INVESTIGATION OF METALLOPEPTIDES UTILIZING HIGH RESOLUTION MASS SPECTROMETRY

A Dissertation

by

ZHAOXIANG WU

Submitted to the Office of Graduate Studies of
Texas A&M University
in partial fulfillment of the requirements for the degree of

DOCTOR OF PHILOSOPHY

May 2010

Major Subject: Chemistry

INVESTIGATION OF METALLOPEPTIDES UTILIZING HIGH RESOLUTION MASS SPECTROMETRY

A Dissertation

by

ZHAOXIANG WU

Submitted to the Office of Graduate Studies of
Texas A&M University
in partial fulfillment of the requirements for the degree of

DOCTOR OF PHILOSOPHY

Approved by:

Chair of Committee,	David H. Russell
Committee Members,	Emile A. Schweikert
	Simon W. North
	Jean-Philippe Pellois
Head of Department,	David H. Russell

May 2010

Major Subject: Chemistry

ABSTRACT

Investigation of Metallopeptides Utilizing High Resolution Mass Spectrometry.

(May 2010)

Zhaoxiang Wu, B.S., University of Science and Technology of China

Chair of Advisory Committee: Dr. David H. Russell

Copper ions (Cu^{+}, Cu^{2+}) play important roles in many biological processes (*i.e.,* oxidation, dioxygen transport, and electron transfer); many of the functions in these processes result from copper ions interacting with proteins and peptides. Previous studies using matrix assisted laser desorption/ionization (MALDI) mass spectrometry (MS) have shown that Cu^{+} ions preferentially bind to electron rich groups in gas phase (*i.e.,* N-terminal amino group, the side-chains of lysine, histidine and arginine). For peptides with more than one Cu^{+} ligand, the interaction between Cu^{+} ions and ligands is described in terms of competitive binding; however, Cu^{+} coordination chemistry for multiple Cu^{+}-containing proteins and peptides in gas phase is still not fully understood. In addition, no studies on the fragmentation chemistry for multiple Cu^{+}-binding peptides, such as $[M + 2Cu - H]^{+}$ ions, have been reported.

The synthesized dinuclear copper complex (α-cyano-4-hydroxycinnamic acid (CHCA) copper salt $(CHCA)_4Cu_2$) enhances the ion

abundances for $[M + xCu – (x-1)H]^+$ (x = 1-6) ions in gas-phase when used as a MALDI matrix. Using this matrix we have investigated site-specific copper binding of several peptides using fragmentation chemistry of $[M + Cu]^+$ and $[M + 2Cu - H]^+$ ions. The fragmentation studies reveal that the binding of a single Cu^+ ion and two Cu^+ ions are different, and these differences are explained in terms of intramolecular interactions of the peptide-Cu ionic complex. The competitive Cu^+ binding to C-terminus (*i.e.*, amide, carboxyl, methyl ester) versus lysine, as well as cysteine (SH/SO_3H) versus arginine (guanidino), was also examined by MALDI MS and theoretical calculations (Density Functional Theory (DFT)). For example, results from theoretical and experimental (fragmentation reactions) studies on $[M + Cu]^+$ and $[M + 2Cu – H]^+$ ions suggest that cysteine side chains (SH/SO_3H) are important Cu^+ ligands. Note that, the proton of the SH/SO_3H group is mobile and can be transferred to the arginine guanidino group. For $[M + 2Cu – H]^+$ ions, deprotonation of the $-SH/SO_3H$ group is energetically more favorable than that of the carboxyl group, and the resulting thiolate/sulfonate group plays an important role in the coordination structure of $[M + 2Cu - H]^+$ ions.

DEDICATION

This dissertation is dedicated to my parents and my whole family. They have always encouraged me during my many years of education, no matter what I did and where I went. Without their support, this dissertation would not exist. I can never thank them enough.

ACKNOWLEDGEMENTS

First, I would like to thank my advisor, Prof. David H. Russell, for his guidance and support during the years of my Ph.D study at Texas A&M University and for providing me an excellent research environment in mass spectrometry. I am so thankful to have been a part of the Russell group from whom I have learned how to become a good scientist. I would like to thank Dr. William K. Russell who taught me a lot in proteomics study, and Dr. Francisco A. Fernandez-Lima for his contributions in the computational calculations of the gas-phase metal-peptide ion structures in this project.

Also, I would like to thank all the graduate students, postdocs and staff in Russell's research group, particularly, Dr. Wenjian Sun, Dr. Stacy Sherrod, Dr. Jody May, Lei Tao, Brad Williams, Stephanie Cologna, and Liuxi Chen, for their helpful discussions on this project. I am also indebted to my advisory committee members, Prof. Emile A. Schweikert, Prof. Simon W. North and Prof. Jean-Philippe Pellois, for contributing their time and thoughts on this project.

I am greatly indebted to my parents and my whole family for their never-ending encouragement and support during the years of my education. Without their support, this dissertation would not exist.

This work was funded by the Robert A. Welch Foundation (A-1176) and the U. S. Department of Energy, Division of Chemical Sciences, BES (DE-FGO2-04ER15520), and the National Science Foundation (DBI-0821700).

NOMENCLATURE

MALDI	Matrix Assisted Laser Desorption/Ionization
TOF	Time-of-Flight
MS	Mass Spectrometry
IM	Ion Mobility

TABLE OF CONTENTS

CHAPTER Page

LIST OF FIGURES

FIGURE Page

FIGURE Page

FIGURE Page

FIGURE Page

LIST OF TABLES

CHAPTER I

INTRODUCTION

Copper ions (Cu^{+}, Cu^{2+}) play important roles in many chemical and biological processes, such as oxidation, dioxygen transport, and electron transfer; many of these functions result from copper ions interacting with proteins and peptides [1-3]. Most of the copper proteins exist as primary oxidase, oxygenases and oxygen carries in animal cells; for example, hemocyanin is a two-copper containing protein which carries oxygen in the hemolymph of many molluscs and arthropods. It has been reported that hemocyanin reversibly bind to a single oxygen molecule, resulting in a color change between the colorless Cu(I) deoxygenated form and the blue Cu(II) oxygenated form [4-6]. Cytochrome c oxidase is the terminal oxidase in the the respiratory electron transport chain of mitochondria, and it receives electrons and transfers them to oxygen molecules, converting oxygen to water. Previous studies have been suggested that electrons are passed from cytochrome c molecules through the Fe_{a3}-Cu_B binuclear center, reducing Cu^{2+} to Cu^{+} [7-10]. In plants, copper is a cofactor for plastocyanin, copper/zinc superoxide dismutase (Cu/Zn SOD), ethylene receptors for the

---

This dissertation follows the style of the *Journal of American Society for Mass Spectrometry.*

apoplastic oxidases, and plays important roles in photosynthesis, respiration, and antioxidant activity [11-13]. Copper has also been implicated in human neurodegenerative diseases such as Alzheimer's Disease, presumably such affects involve the interaction of copper ions with peptides and/or proteins [14-16].

In general, copper proteins in their native state contain either Cu^{2+} or Cu^{+} or both [2,3]. Redox chemistry ($Cu^{2+} \Leftrightarrow Cu^{+}$) is involved in many enzymatic processes, but there are numerous examples, such as copper chaperone proteins and copper transport proteins, where the biological processes are limited to a single oxidation state, *i.e.*, Cu^{2+} or Cu^{+} [17]. Most of our knowledge concerning copper in the biological system is derived from solution and solid-state studies [18]; for example, dopamine β-hydroxylase (Figure 1) is an oxygenase which catalyzes the penultimate step in the biosynthesis of adrenaline, and the copper binding sites of this physiologically important enzyme has been studied using various analytical techniques, including nuclear magnetic resonance (NMR), X-ray crystallography and electron paramagnetic resonance (EPR) [2,19]. Results from NMR and radioactive binding experiments suggest that dopamine β-hydroxylase requires eight copper ions per tetramer for maximal activity. Spin-echo EPR and X-ray crystallography data indicate that three to four histidine ligands coordinated to each copper ion in a square planar geometry [2].

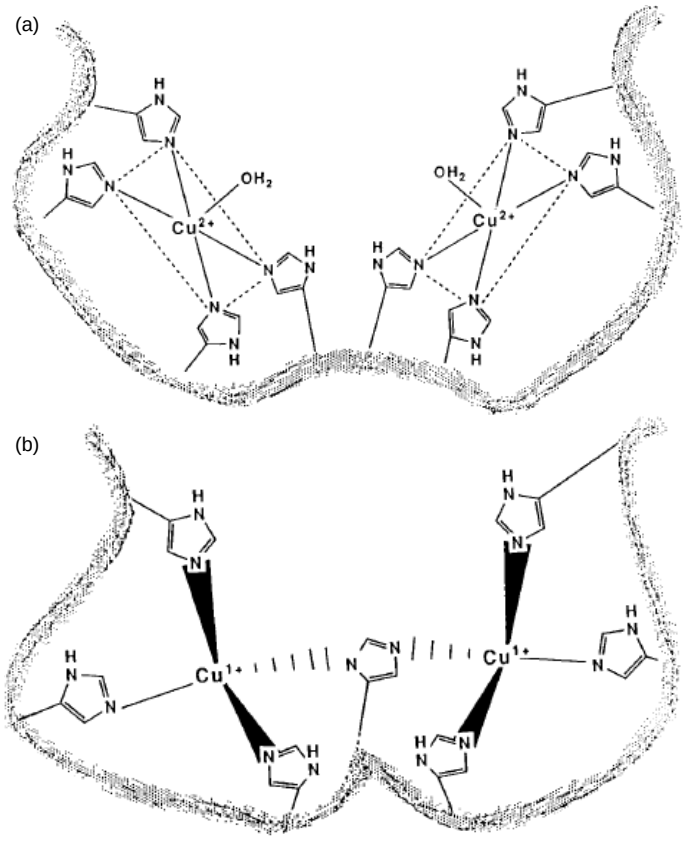

Figure 1. (A) Cu(II) binding sites in native dopamine β-hydroxylase and (B) Cu(I) binding sites in reduced dopamine β-hydroxylase [2].

Studies of gas-phase species can be used to probe intrinsic metal-peptide and metal-protein interactions in the absence of solvent, which simplify the chemistry and eliminates solvent stabilization of metal ion-ligand interactions and are more closely related to low dielectric environments such as biological membrane systems [7,20,21]. Mass spectrometry has been used as a comprehensive and versatile tool for analysis of non-covalent interactions of proteins or peptides with metal ions in gas phase [22-33]. Wood and coworkers studied the binding of Cu^{2+} and Co^{2+} to a zinc finger

peptide of the transcription factor IIIA (Cys^2-His^2) and they suggested that mass spectrometry can be used to detect noncovalently metal-bound compounds if conditions were used to prepare the samples that allowed macromolecular assemblies to retain tertiary structure [34]. Hornshaw and coworkers have shown that synthetic peptides containing three or four copies of an octapeptide repeat sequence (PHGGGWGQ), which is found in a highly conserved N-terminal domain of prion protein, preferentially bind copper over other metals [35]. Although comparison of gas-phase and solution-phase data could potentially yield important information regarding solvent dependent metal-protein interactions, the ligand interactions are typically very different [7]. For example, in solution the side chains of basic amino acid residues are protonated, which reduces the binding energy of N-donor ligands, whereas in the gas-phase Cu^+ and Cu^{2+} have strong preferences for binding to arginine, lysine, and histidine [1,7,33,36].

The kinetic method, developed by Cooks and co-workers, has been successful used for the measurement of proton affinities [37,38], metal affinities [39], gas-phase acidities [40] and electron affinities [41]. Wesdemiotis and co-workers have determined the relative Cu^+ ion affinities of amino acids in gas-phase based on the unimolecular dissociations of the Cu^+-bound heterodimers ($AA_1…Cu^+…AA_2$) [42]. In their experiments, the relative Cu^+ affinities of amino acid AA_1 and AA_2 are obtained by comparing the rates of dissociation of the Cu^+-bound heterodimer $AA_1…Cu^+…AA_2$ to

each of the individual Cu^+-attached monomers (*i.e.,* AA_1Cu^+, or AA_2Cu^+) (eq 1).

$$AA_1 \ldots Cu^+ \ldots AA_2 \xrightarrow{k1} AA_1Cu^+ + AA_2 \quad (1a)$$

$$AA_1 \ldots Cu^+ \ldots AA_2 \xrightarrow{k2} AA_1 + AA_2Cu^+ \quad (1b)$$

Application of transition state theory [43] to the competing reactions (1a and 1b) leads to:

$$\ln\left(\frac{k1}{k2}\right) = \ln(Q_1^* Q_2 / Q_2^* Q_1) + \Delta\epsilon_0 / RT_{eff} \quad (2)$$

where Q and Q^* are the partition functions for the ion and the activated complex, T_{eff} is the effective temperature of the heterodimer ion (*i.e.,* $AA_1…Cu^+…AA_2$) undergoing dissociation. Both reaction channels originate from the same reactant ion (*i.e.,* $AA_1…Cu^+…AA_2$), Q_1 and Q_2 are identical. Since the unimolecular dissociations (1a and 1b) proceed by simple bond cleavages from the loosely bound dimer $AA_1…Cu^+…AA_2$, the reverse activation energies for channels 1a and 1b are negligible. $\Delta\epsilon_0$ can be approximated by the difference in Cu^+ affinities between the two amino acids (*i.e.,* ΔCu^+A). In addition, AA_1 and AA_2 are chemically similar species, $\Delta(\Delta S^o_{Cu^+})$ should be close to zero and $Q_1^* \approx Q_2^*$, eq2 is simplified to

$$\ln\left(\frac{k1}{k2}\right) = \Delta Cu^+A / RT_{eff} \quad (3)$$

By measuring the experimental abundance ratio of AA_1Cu^+/AA_2Cu^+, which is equal to $k1/k2$, Wesdemiotis reported that the Cu^+ affinities for the 20 common amino acids decrease in the order Arg > Lys > His > Trp > Met >

Gln > Cys > Tyr > Phe > Glu > Asn > Asp > Pro > Thr > Ile > Leu > Val > Ser > Ala > Gly [42].

Matrix assisted laser desorption/ionization (MALDI) time-of-flight (TOF) mass spectrometry (MS) has also been widely used to study the energetics of copper binding sites in model peptides [25,27,29,33,36,44-49]. Bluhm and coworkers used a combination of theoretical calculations and experimental data to determine copper binding sites for modeled systems based on monodentate and bidentate interactions [50], and the measured and calculated Cu^+ ion affinity order were in agreement with previous data reported by Wesdemiotis [42]; the monodentate Cu^+ binding energies for amino acids follow the order Arg > His > Lys > Cys > Ser, and bidentate Cu^+ relative binding energies are Arg > Lys > His > Gln > Asn > Glu >Asp. In both cases, arginine is the most favorable binding site of Cu^+ for gas-phase peptides. Peptides that do not possess basic amino acids (*i.e.,* Arg, Lys, and His) do not strongly bind to copper ions and the $[M + Cu]^+$ ions are either not observed by MALDI mass spectrometry or are formed at very low abundance.

Unlike electrospray ionization (ESI), which yields almost exclusively Cu(II) complexes such as $[M + Cu(II) - H]^+$ ions in gas phase [51], MALDI studies suggest that peptide-metal ion complexes are formed by a reductive process which yields primarily $[M + Cu(I)]^+$ ions. Nelson and coworkers investigated the affinity of aqueous copper ions for a model peptide (sequenced $(GHHPH)_5G$)), which comes from human histidine-rich

glycoprotein (HRG). Their results suggest that the copper is bound as Cu^+ in the desorbed ion [27].

Zenobi and coworkers proposed a mechanism of the reduction of Cu(II) in MALDI experiments [52,53]. They reported that Cu(II) is reduced to Cu(I) by gas-phase charge exchange with matrix molecules, and under some conditions, Cu(II) can be even more efficiently reduced to Cu(I) by free electron capture in the gas-phase [52]. More recently, Prudent and Girault have shown that both $[M + Cu(I)]^+$ and $[M + Cu(II) – H]^+$ ions can be formed by ESI; however, formation of $[M + Cu]^+$ ions is only observed if the ESI emitters are composed of solvable copper anodes [51].

Tandem mass spectrometry can provide structural information of peptide ions in the gas phase (Table 1), and the fragmentation reactions of copper bound peptides have been used for the determination of copper binding sites. Based on fragmentation studies, Shields and coworkers proposed that the primary Cu^+ binding site in peptides with an N-terminal arginine is the guanidino group of arginine and the N-terminal amine [36]. That is, the principal fragment ions of $[M + Cu]^+$ peptide ions containing an N-terminal arginine are $[a_n + Cu - H]^+$ and $[b_n + Cu - H]^+$ fragment ions. They also described the fragmentation reactions of $[M + Cu]^+$ in terms of a “mobile proton” model, by which the fragmentation occurs remote from the Cu^+ ion attachment site, and involves metal ion promoted deprotonation to generate a new site of protonation.

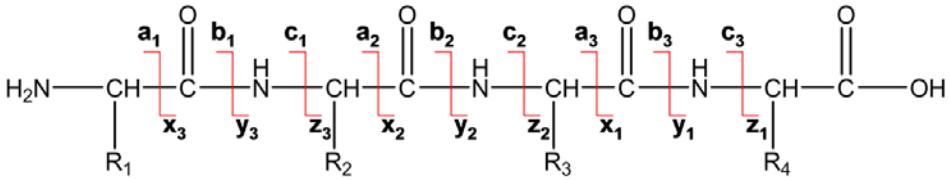

Recently, Vachet and coworkers developed a methodology based on metal-catalyzed oxidation (MCO) reactions and mass spectrometry (MS) to determine the Cu^{2+} binding sites in copper proteins [54-56]. They incubated the copper proteins or copper-bound peptides with a reducing agent (*i.e.*, ascorbate) and an oxidating agent (*i.e.*, O_2, H_2O_2), and the redox cycling of the metal generates highly reactive oxygen species such as $O_2^{-\cdot}$ and $OH\cdot$ by Fenton-like chemistry, resulting in oxidative modifications or cleavages at amino acids that bound copper ions. MS and tandem MS are then used to identify the amino acids that have been oxidized, and thus to determine the copper binding sites [54].

Table 1. Nomenclature for peptide fragment ions [57].

$\mathbf{a_n}$	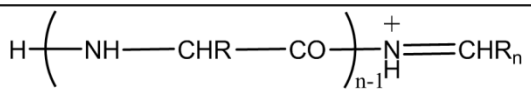
$\mathbf{b_n}$	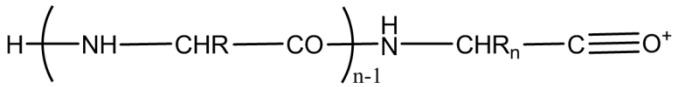
$\mathbf{c_n}$	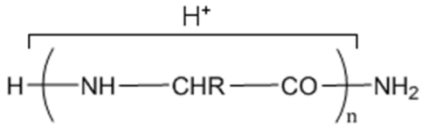
$\mathbf{x_n}$	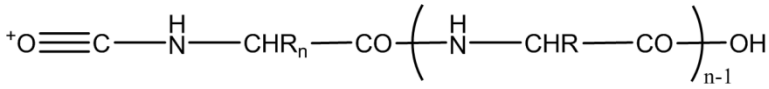
$\mathbf{y_n}$	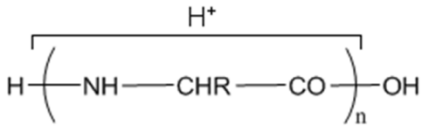
$\mathbf{z_n}$	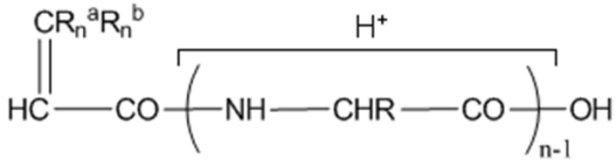

For peptides with more than one basic residue, the interaction between the Cu^+ and the basic residues is described in terms of competitive binding; *i.e.,* Cu uptake by biologically important peptides and proteins. That is, if a peptide contains multiple Cu^+ binding sites, are there other factors that determine Cu^+ binding; does the addition of Cu^+ to a peptide influence the binding site of subsequent Cu^+ ions? How does accumulation of Cu^+ by

specific amino acids influence Cu^+ binding? In addition, for peptides containing multiple Cu^+ ions, such as $[M + 2Cu - H]^+$, how would the deprotonation affects the fragmentation chemistry of peptides? Few studies have been reported to answer these questions, and addressing these issues will shed light on the intrinsic Cu^+ binding to peptides and gain a better understanding of the functions of Cu^+ ions in biological systems.

CHAPTER II

A NOVEL COPPER CONTAINING MALDI MATRIX*

Introduction

Previous studies have shown that gas-phase peptide-metal complex ions (*i.e.,* peptide-Cu^{2+} complex) can be generated by electrospray method [22,28,30,32]. Gatlin and coworkers reported the gas-phase chemistry of amino acid complexes with copper (II) and 2,2'-bipyridyl (bpy). They found that electrospraying CH_3OH/H_2O (50/50) solutions of amino acids, $CuSO_4$-$5H_2O$, and bpy produces abundant gas-phase $[Cu(II)(RCOO)bpy]^+$ ions; however, only Cu^{2+} ions are observed in the copper complexes for electrospray experiments [22]. Therefore, electrospray may not be suitable for analysis of the copper proteins containing Cu^+ ions.

As we discussed in Chapter I, MALDI experiments generate primarily $[M + Cu(I)]^+$ ions in gas phase by a reductive process [53], and there are two commonly used sample preparation methods to generate gas-phase peptide-Cu ions using MALDI: (i) co-mixing a metal salt such as $CuCl_2$, CuO or $CuSO_4$ with the peptide and organic matrix [22,23,26,28,30-32,58], and (ii)

---

* Reproduced with permission from Wu, Z.; Fernandez-Lima, F.A.; Perez, L.M.; Russell, D.H. A New Copper Containing MALDI Matrix That Yields High Abundances of $[Peptide+Cu]^+$ ions. *J. Am. Soc. Mass. Spectrom*. **2009**, 20, 1263-1271. Copyright [2009] by Elsevier.

the method first reported by Shields where $[M + Cu]^+$ is generated by desorbing the sample from a CHCA matrix deposited onto an oxidized copper plate [59]. Presumably the latter method involves dissolution of CuO from the metal surface followed by reaction of CuO with the peptide and/or matrix to yield peptide-Cu complexes. Both methods produce abundant peptide $[M + Cu]^+$ ions; however, the dominant ions observed in the mass spectrum usually correspond to the $[M + H]^+$ ion with a lower abundance of the $[M + Cu]^+$ ions.

Here, we introduce a dinuclear copper complex (α-cyano-4-hydroxycinnamic acid (CHCA) copper salt $(CHCA)_4Cu_2$), which is synthesized by reacting CHCA with copper oxide (CuO) [60]. The dinuclear copper complex yields increased abundances of $[M + xCu – (x-1)H]^+$ (x = 1-6) ions when used as a matrix for matrix-assisted laser desorption ionization (355 nm Nd:YAG laser). The yield of $[M + xCu - (x-1)H]^+$ (x = 1~6) ion is much greater than that obtained by mixing peptides with copper salts or directly depositing peptides onto oxidized copper surfaces. The increased ion yields for $[M + xCu - (x-1)H]^+$ result in higher quality tandem MS signals, which enable studies of the binding and fragmentation chemistry of peptide-Cu complexes. For example, using this matrix we have investigated site-specific copper binding of several peptides using fragmentation chemistry of $[M + Cu]^+$ and $[M + 2Cu - H]^+$ ions. The fragmentation studies reveal interesting insight on Cu binding preferences for basic amino acids. Most

notable is the fact that the binding of a single Cu^+ ion and two Cu^+ ions are quite different, and these differences are explained in terms of intramolecular interactions of the peptide-Cu ionic complex.

Experimental

Chemicals and Materials

Copper oxide (CuO) and α-cyano-4-hydroxycinnamic acid (CHCA) were obtained from Sigma (St. Louis, MO). CHCA was recrystallized prior to use. The organic solvents used for mass spectrometry were HPLC grade, all the other chemicals were reagent grade, and the water is in high purity (18MΩ; Barnstead International, Dubuque, IA). The peptides Ac-$(AAKAA)_n$-NH_2 (n = 2 - 4) were purchased from Genscript Corporation (Piscataway, NJ). Other peptides used in the experiments were purchased from Sigma (St. Louis, MO) and used without further purification. Ac-$(AAKAA)_2$-OH and Ac-$(AAKAA)_2$-OCH_3 peptides were synthesized from Ac-$(AAKAA)_2$-NH_2 following standard protocols [61,62].

Peptide Methylation

A solution of 2M hydrochloric acid in methanol was prepared by dropwise addition of acetyl chloride (800 µl) into anhydrous methanol (5 ml) and then stirring for 5 min at room temperature. The solution (1 ml) was added to the peptide (50 µg) and then the mixture was stirred for 3 h at room temperature. The resulting solution was dried by SC250DDA Speedvac Plus

(Thermo Electron Corporation, Waltham, MA). The methylated peptide was used without any further purification [61,62].

Synthesis of the Copper Complex

The copper α-cyano-4-hydroxycinnamic acid complex (Cu-CHCA) was synthesized by reacting CHCA with copper oxide (CuO). The reaction was carried out by dissolving 200 mg of α-cyano-4-hydroxycinnamic acid (CHCA) and 170 mg of copper oxide (CuO) powder in 7:3 (v:v) distilled deionized H_2O: acetonitrile (ACN) solution, followed by 15 minutes of sonication to form a suspension. The suspension was then incubated in a water bath at 65 ^oC for 8 hours and cooled to room temperature. Following several steps of filtration and recrystallization, needle–like crystals were obtained (Figure 2A).

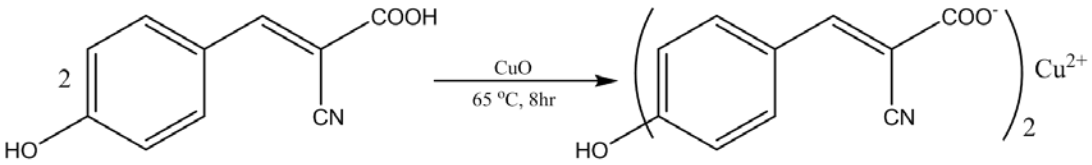

Characterization of the Copper Complex

The Cu-CHCA complex was characterized by single crystal X-ray diffraction, MALDI-TOF mass spectrometry, and UV/VIS spectroscopy. The single crystal X-ray diffraction data (Figure 2B) indicated that four α-cyano-4-hydroxycinnamic acid ligands complexed to a dinuclear copper center in a paddlewheel-like structure [63]. The distance between the two copper ions of approximately 2.6Å is typical of the noncovalent binding of Cu-Cu in other paddlewheel complexes. Each copper ion is five-coordinated with 4 oxygen atoms from the two carboxylate groups and one oxygen atom from the

solvent molecule (tetrahydrofuran), thus the chemical formula of the complex is $(CHCA)_4Cu_2$. The MALDI mass spectrum (Figure 3A) of the Cu-CHCA complex contains a dominant peak at m/z 441.0 which corresponds to the protonated $(CHCA)_2Cu$ species. The UV/VIS spectrum (Figure 3B) shows that the Cu-CHCA complex has a strong absorption in the UV wavelength range, which is similar to that of CHCA. Also, the Cu-CHCA complex has a weak absorption in the visible light wavelength range, indicating the existence of Cu^{2+} ions.

Mass Spectrometry

The MALDI MS experiments described herein were performed on a tandem time-of-flight mass spectrometer (4700 Proteomics Analyzer, Applied Biosystems, Framingham, MA), and all tandem MS experiments were performed using a collision energy setting of 1 kV and air as the collision gas.

Theoretical Calculations

Theoretical calculations using Density Functional Theory (DFT) have been performed to gain a better understanding of peptide-Cu ion structure. The B3LYP functional was used [64-66]. The triple-ξ quality basis set with a small-core effective core potential (SDD) was used for the Cu ions [67], while all the other atoms were treated with the triple- ξ quality Pople style basis set with diffuse and polarization functions (6-311++G(d,p)) [68,69]. This combination of basis sets will be referred to as TZBS. No symmetry

restriction of any kind was imposed in the process of geometry optimization. All calculations were performed using the Gaussian 03 program suite [70].

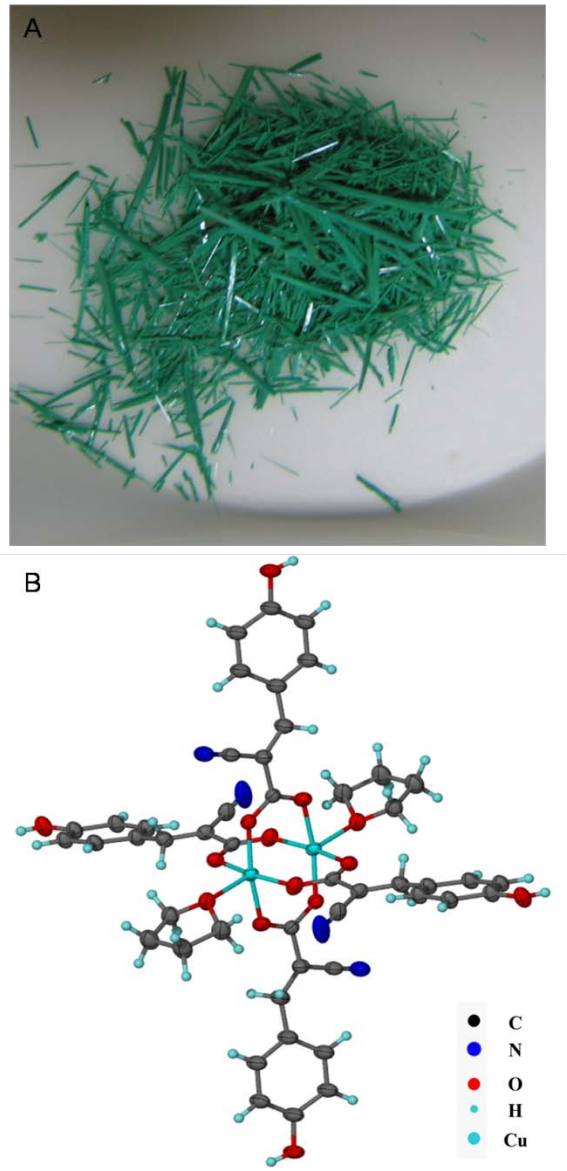

Figure 2. (A) Image of the Cu-CHCA complex crystal. (B) Single crystal X-ray diffraction data of the Cu-CHCA complex. Four α-cyano-4-hydroxycinnamic acid ligands complex to a dinuclear copper center in a paddlewheel-like structure. Each copper atom is five-coordinated with 4 oxygen atoms from the two carboxylate groups and one oxygen atom from the solvent molecule (tetrahydrofuran).

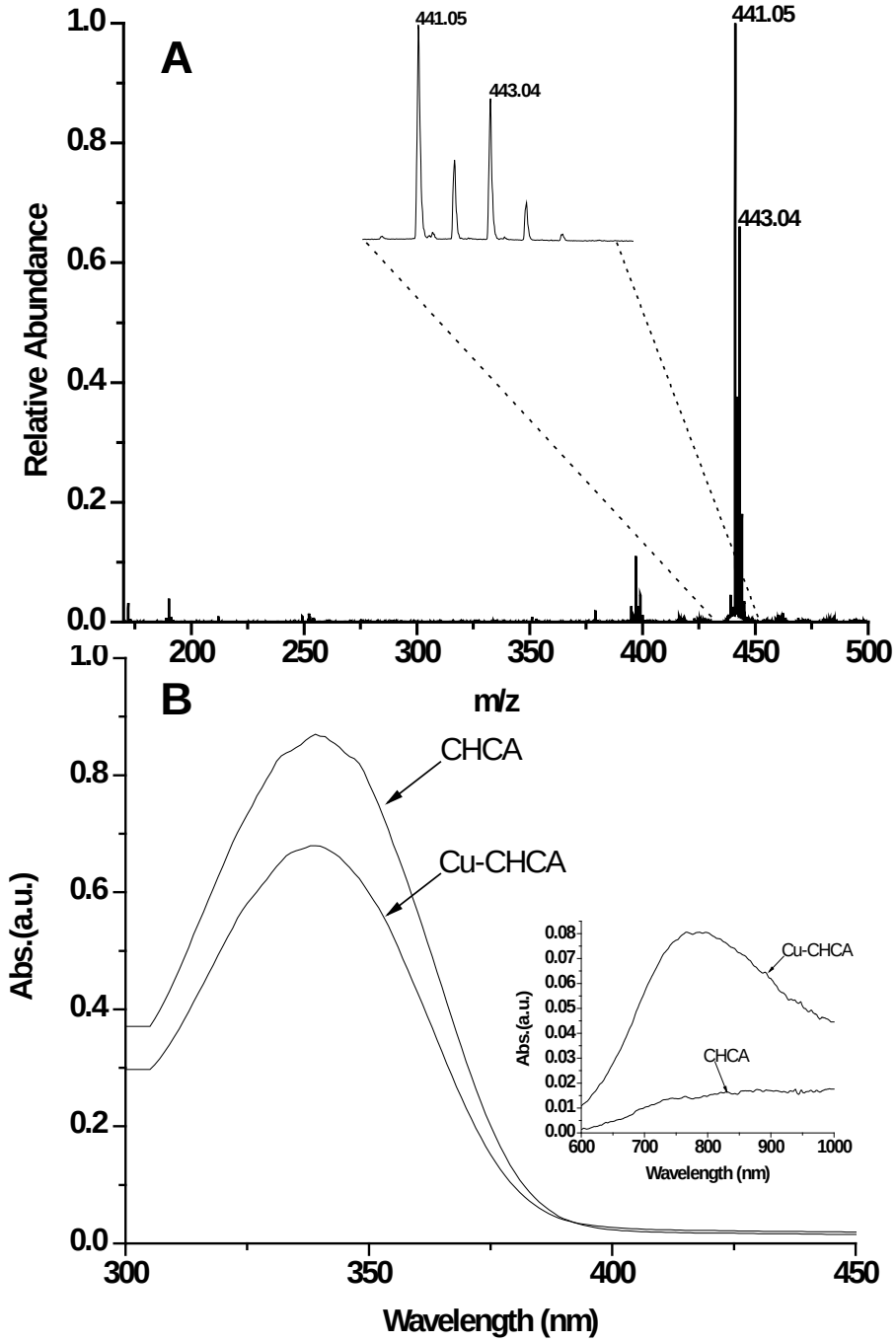

Figure 3. (A) MALDI-TOF mass spectrum of Cu-CHCA complex. The dominant peak at m/z 441.0 corresponds to the protonated $(CHCA)_2Cu$ species. (B) UV/VIS spectrum of CHCA and Cu-CHCA complex.

Results and Discussion

Here, we describe the utility of the Cu-CHCA complex as a MALDI matrix. LDI from crystals of Cu-CHCA yield higher abundances of $[M + xCu – (x-1)H]^+$ ions (x = 1-6). To illustrate this point, LDI mass spectra obtained by using copper sulfate, a copper plate (CuO) and the Cu-CHCA complex are shown in Figure 4. Note that the yield of $[M + Cu]^+$ ions using Cu-CHCA is considerably higher than that obtained using copper salt or a copper plate and that the ratio of $[M + Cu]^+$ to $[M + H]^+$ ions has also increased (Figure 4). For the peptide ACTH (1-17) (SYSMEHFRWGKPVGKKR), which contains six basic amino acids, we observe $[M + xCu - (x-1)H]^+$ where x ranges from 1 to 6, and the ratio of $[M + Cu]^+$ ions to $[M + H]^+$ is ~1.3:1. Conversely, when using copper sulfate or CHCA/copper plate, the most abundant peaks in the spectra correspond to $[M + H]^+$ ions while a very low abundance of $[M + xCu - (x-1)H]^+$ ions are observed.

The increased abundances for $[M + Cu]^+$ produced by Cu-CHCA reveal rich MS/MS spectra containing Cu^+, which improves our ability to investigate Cu-peptide and Cu-protein complexes. In addition, Cu-CHCA affords opportunities to study the competitive binding of Cu^+ in $[M + xCu – (x-1)H]^+$ ions, *i.e.,* Cu uptake by biologically important peptides and proteins. That is, if a peptide contains multiple Cu^+ binding sites, are there other factors that determine Cu^+ binding; does the addition of Cu^+ to a peptide influence the

binding site of subsequent Cu^+ ions? How does accumulation of Cu^+ by specific amino acids influence Cu^+ binding?

Figure 5 contains fragment ion spectra for $[M + Cu]^+$ ions of $[Val]^5$–Angiotensin II and ACTH (1-17). Both spectra contain abundant $[b_i + Cu]^+$ and $[y_i + Cu]^+$ ions, and all fragment ions contain Cu^+, *i.e.,* the Cu^+ binding affinity of the peptide is higher than the energy required to fragment the molecule. On closer inspection of the fragment ions, we can determine the Cu^+ binding site, and the relative abundance of *b* and *y*-type ions indicates whether Cu^+ prefers to bind to the basic residues close to the N-terminus or the C-terminus. For example, on the basis of relative binding energies (BE) we would predict that Cu^+ preferentially binds to Arg^2 and His^6; BE for Arg^2 (~73 kcal/mol) is greater than that for His^6 (~64 kcal/mol) [50]. We would also expect to observe b_2, b_3, b_4 and b_5 fragment ions for $[M + Cu]^+$ ions if Cu^+ is bound to Arg^2. Similarly, signature fragment ions for Cu^+ binding to His^6 would be y_3, y_4, y_5 and y_6. The relative abundances of these signature *b* and *y*-type ions is about 2:1, thus it appears that ~67% of the Cu^+ ions bind to Arg^2 and ~33% of the Cu^+ ions bind to His^6. On the basis of our previous studies we would argue that Cu^+ prefers to bind to Arg^2, owing to the stabilization afforded by bidentate complexation to the N-terminal NH_2 group [50].

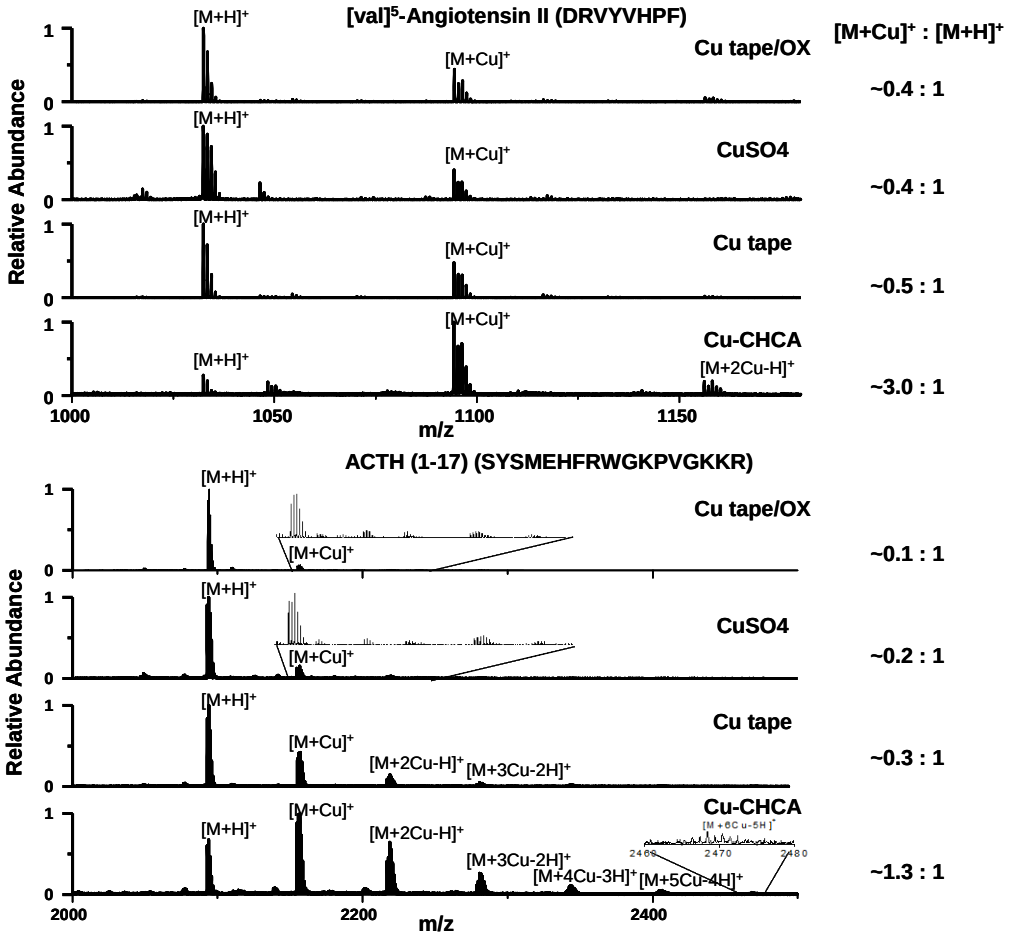

Figure 4. Partial mass spectra for [Val]^5-Angiotensin II and ACTH (1-17) obtained by using four different copper sources: copper tape with an oxidized surface; $CuSO_4$ solution; copper tape with a non-oxidized surface; copper matrix Cu-CHCA. The peptides amounts deposited on the MALDI plate were kept constant at 1pmol for all the experiments. The molar ratio of $CuSO_4$/peptide and Cu-CHCA/peptide was kept constant at 5.

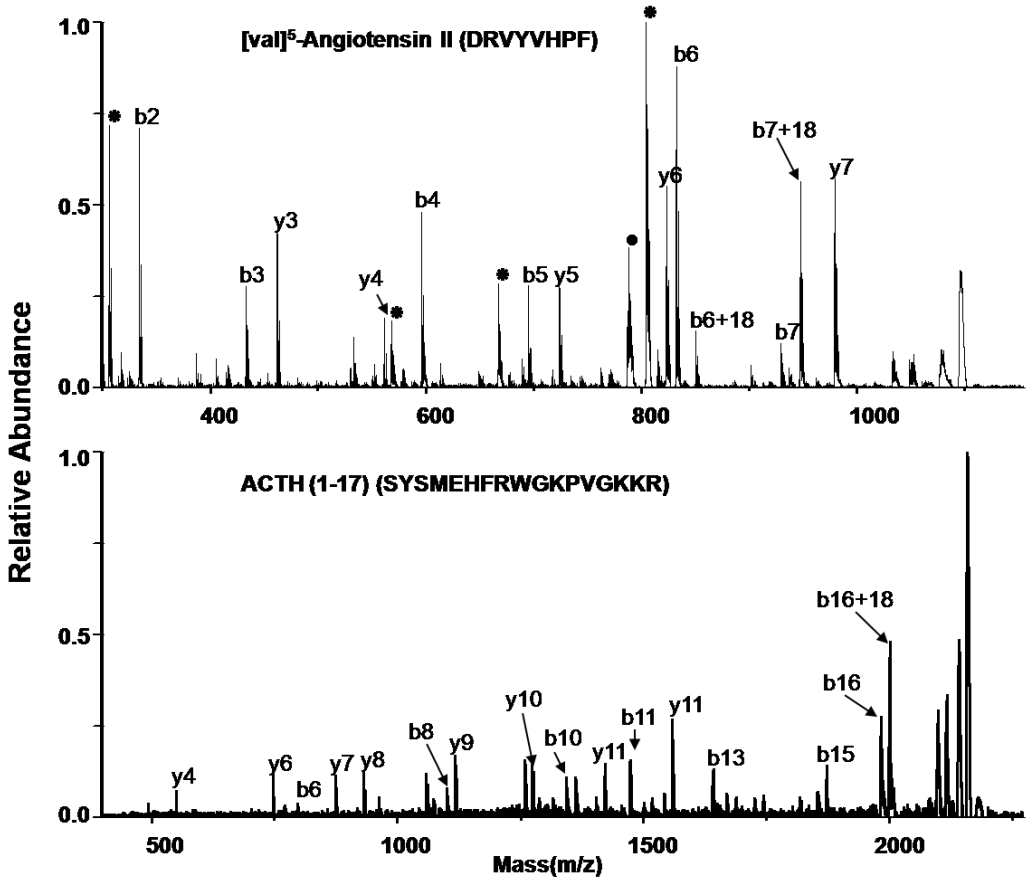

Figure 5. Fragment ion spectra of $[M + Cu]^+$ of two peptides: $[Val]^5$-Angiotensin II and ACTH(1-17). All fragment ions in the spectra have bound Cu^+. (•) denotes internal fragment ions with Cu^+ attached; (*) denotes a-type fragment ions with Cu^+ attached. *b*- and *y*- type fragment ions with Cu^+ attached are the dominant ions for both peptides.

Figure 6 contains the fragment ion spectra of Ac-$(AAKAA)_2Y$ $[M + Cu]^+$ ions with three different C-terminal groups: an amide group, a free acid and a methyl ester. This peptide contains two basic lysine residues; thus, Cu^+ ions can bind to either Lys^3 or Lys^8. In addition, our previous studies suggest a preference for binding to Lys^3 because of its ability to form a bidentate interaction with the N-terminus [50]. The fragmentation spectra of the $[M + Cu]^+$ ions of the peptide ion with different C-termini are dominated by both *b*- and *y*-type fragment ions, all of which contain Cu^+. The b_3 ion is the lowest m/z *b*-type fragment ion observed and the lowest m/z *y*-type fragment ions correspond to y_4 ion, which supports our assignment of Cu^+ binding to either Lys^3 or Lys^8. Note also that the *b*-type fragment ions are more dominant than the *y*-type fragment ions; the ratio of *b*- to *y*-type ions is approximately 70% to 30% for all the three spectra, respectively. Presumably, the higher abundance of *b*-type fragment ions indicates that Lys^3, which is close to the N-terminus, has a higher binding affinity for Cu^+ than the Lys^8; thus, the position of the lysine residues plays an important role in the binding preference of Cu^+ to peptides. Also, this data suggests that the C-terminus has less influence on the fragmentation of $[M + Cu]^+$ ions compared to the position of the lysine residue.

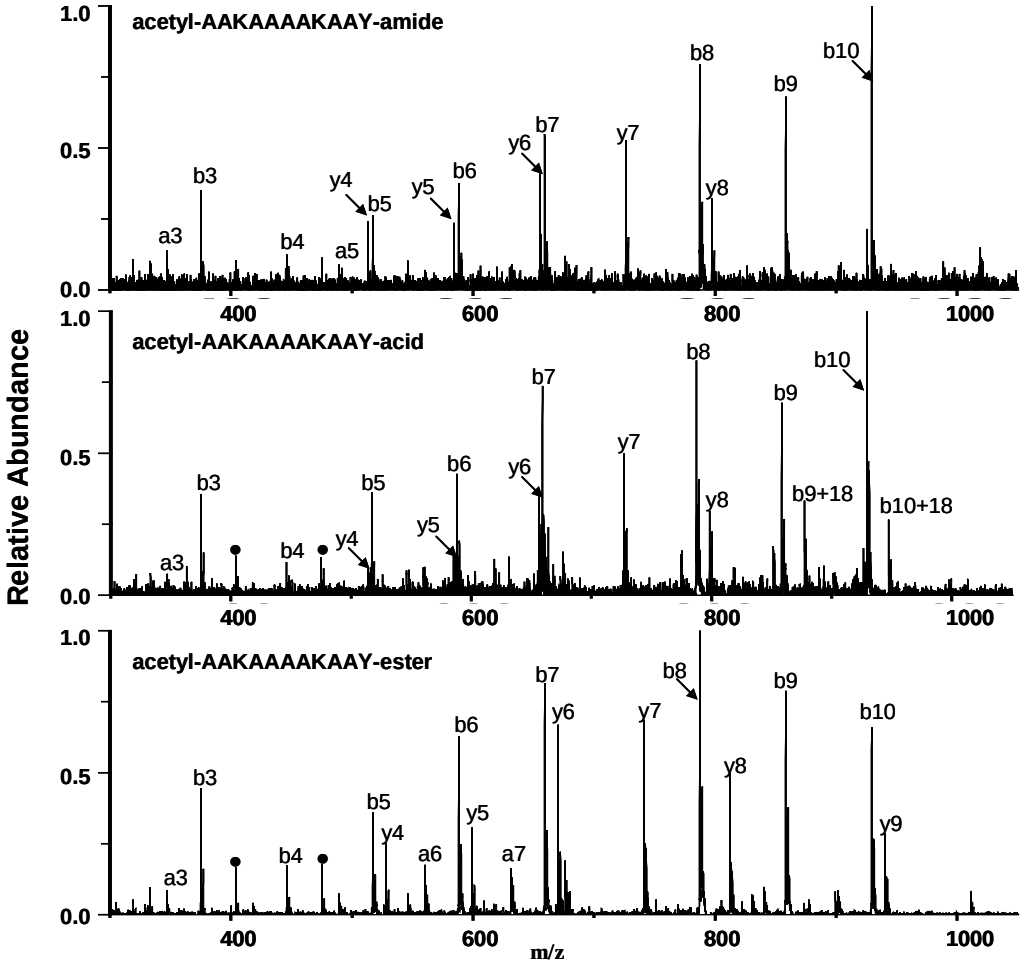

Figure 6. Fragment ion spectra of $[M + Cu]^+$ of Ac-$(AAKAA)_2$Y with three different C-terminal groups: amide, free acid and ester. All fragment ions in the spectra have bound Cu^+. (•) denotes internal fragment ions with Cu^+ attached. The fragment ion spectra of the $[M + Cu]^+$ ions of the peptide ion with different C-termini are dominated by both *b*- and *y*-type fragment ions, all of which contain Cu^+, and the abundance ratio of *b*- to *y*-type ions is approximately 70% to 30% for all the three spectra, respectively.

We also examined the fragmentation chemistry for model peptide ions containing multiple Cu ions. For these ions, the C-terminus strongly affects the fragmentation reactions. For example, the fragment ion spectra of the $[M + 2Cu - H]^+$ ions of the peptide Ac-$(AAKAA)_2$-Y with three different C-terminal groups (Figure 7) are quite different from those of the $[M + Cu]^+$ ions (Figure 6). Specifically, inspection of the $[M + 2Cu - H]^+$ fragment ion spectra shows that all the observed fragment ions contain two coppers while fragment ions containing a single Cu^+ are not observed, which suggests that both copper ions are bound to the same site or in close proximity. The $[M + 2Cu - H]^+$ fragment ion spectra are dominated by *b*- and *y*- type fragment ions, and the ratio of *b*- to *y*-type ions varies depending on the nature of the C-terminal group. For peptide ions with an amide or ester C-terminus, the ratio of *b*- to *y*- type ions is approximately 45% to 55% (Table 2), which suggests that the copper ions bind to the two lysine residues with roughly equal probability. On the other hand, peptide ions with a free acid C-terminus yield a very different ratio of *b*- to *y*-type ions, viz. 5% to 95% (Table 2), which suggest that the copper ions strongly prefer Lys^8. Our interpretation of this experimental result is that the free acid C-terminus is a better Cu^+ ligand than the amide or methyl ester groups; this is probably an indication that the –COOH proton is lost in forming $[M + 2Cu – H]^+$ ions.

Table 2. Cu^+ binding preference for peptides with multiple basic residues. For example, K^3 is the percentage of peptide with Cu^+ bound to the third lysine. For multiple lysine containing peptides Ac-$(AAKAA)_n$Y-NH_2 (n = 3,4), the Cu^+ ions preferentially bind to the lysine near the termini; However, for multiple histidine containing peptide WGGHDGPHAPGDH, the most favorable binding sites for Cu^+ ions are His^8 and His^{13}.

peptide	$[M+Cu]^+$	$[M+2Cu-H]^+$
R^1PGFSPFR^8	R^1: 57%; R^8: 43%	R^1: 58%; R^8: 42%
R^1PPGFSPFR^9	R^1: 73%; R^9: 27%	R^1: 74%; R^9: 26%
acetyl-AAK^3AAAAK^8AAY-amide	K^3: 70%; K^8: 30%	K^3: 47%; K^8: 53%
acetyl-AAK^3AAAAK^8AAY-free acid	K^3: 68%; K^8: 32%	K^3: 5%; K^8: 95%
acetyl-AAK^3AAAAK^8AAY-ester	K^3: 70%; K^8: 30%	K^3: 45%; K^8: 55%
acetyl-AAK^3AAAAK^8AAAAK^{13}AAY-amide	K^3: 69%; K^{13}: 31%	K^3: 49%; K^{13}: 51%
acetyl-AAK^3AAAAK^8AAAAK^{13}AAAAK^{18}AAY-amide	K^3: 68%; K^{18}: 32%	K^3: 46%; K^{18}: 54%
WGGH^4DGPH^8APGDH^{13}	H^8: 46%; H^{13}: 54%	H^8: 42%; H^{13}: 58%

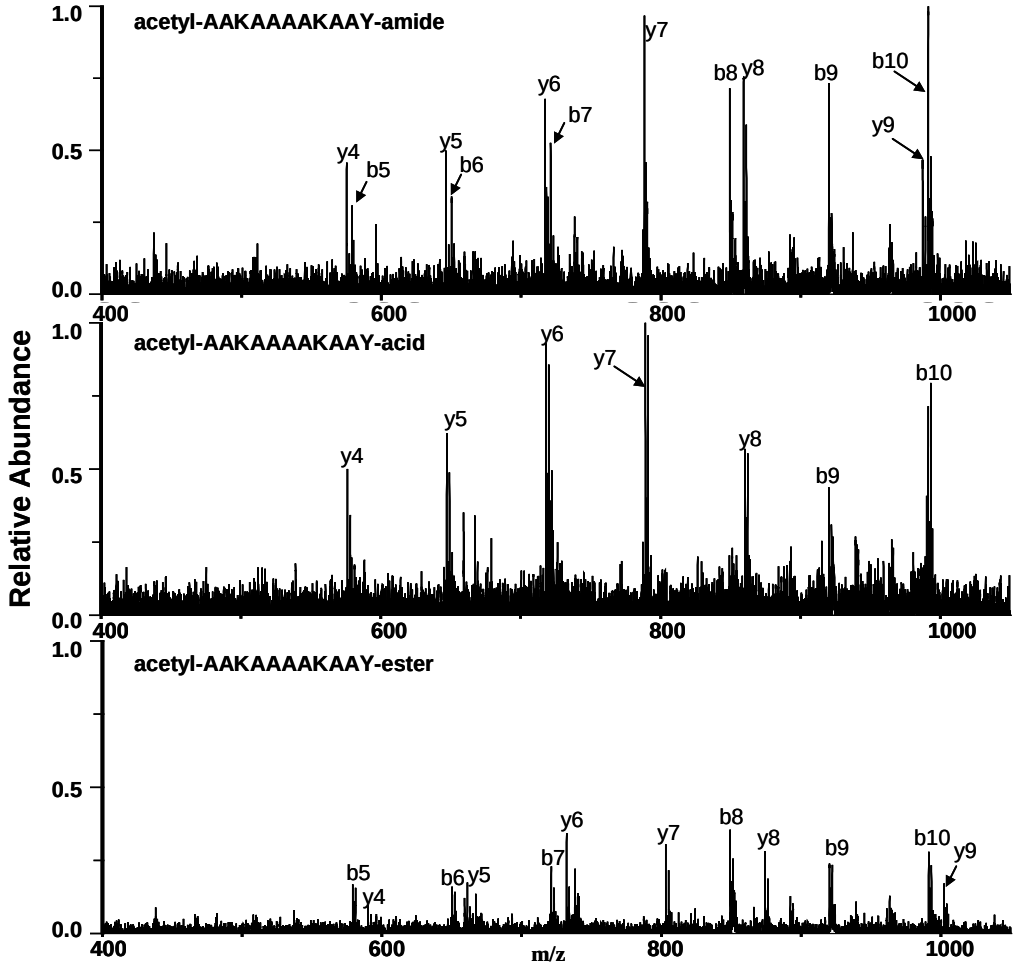

Figure 7. Fragment ion spectra of the $[M + 2Cu - H]^+$ of Ac-$(AAKAA)_2$Y with three different C-terminal groups: amide, free acid and ester. All fragment ions in the spectra contain two Cu^+. Both copper ions are bound to the same site or in close proximity. For peptide ions with an amide or ester C-terminus, the abundance ratio of *b*- to *y*-type ions is approximately 45% to 55%, whereas peptide ions with a free acid C-terminus yield very different ratio of *b*- to *y*-type ions, *viz.* 5% to 95%.

A plausible way to describe the $[M + 2Cu – H]^+$ ions is in terms of individual Cu^+ ions attached to the €-amino group of Lys^3 and Lys^8 and the deprotonated C-terminus because it is unlikely that the Cu^+ ions are bound as a Cu_2^{2+} [71]. These ideas were explored using theoretical studies (at the DFT/B3LYP/TZBS level) on several model systems, *viz.* various structures of deprotonated Lys-Ala containing two Cu^+ ions $[M + 2Cu – H]^+$ (Figure 8a), the dinuclear Cu^+ complex of deprotonated Ala-Ala (AA, label A) and n-propylamine (PA, label B) $[M + 2Cu - H]^+$ (Figure 8b), and the $[M + 2Cu – H]^+$ ion of peptide KAAY (Figure 9). The lowest energy structure obtained for the Lys-Ala dinuclear complex has both Cu^+ ions interacting with the carboxylate group and the amide oxygen. The lowest energy structure obtained for the AA/PA-2Cu $[M + 2Cu - H]^+$ complex (Figure 8b) is similar to the Lys-Ala dinuclear complex in that both Cu^+ ions interact with the carboxylate group and an amide oxygen. The large binding energies (49.83 and 38.81 kcal/mol) observed in the AA/PA-2Cu $[M + 2Cu - H]^+$ complex suggest that the Cu ions can be better coordinated by the carboxylate and amide groups, and this information was further used to developed a series of candidate structures for the $[M + 2Cu – H]^+$ ions of peptide KAAY(Figure 9). The lowest energy structures (labeled A, B and C) are all quite similar, having the two Cu^+ ions interacting with the carboxylate group and backbone amide groups of Lys. Higher energy conformations, *i.e.,* Cu^+ ions located at the Tyr and the carboxylate group (structure F, 87.13 kcal/mol) and at the Lys and Tyr

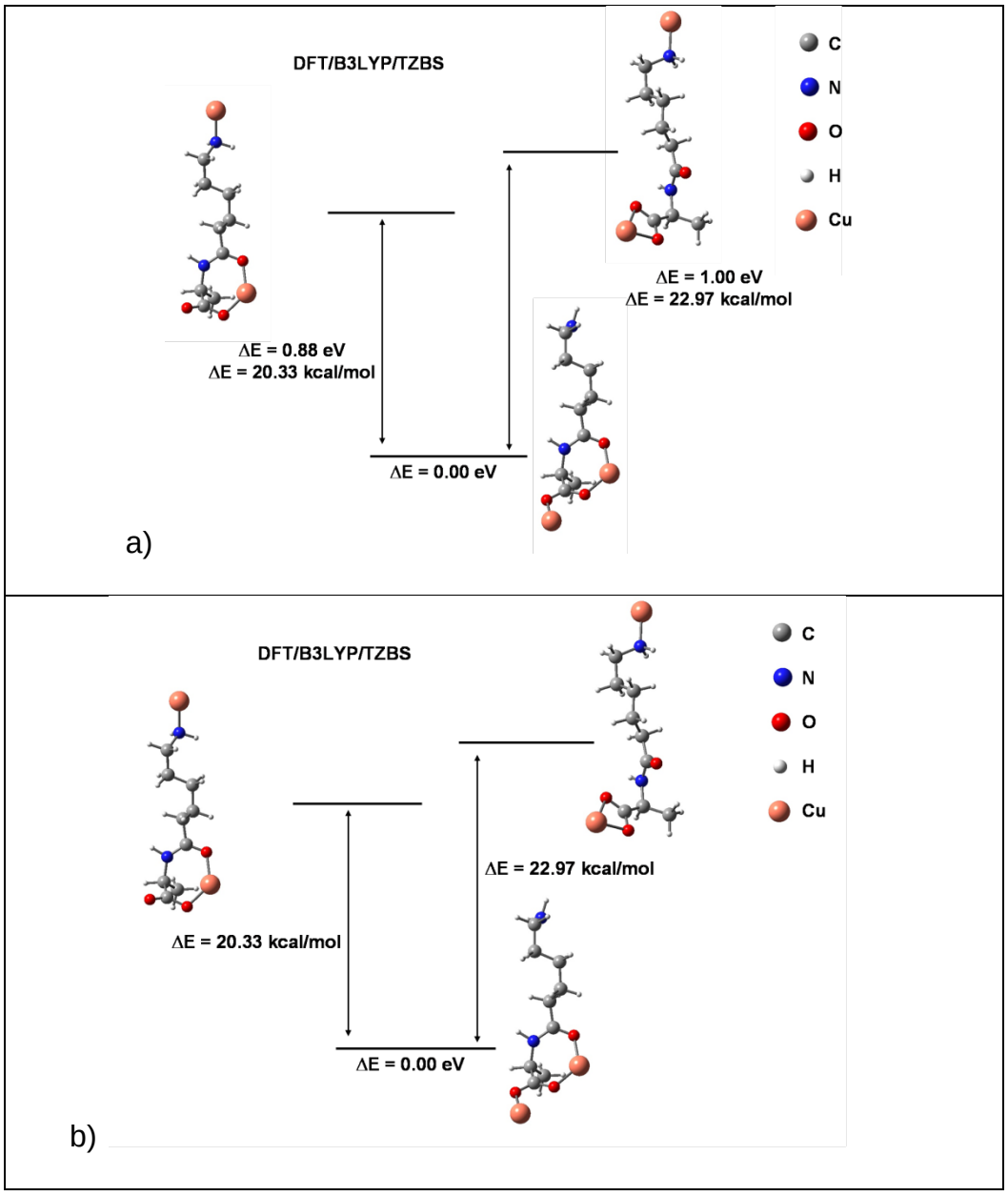

Figure 8. Model structures used to study the copper binding site and energy for: a) deprotonated Lys-Ala containing two Cu^+ ions $[M + 2Cu - H]^+$, and b) the dinuclear Cu^+ complex of deprotonated Ala-Ala (AA, label A) and n-propylamine (PA, label B) $[M + 2Cu - H]^+$. All calculations were performed at the DFT/B3LYP/TZBS level.

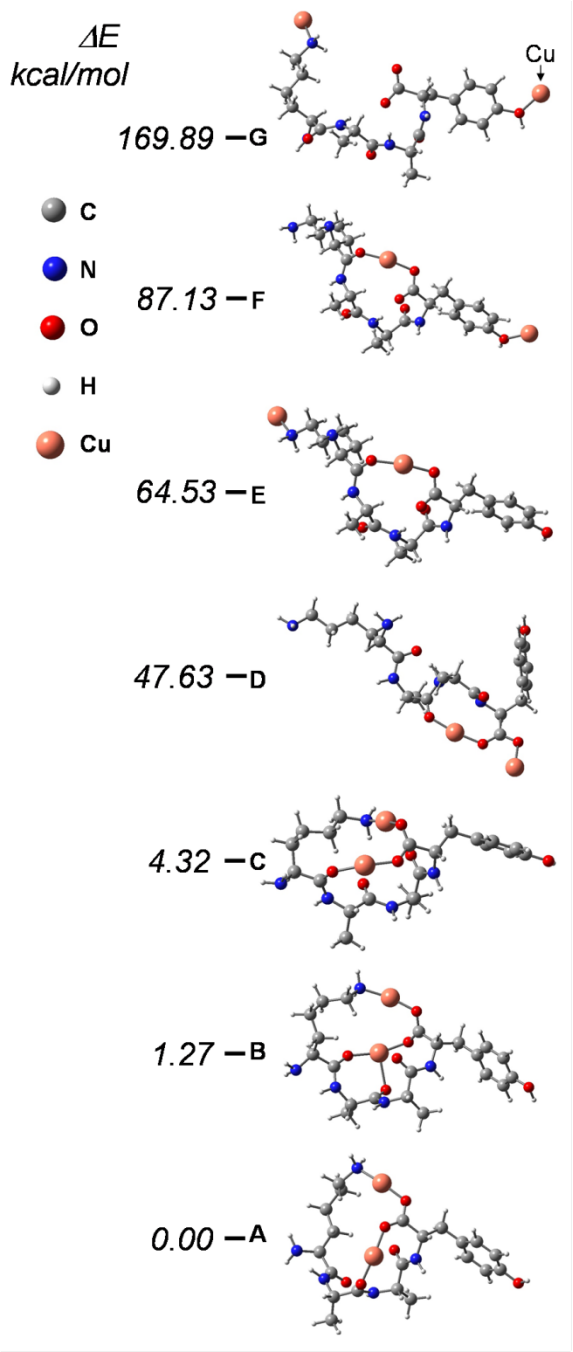

Figure 9. Candidate structures obtained at the DFT/B3LYP/TZBS level for the $[M + 2Cu – H]^+$ ion of the peptide motif KAAY.

(structure G, ~ 169.89 kcal/mol), are also shown for comparison in Figure 9. In the case of the high energy structure G, it should be pointed out that the loss of the desired conformation was avoided by terminating the optimization process after ten geometry optimization cycles. Using the model structures contained in Figures 8 and 9 the preference for forming y-type CID product ions which retain both Cu^+ ions can be rationalized. For example, the collisional activation of the Ac-$(AAKAA)_2$-Y $[M + 2Cu - H]^+$ ion weakens the interaction between the €-amino group of Lys^3 and subsequent backbone cleavage yields fragment ions with the charge carried by the C-terminus. The lowest energy C-terminal charge carrying ions are the y-type ions.

We also examined fragmentation reactions of $[M + Cu]^+$ and $[M + 2Cu - H]^+$ for histidine and arginine containing peptide ions (Table 2). The arginine containing peptides RPGFSPFR and RPPGFSPFR (bradykinin) contain abundant *b*-type ions which we interpret as evidence for binding preferences to the N-terminal arginine (Figure 10). Note also that this trend is observed for both $[M + Cu]^+$ and $[M + 2Cu - H]^+$ ions. The peptides Ac-$(AAKAA)_nY$-NH_2 (n = 3, 4) yield fragment ions that suggest the Cu^+ ion is bound to Lys^3 and Lys^{13} (n = 3) (Figure 11) and Lys^3 and Lys^{18} (n = 4) (Figure 12), *i.e.,* the N- and C-terminal residues, thus it appears that the Cu^+ ions preferentially bind to the lysine near the termini. The ratio of *b*- to *y*-type ions of $[M + Cu]^+$ is approximately 70% to 30%, which suggests that lysine residues near the N-terminus has a higher Cu^+ affinity than lysine residues that are located near

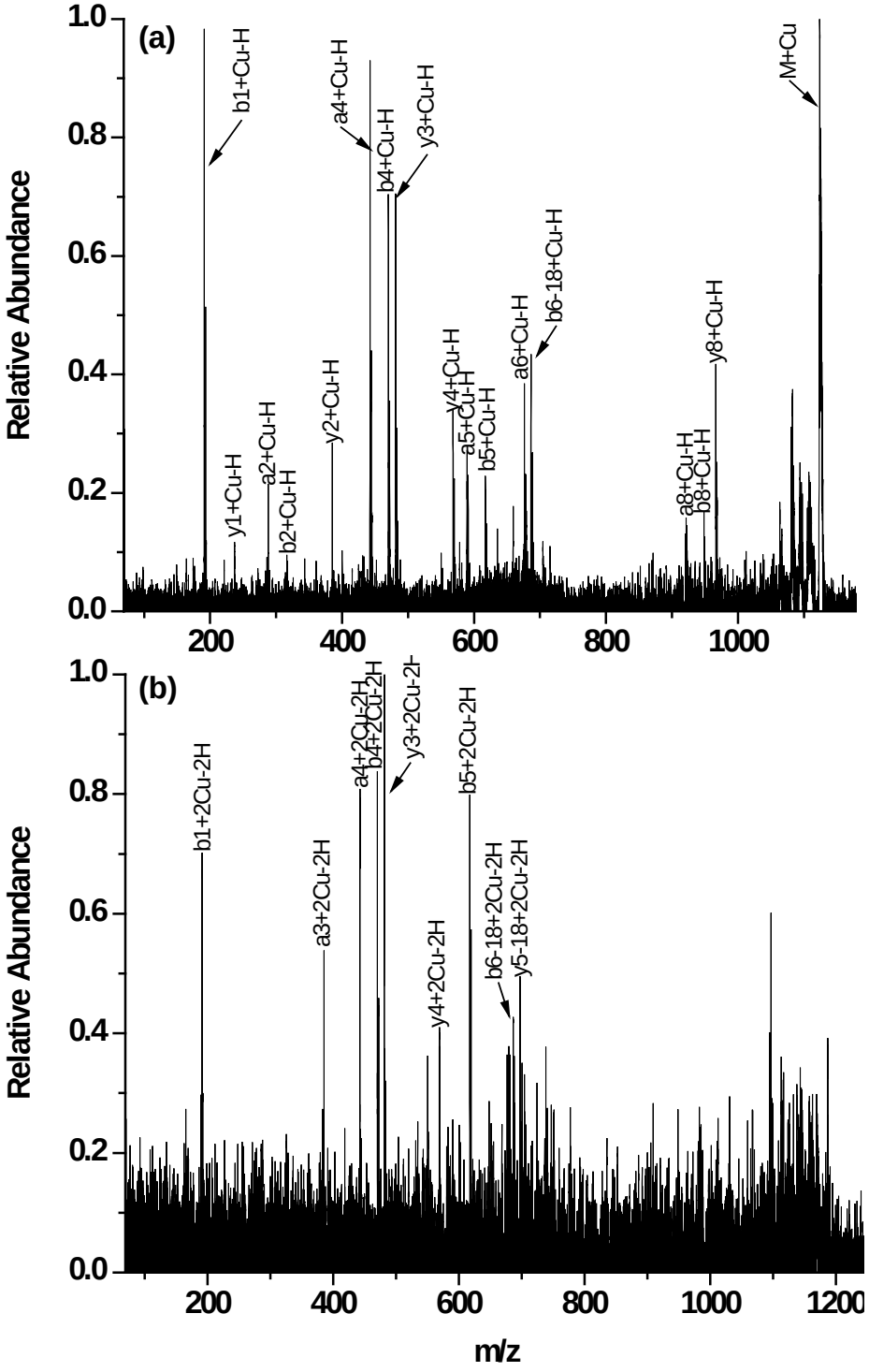

Figure 10. Fragment ion spectra of the (a) $[M + Cu]^+$ and (b) $[M + 2Cu – H]^+$ ions for bradykinin (RPPGFSPFR).

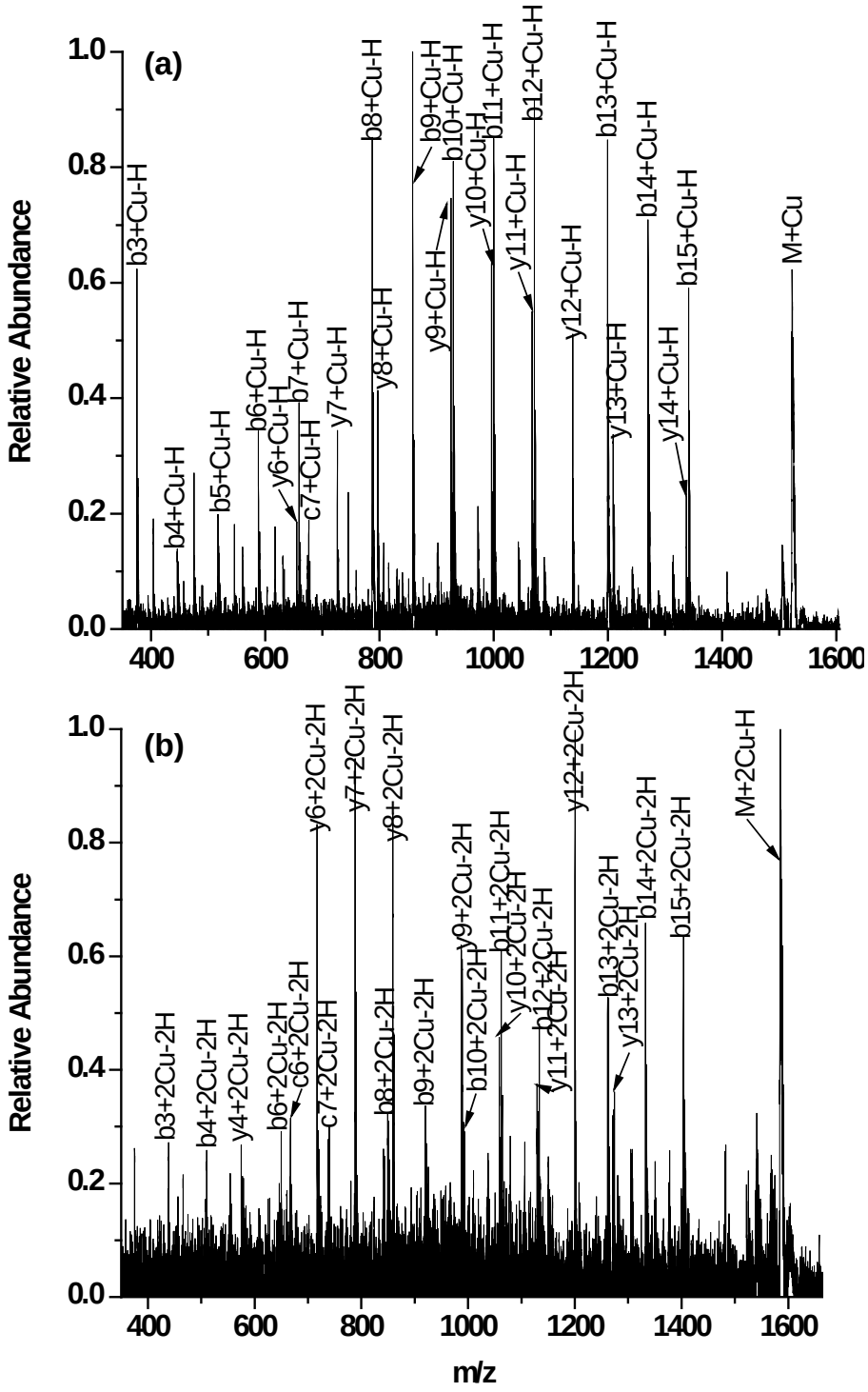

Figure 11. Fragment ion spectra of the (a) $[M + Cu]^+$ and (b) $[M + 2Cu – H]^+$ ions for the peptide Ac-AAKAAAAKAAAAKAAY-NH_2.

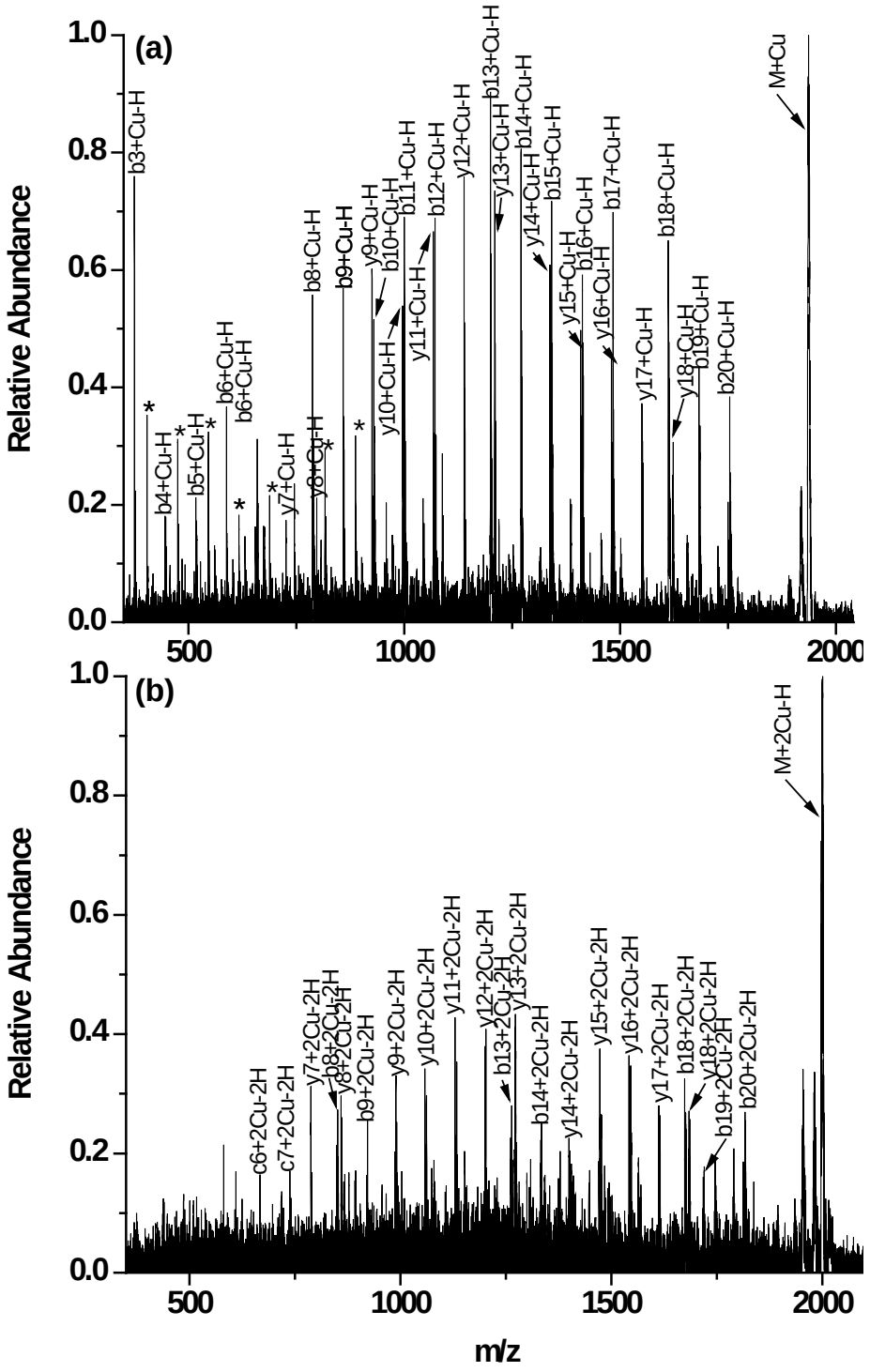

Figure 12. Fragment ion spectra of the (a) $[M + Cu]^+$ and (b) $[M + 2Cu – H]^+$ ions for the peptide Ac-AAKAAAAKAAAAKAAAAKAAY-NH_2.

the C-terminus. We also found that the competitive binding of Cu^+ to basic residues close to N-terminus versus C-terminus depends on the amino acid. For example, for a multiple histidine containing peptide such as Ac-WGGHDGPHAPGDH-NH_2 (Figures 13, 14, 15), we do not observe signature fragment ions for $[M + Cu]^+$ and $[M + 2Cu - H]^+$ in which Cu^+ ions bind at His^4 (Figure 13)). Thus, the most favorable binding sites for Cu^+ ions are His^8 and His^{13} probably because of the peptide secondary structure, *i.e.*, His^4 may be sterically hindered by other amino acid residues, thereby reducing the Cu^+ ion affinity of His^4. Residues such as tryptophan and aspartic acid may also play roles in copper binding. For example, we have found that acidic groups such as oxidized cysteine strongly influence Cu^+ ion binding. Specifically, for the peptide laminin (CDPGYIGSR), we found that the oxidized cysteine (via sulfonic acid) will partially shift the Cu^+ binding from the arginine to the C-terminal cysteine, owing to the bidentate binding of Cu^+ by the acidic sulfonic acid, similar to that for the carboxylic acid group discussed above. We will discuss this issue in detail in Chapter III.

Conclusions

We have synthesized a novel copper matrix and demonstrated the utility of the copper matrix for studies of copper binding peptides. The yields of copper adducted peptides in the gas-phase are increased significantly using this copper matrix as compared with other methods previously used to generate peptide-Cu^+ ions. We investigated the fragmentation chemistry of

$[M + Cu]^+$ and $[M + 2Cu -H]^+$ of model peptides, and explored the influence of modifying the C-terminal group on the fragmentation pattern of the peptide-Cu^+ ions. We have also explored the influence of the amino acid on the copper binding site and the fragmentation pattern. This work provides a new approach towards investigating the binding of copper ions to peptides and this new method will likely help understand the interactions of copper ions with peptides and proteins in the gas-phase.

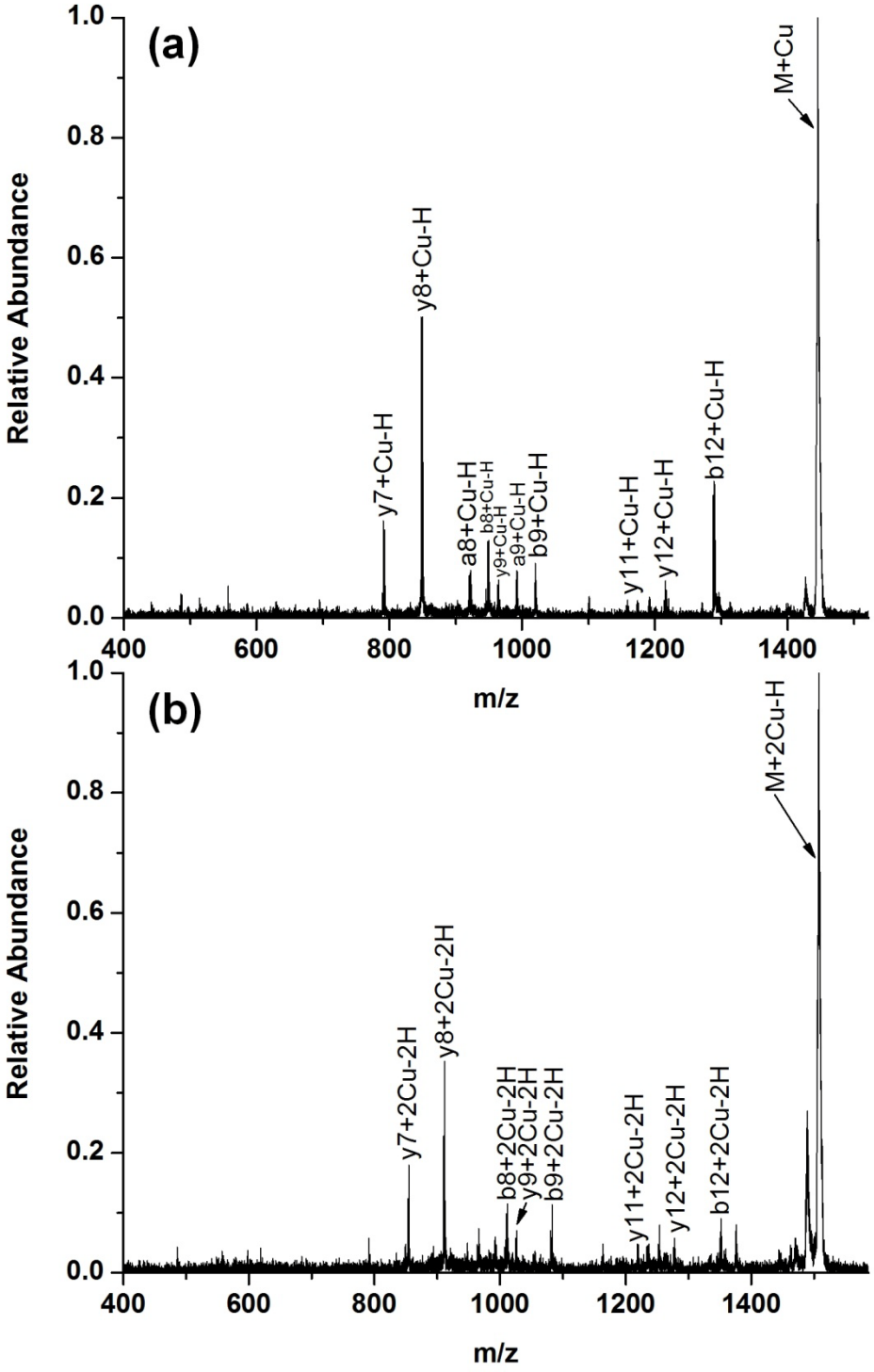

Figure 13. Fragment ion spectra of the (a) $[M + Cu]^+$ and (b) $[M + 2Cu – H]^+$ ions for the peptide Ac-WGGHDGPHAPGDH-NH_2.

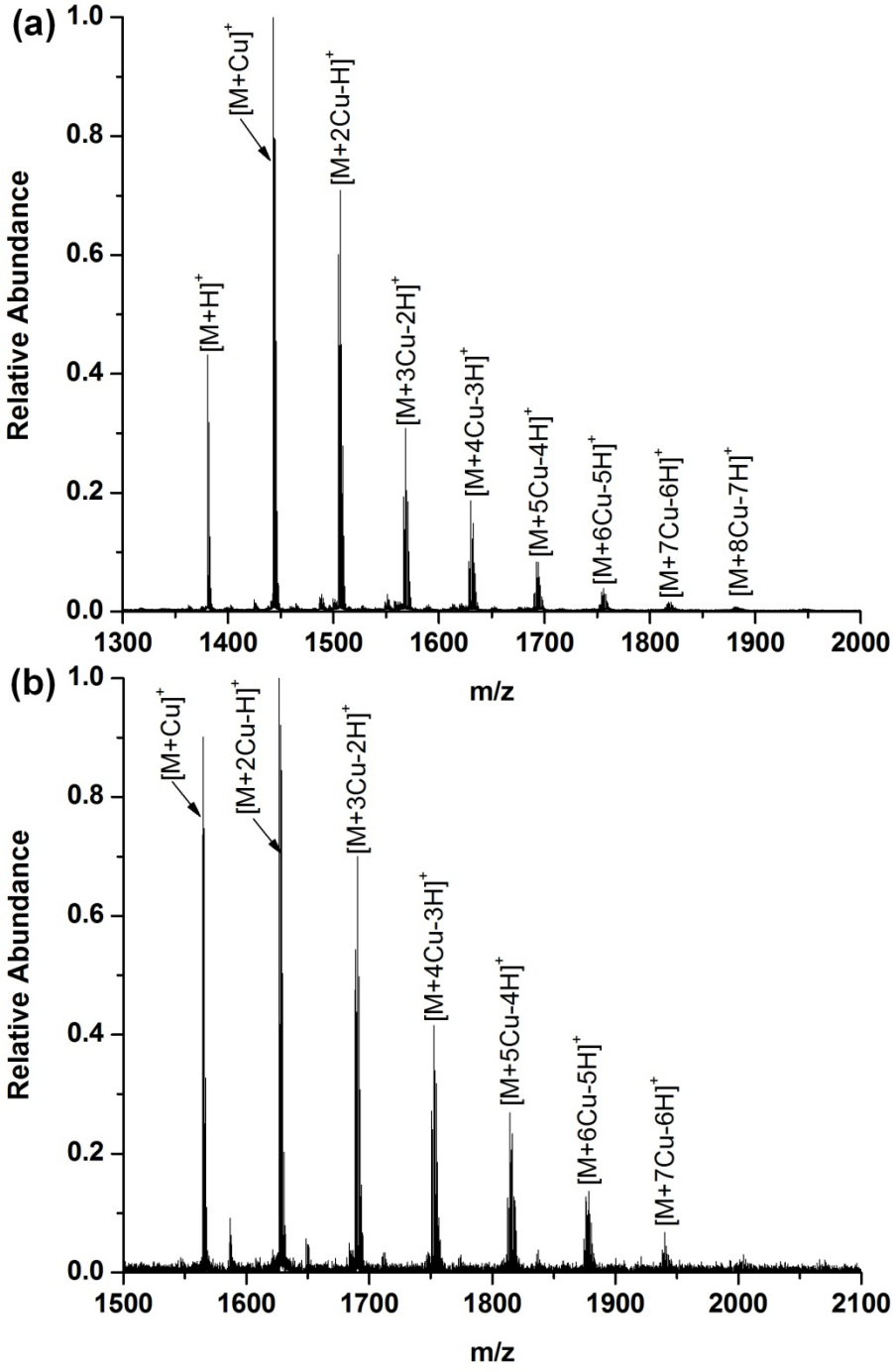

Figure 14. MALDI mass spectra of the peptides (a) Ac-WGGHDGPHAPGDH-NH_2 and (b) Ac-WGHGHGHGPGHGHGH-NH_2 using $(CHCA)_4Cu_2$ as a matrix.

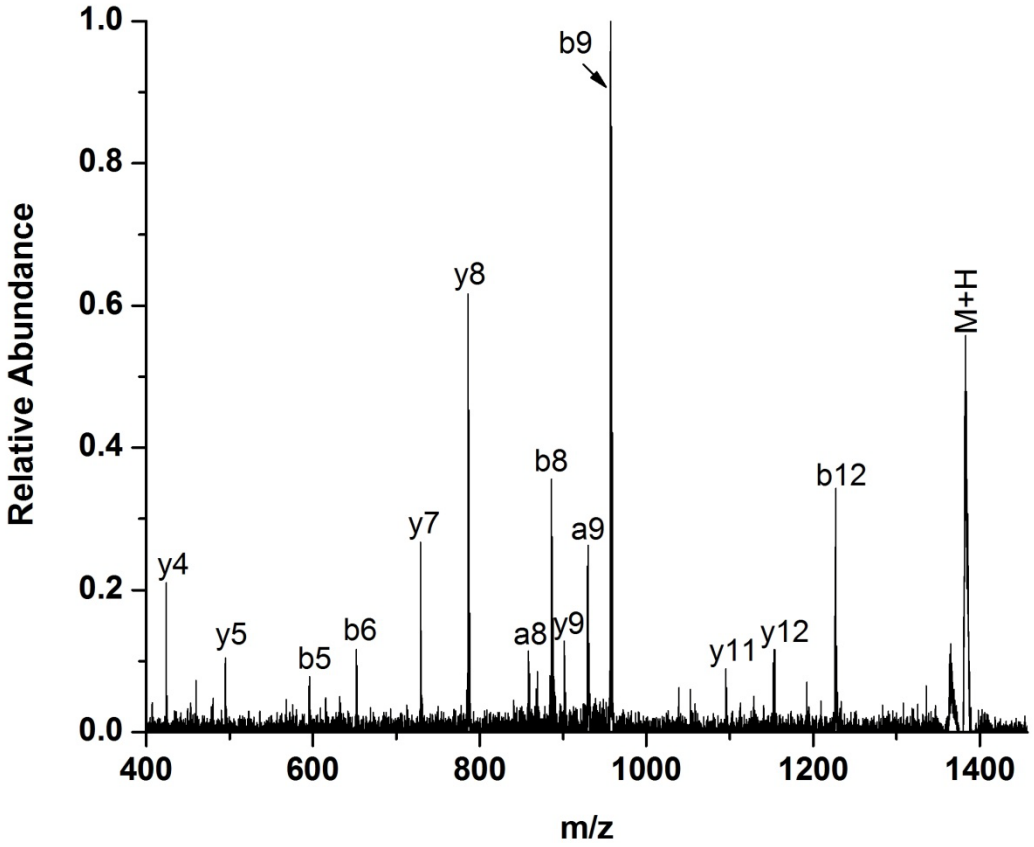

Figure 15. Fragment ion spectra of the $[M + H]^+$ ions for the peptide Ac-WGGHDGPHAPGDH-NH_2.

CHAPTER III

AMINO ACIDS INFLUENCE ON COPPER BINDING: CYSTEINE VERSUS ARGININE*

Introduction

MALDI mass spectrometry has been used widely to investigate the copper binding affinities to peptides in gas phase [36,50,59,72]. Results from these studies indicate that Cu^+ ions preferentially bind to electron rich systems (*i.e.* N-terminal amino group, the side-chain of lysine, histidine and arginine). Bluhm and Wesdemiotis reported the relative copper binding affinities for amino acids, suggesting that arginine guanidine is the most favorable binding site of Cu^+ for gas-phase peptides [42,50]. In last chapter, We reported the synthesis of a 'paddle-wheel' dinuclear copper matrix that afforded new capabilities for studies of both mono-metal and multi-metal containing peptide complexes [60]. These studies clearly illustrated that the C-terminal carboxyl group is an important Cu^+ ligand especially for multi-copper peptide ions such as $[M + 2Cu - H]^+$, whereas the C-terminal amide or the methyl ester group has less influence on the Cu^+ coordination. The

---

* Reproduced with permission from Wu, Z.; Fernandez-Lima, F.A.; Russell, D.H. Amino Acid Influence on Copper Binding to Peptides: Cysteine versus Arginine. *J. Am. Soc. Mass. Spectrom*. **2010**, 21, 522-533. Copyright [2010] by Elsevier.

difference in the binding sites for the mono-metal and di-metal species arises as a result of deprotonation of the acidic C-terminal carboxyl, and as a consequence, the Cu^+ ions are charge-solvated by the resulting carboxylate, the lysine €-amino group and the backbone amide groups [60].

In biological systems, cysteine is an important ligand in terms of the functions of copper proteins [73-76], and 35% of the copper (Cu^+, Cu^{2+}) ligands are cysteine residues [77-79]. For example, copper-zinc superoxide dismutase (Cu/Zn SOD), a copper containing protein which catalyzes the conversion of superoxide anion (O_2^-) into O_2 and H_2O_2, protects cells against oxidative stress [80]. It has been suggested that cysteine (position 111) in Cu/Zn SOD is a potential copper ligand which is responsible for the function of Cu/Zn SOD [76]. Cys^{111} is also a primary target for oxidative modification and the so-called “copper hypothesis” suggests that copper bound to or released by mutant SOD generates free radicals that cause oxidative damage to motor neurons [75]. These studies suggest that understanding how copper ions (Cu^+, Cu^{2+}) interact with cysteine residues is essential to understanding the biological functions of copper proteins.

In this chapter, we investigate the fragmentation chemistry of $[M + xCu - (x-1)H]^+$ (x = 1,2) ions in an effort to determine the influence of the cysteine residue on the Cu^+ binding, specifically competition for Cu^+ between cysteine and arginine. Theoretical calculations are also used to generate the candidate structures of the peptide-metal ion complex, which provide

theoretical evidences to support our experimental observations. In related work, Vachet and coworkers compared the effects of ligand donor group on dissociation of Cu(II) complexes, and their results suggest that Cu^{2+} ions prefer to remain coordinated to thio group rather than other functional groups such as amino and imidazole [81,82]. Kass and coworkers utilized H/D exchange experiments and high level calculations to compare the gas-phase acidities of the cysteine thiol group and carboxyl group [83]. They reported that the side-chain thiol in cysteine is more acidic than the carboxyl group in gas phase, and deprotonated cysteine is thus predicted to be a thiolate ion [83]. If this is the case, the deprotonation of the thiol group would be highly competitive with that at the carboxyl group. For peptides containing both cysteine and arginine residues, it appears likely that the thiolate group could function as an important Cu^{+} ion ligand. This study focuses on the competitive binding of Cu^{+} ions to peptides that contain both cysteine and arginine.

Experimental

Copper oxide (CuO) and α-cyano-4-hydroxycinnamic acid (CHCA) were obtained from Sigma (St. Louis, MO). CHCA was recrystallized in ethanol prior to use. The α-cyano-4-hydroxycinnamic acid (CHCA) copper salt $(CHCA)_4Cu_2$) was synthesized as described in Chapter II. The organic solvents (CH_3OH, CH_3CN) used for mass spectrometry were HPLC grade, and the water is in high purity (18MΩ; Barnstead International, Dubuque, IA).

Laminin (925-933) (CDPGYIGSR) and Cys-Kemptide (CLRRASLG) were purchased from Sigma (St. Louis, MO) and used without further purification. Cysteine residues were alkylated [84] or oxidized [85] following standard protocols.

Cysteine Oxidation with Performic Acid

Fresh performic acid is prepared by adding 1 ml of 30% hydrogen peroxide to 9 ml formic acid. Mix and incubate for 30 min at 60°C. Chill performic acid in an ice bath to 0°C. To a chilled tube containing 10 µg lyophilized peptides, add 20 µl chilled performic acid to thoroughly dissolve the peptide. Incubate 1 hr on ice water. Lyophilize the peptide solution via Speedvac evaporation [85].

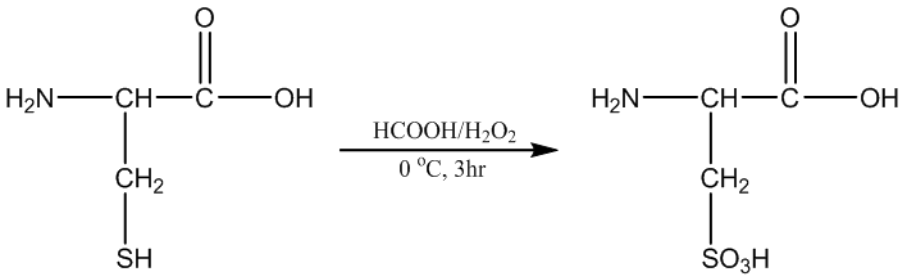

Cysteine Alkylation with Iodoacetamide

2 µl of iodoacetamide stock solution (100 mM in water) was added to 10 µl of the peptide solution (1 mg/ml in 50 mM ammonium bicarbonate). The resulting mixture was incubated in the dark for 1 h at room temperature [84].

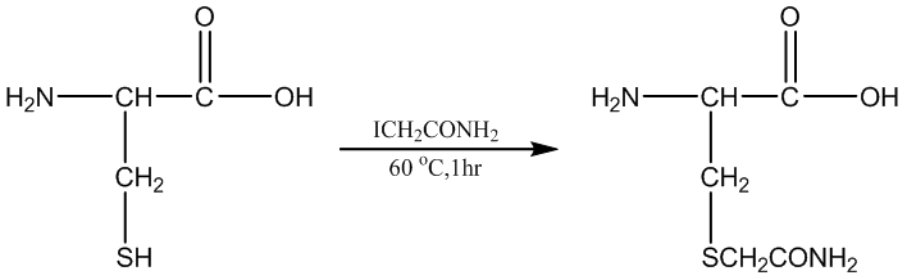

Mass Spectrometry

The MALDI experiments described herein were performed on a tandem time-of-flight mass spectrometer (4700 Proteomics Analyzer, Applied Biosystems, Framingham, MA). Tandem mass experiments were performed using a collision energy setting of 1 kV and air as the collision gas. $(CHCA)_4Cu_2$ (10 mg/ml in 60% acetonitrile containing 0.1% trifluoacetic acid) was used as the MALDI matrix to generate [peptide + xCu - (x-1)H]$^+$ ions. Peptide samples (0.5 nmol) were mixed with matrix solution at a ratio of 1:3 (v:v) and a 1µl aliquot was deposited to a stainless steel target. Samples were dried in air at room temperature.

Theoretical Calculations

Theoretical calculations using Density Functional Theory (DFT) have been performed to gain a better understanding of the stability of the peptide-Cu ion structures. The B3LYP functional was used [64-66] using the LACV3P basis set (DFT/B3LYP/LACV3P**). The LACV3P basis set is a triple-zeta contraction of the LACVP basis set [86] developed and tested at Schrödinger, Inc [87]. In particular, Cu ions were treated using effective core potentials, while all the other atoms were treated with the 6-311G** basis set.

No symmetry restriction of any kind was imposed in the process of geometry optimization. A vibration frequency analysis was performed for all the optimized structures at the level of calculation employed. For the reported structures, all frequencies are observed to be real, indicating that they correspond to the true minima in the respective potential energy hypersurfaces. All calculations were performed with the Jaguar 6.0 software using the pseudospectral method to minimize the computational time [87].

Candidate structures were constructed to study the copper ion(s) attachment to a small, model peptide sequence CLR. Initial calculations of copper ion(s) interacting with the oxidized and non-oxidized form of the Cys side chain were performed to minimize the computational time. As a result, the backbone orientations and docking sites of the copper ion(s) for both forms of the Cys side chain were obtained. Analogous, backbone orientations and docking sites for the Arg side chain were explored. These configurations were used as starting geometries for the peptide sequence CLR. Copper attachments involving the C-terminus were explored in a previous paper [60] and were not considered here. Candidate structures and geometry files of the peptide sequence CLR for the oxidized and non-oxidized form of the Cys side chain are included in the Supplemental Information.

Results and Discussion

Previous work has shown that Cu^{+} ions preferentially bind to electron

rich systems in gas phase (*i.e.,* N-terminal amino group, the side-chain of lysine, histidine and arginine, and the deprotonated C-terminal carboxyl group) [50,60]. Kass and coworkers reported that in gas-phase the cysteine side-chain thiol is more acidic than the carboxyl group, and deprotonated cysteine is thus predicted to be a thiolate ion, making it a potential electron rich group [83]. Therefore, it would be interesting to see how the Cu^+ ions competitively bind to the cysteine thiol versus other electron rich system such as the guanidino group of arginine. The potential for interactions of cysteine thiol with Cu^+ ions were first examined by using theoretical calculations (at the DFT/B3LYP/LACV3P** level) on a small, model peptide sequenced CLR. The C-terminus was blocked by addition of an aldehyde group to eliminate the possible interaction of a carboxyl group with Cu^+ ions, which was described previously [60]. For a comparison, the interactions of Cu^+ ions with cysteine thiol versus cysteine sulfonic acid were also examined. Figure 16 contains the lowest energy structures obtained at the DFT/B3LYP/LACV3P** level for the $[M + Cu]^+$ and $[M + 2Cu - H]^+$ ions of CLR_{CHO} and $C_{ox}LR_{CHO}$ ('$_{CHO}$' denotes an aldehyde C-terminus). These simulated structures reveal that the guanidino group of arginine is an important ligand for Cu^+ ions; however, the cysteine side chain also participates in the coordination of Cu^+ ions. That is, a plausible configuration for $[M + Cu]^+$ ions is that the proton from the initial thiol or the sulfonic acid group is transferred to the basic guanidine, resulting in a protonated arginine

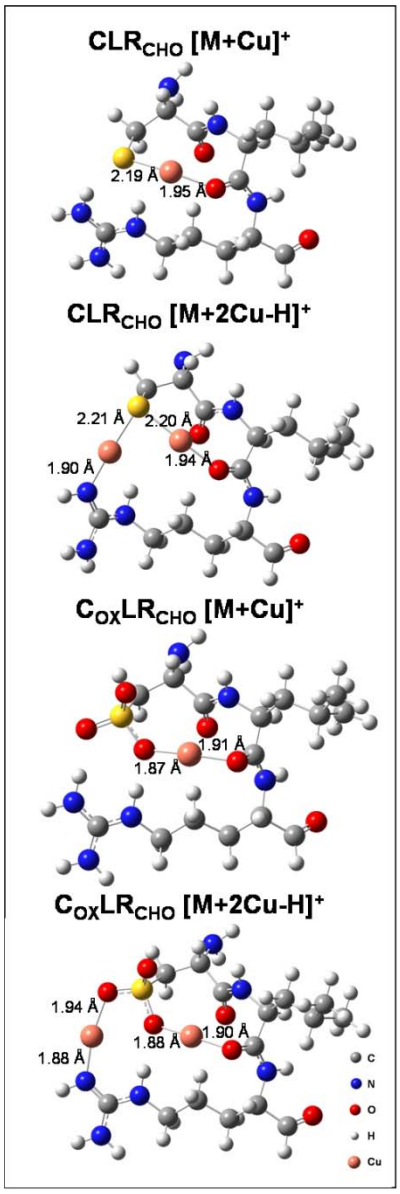

Figure 16. Lowest energy candidate structures obtained at the DFT/B3LYP/LACV3P** level for the $[M + Cu]^+$ and $[M + 2Cu - H]^+$ ions of peptides CLR_{CHO} and $C_{ox}LR_{CHO}$. The'$_{CHO}$' denotes an aldehyde C-terminus. Bonds smaller than 2.7 Å involving Cu ions are denoted. For comparison purposes, other candidate structures are contained in the figures on page 64 - 67.

side chain, and the Cu^+ ion is charge-solvated by the resulting thiolate or sulfonate group and the backbone carbonyls (see Figure 16). In addition, deprotonation of the thiol or sulfonic acid is energetically favorable for $[M + 2Cu - H]^+$ ions, and as a consequence, the interaction of the resulting thiolate or sulfonate group with Cu^+ ions contributes to the gas-phase structure of the $[M + 2Cu - H]^+$ ions. These results raise several questions regarding the binding of Cu^+ ions to thiol/sulfonic acid versus guanidine in larger peptide ions? How does the competitive Cu^+ binding affect the fragmentation of the peptides?

To address these questions we examined the fragmentation reactions of the $[M + Cu]^+$ and $[M + 2Cu – H]^+$ ions of cys-kemptide (CLRRASLG). We also examined the modified cys-kemptide where the N-terminal cysteine was modified by iodoacetamide [84] or performic acid [85], denoted as C_{alkyl} or $C_{ox,}$ respectively. Figure 17 contains the fragment ion spectra of the $[M + Cu]^+$ ions for peptides XLRRASLG (X = C, C_{alkyl} and C_{ox}). In the case of CLRRASLG, the fragment ion spectrum of $[M + Cu]^+$ ions contains both C- and N-terminal fragment ions, including $[a_i + Cu - H]^+$, $[b_i + Cu – H]^+$ and $[y_i + Cu - H]^+$ ions. The relative abundance ratios of C- and N-terminal fragment ions are 52% and 48%, respectively. We interpret this observation as evidence that Cu^+ can bind to either Arg^3 or Arg^4, and there is no strong preference for binding of Cu^+ to the N-terminal cysteine. Scheme 1A(i) contains a proposed configuration showing that Cu^+ interacts with the

guanidine group(s) of arginine(s), the backbone carbonyls and the N-terminal amine group. Note, however, that a small peak corresponding to the y_5 ion without Cu^+ is observed. An explanation for the formation of the y_i ions, which is consistent with the theoretical results for CLR, is that Cu^+ promotes intramolecular proton transfer from the cysteine thiol to the arginine guanidine and the arginine side chain is protonated (Scheme 1A(ii). Note that the protonated guanidine group is projected away from the Cu^+ charge solvating center because this group is not a good Cu^+ ligand, *i.e.*, the group acts as an isolated charge site). This explanation is further supported by the absence of y_i fragment ions for the peptide C_{alkyl}LRRASLG (Figure 17b). That is, the $–CH_2CONH_2$ group blocks the pathway for the intramolecular proton transfer thus all fragment ions are formed with Cu^+ attached (Scheme 1B(i)). Interestingly, when the cysteine thiol is oxidized to sulfonic acid, the abundance of the y_5 is increased (Figure 17C). Thus it appears that oxidation of the cysteine increases the extent of the intramolecular proton transfer, generating larger population of the conformation shown in Scheme 1C(ii) than that shown in Scheme 1A(ii).

We also examined the fragmentation chemistry of the $[M + 2Cu - H]^+$ ions for XLRRASLG (X = C, C_{alkyl} and C_{ox}). Fragment ion spectra of the $[M + 2Cu - H]^+$ ions are very different from that of the $[M + Cu]^+$ ions, and the cysteine modifications significantly affect the fragmentation results. For example, we observe predominantly $[a_3 + 2Cu - 2H]^+$ and $[b_3 + 2Cu - 2H]^+$

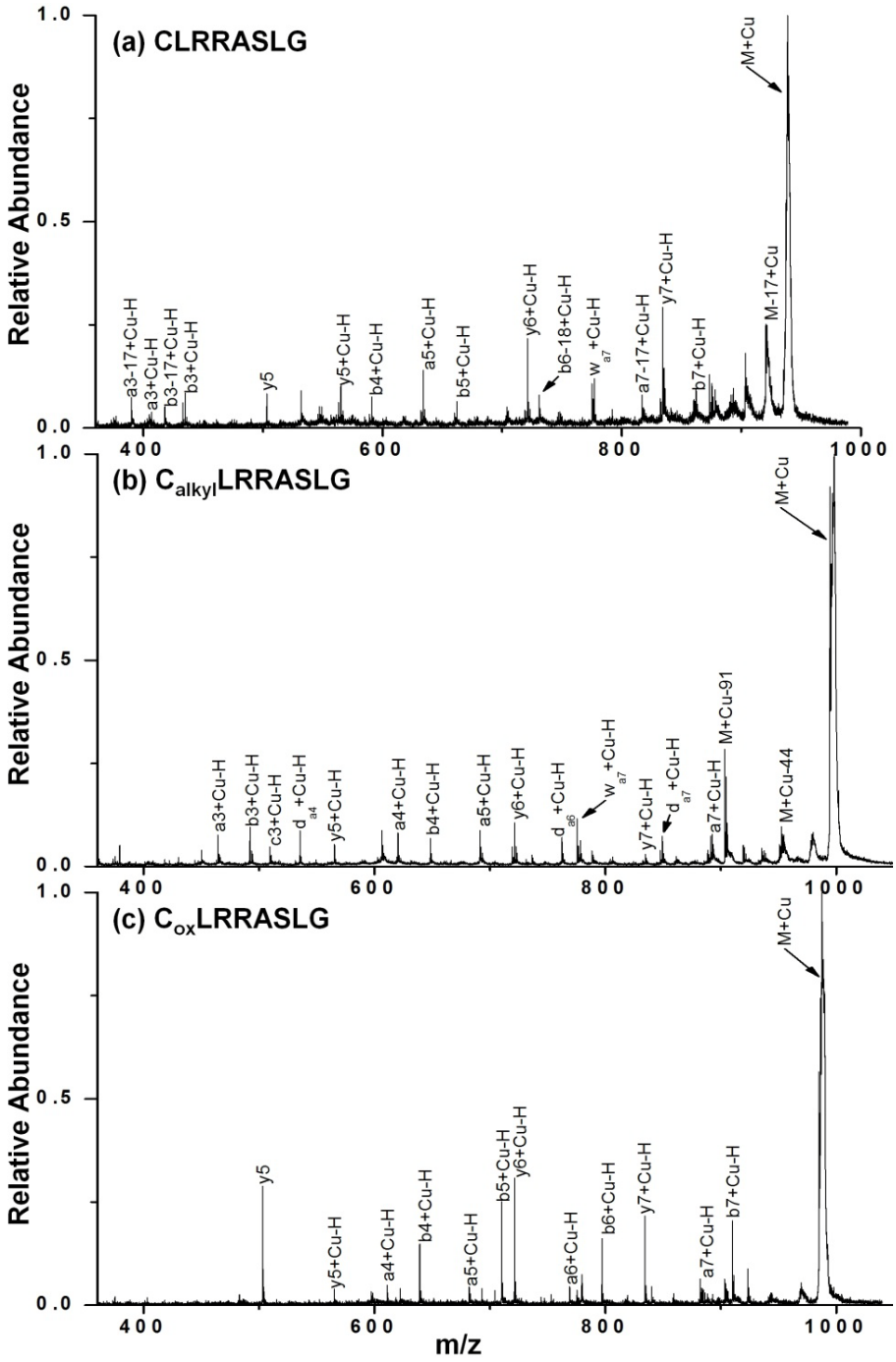

Figure 17. Fragment ion spectra of the $[M + Cu]^+$ ions of (a) CLRRASLG, (b) C_{alkyl}LRRASLG, (c) C_{ox}LRRASLG. The 91 mass shift (*i.e.,* $[M + Cu - 91]^+$ in b) is due to the loss of the alkylated cysteine side chain ($SHCH_2CONH_2$).

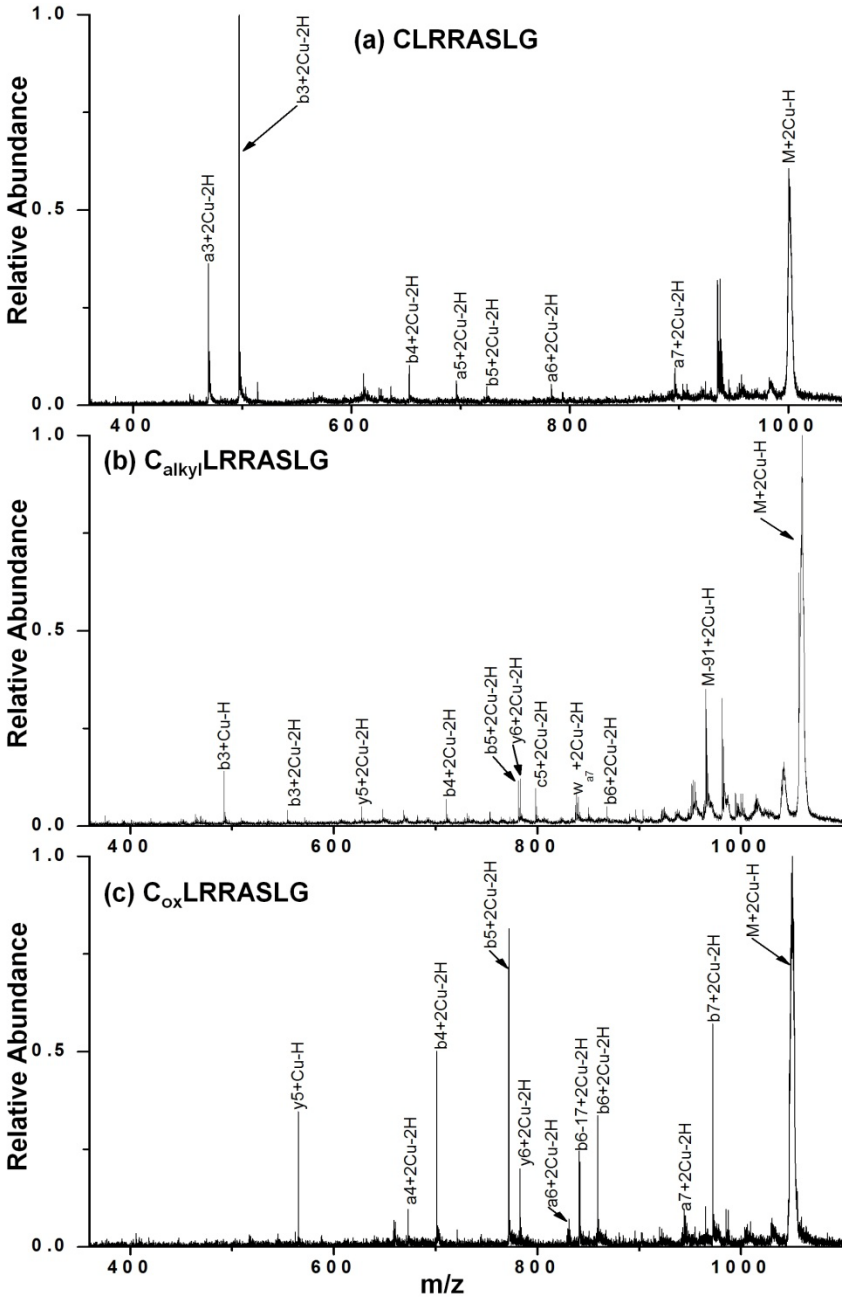

Figure 18. Fragment ion spectra of the $[M + 2Cu - H]^+$ ions of (a) CLRRASLG, (b) C_{alkyl}LRRASLG, (c) C_{ox}LRRASLG. The 91 mass shift (*i.e.* $[M – 91 + 2Cu – H]^+$ in b) is due to the loss of the alkylated cysteine side chain ($SHCH_2CONH_2$).

fragment ions for the $[M + 2Cu - H]^+$ ions of CLRRASLG (Figure 18a); however, very different fragment ions are observed if the cysteine is alkylated (Figure 18b). A plausible explanation for the high abundance of the N-terminal fragment ions is that the deprotonation of the cysteine side chain occurs rather than the C-terminal carboxyl group, owing to its higher gas-phase acidity over that of the carboxyl [83]. Consequence, the two Cu^+ ions are strongly coordinated to N-terminal CLR residues. That is, the two Cu^+ ions are charge-solvated by the resulting thiolate, the arginine guanidine(s), the backbone carbonyl(s) and the N-terminal amine (Scheme 2A(i)). This interpretation is further evidenced by the fragmentation reactions of the peptide C_{alkyl}LRRASLG. That is, no significant preference of the N-terminal fragments for the $[M + 2Cu - H]^+$ is observed, considering that the abundace ratio of N-/C- fragment ions is ~58/42 for C_{alkyl}LRRASLG (Figure 18b) versus ~100/0 for CLRRASLG (Figure 18a). These results are in good agreement with our theoretical calculations, where deprotonation of the cysteine thiol is energetically favorable for $[M + 2Cu - H]^+$ ions, and blocking the thiol results in a different deprotonation site along the peptide backbone, which significantly changes the Cu^+ coordination environment for $[M + 2Cu - H]^+$ ions (Scheme 2B(i)). Oxidizing the cysteine also influences the Cu^+ coordination. For example, the fragment ion spectrum of the C_{ox}LRRASLG $[M + 2Cu - H]^+$ ion contains predominantly $[b_i + 2Cu- 2H]^+$ (i >=4) fragment ions; note that the $[b_3 + 2Cu – 2H]^+$ fragment ions are absent. Thus, it

appears that the position of arginine also plays a role in the Cu^+ coordination, *i.e.*, Cu^+ ions prefer to bind to Arg^4 rather than Arg^3 for C_{ox}LRRASLG. Two additional observations are consistent with our proposed Cu^+ binding preference of Arg^4: (i) the smallest N-terminal fragment ions of $[M + 2Cu - H]^+$ ions for C_{ox}LRRASLG are $[b_4 + 2Cu - 2H]^+$ and $[a_4 + 2Cu - 2H]^+$ (Figure 18c), indicating that at least one Cu^+ ion is attached to either Arg^3 or Arg^4; and (ii) the peak at m/z 565.1, which is assigned as $[y_5 + Cu - H]^+$, suggests that Arg^4 is the preferred Cu^+ binding site otherwise we would expect $[y_6 + Cu - H]^+$ to also be observed (Scheme 2C(ii)).

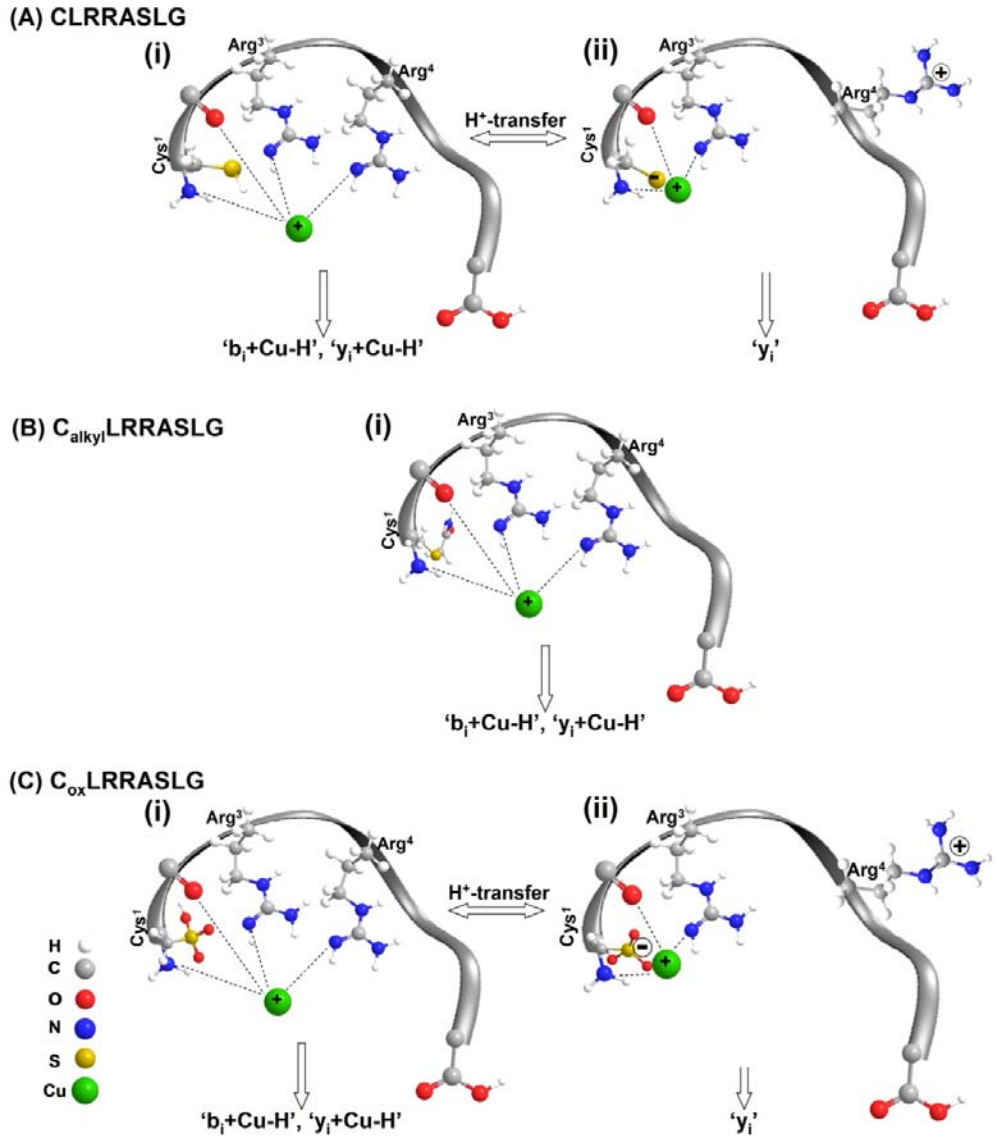
(A) CLRRASLG
(i)
Arg3
Arg4
Cys1
H+-transfer
(ii)
Arg3
Arg4
Cys1
'bi+Cu-H', 'yi+Cu-H'
'yi'
(B) CalkylLRRASLG
(i)
Arg3
Arg4
Cys1
'bi+Cu-H', 'yi+Cu-H'
(C) CoxLRRASLG
(i)
Arg3
Arg4
Cys1
H+-transfer
(ii)
Arg3
Arg4
Cys1
H
C
O
N
S
Cu
'bi+Cu-H', 'yi+Cu-H'
'yi'

Scheme 1

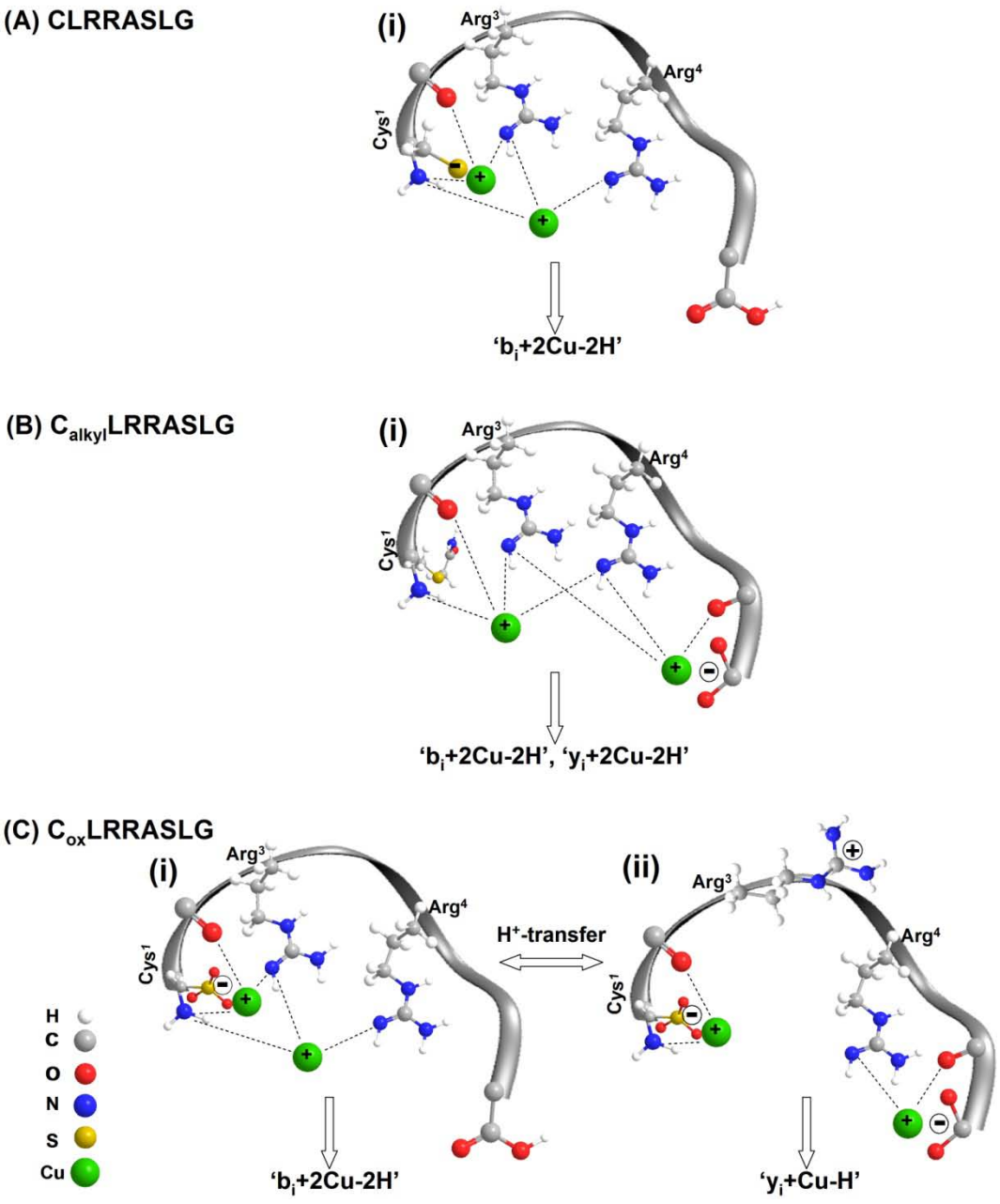
(A) CLRRASLG
(i)
Arg3
Arg4
Cys1
'bi+2Cu-2H'
(B) CalkylLRRASLG
(i)
Arg3
Arg4
Cys1
'bi+2Cu-2H', 'yi+2Cu-2H'
(C) CoxLRRASLG
(i)
Arg3
Arg4
Cys1
'bi+2Cu-2H'
H+-transfer
(ii)
Arg3
Arg4
Cys1
'yi+Cu-H'
H
C
O
N
S
Cu

Scheme 2

For comparison we also examined the peptide Laminin (CDPGYIGSR) aimed at addressing how the Cu^+ ion interacts with cysteine versus arginine if the two side chains are located at the two termini. For example, is the intramolecular proton transfer process noted above the result of close proximity of the two groups? The $[M + Cu]^+$ ion of CDPGYIGSR yields exclusively C-terminal fragment ions (Figure 19a). The $[y_7 + Cu - H]^+$ ion is the most abundant, which indicates an enhanced backbone cleavage between the aspartic acid and proline residue with the Cu^+ remaining on the C-terminus. We interpret the preference for $[y_i + Cu - H]^+$ ions, esp. $[y_1 + Cu – H]^+$, as evidence that Cu^+ ion is bound to the arginine side chain (Scheme 3A(i)). Interestingly, we also observed a small peak corresponding to the y_7 ion that does not contain Cu^+; however, the y_7 peak is absent for $[M + Cu]^+$ ions of C_{alkyl}DPGYIGSR (Figure 19b); a result that suggests that the formation of y_7 ion for $[M + Cu]^+$ ions of CDPGYIGSR is also owing to an intramolecular proton transfer. That is, the proton from the thiol is transferred to the arginine guanidine, and Cu^+ is charge-solvated by the resulting thiolate group (Scheme 3A(ii)). More interestingly, however, when the cysteine thiol group is oxidized to sulfonic acid, the intramolecular proton transfer appears to occur to a larger extent. For example, in Figure 19c, we observe a significantly high abundance of y_i ions that do not contain Cu^+. The abundance ratio of the $[y_i + Cu - H]^+$ to y_i is approximately 70% to 30%. We interpret this result as evidence that the coordination structure of the [M +

$Cu]^+$ ions is dependent on the position of the cysteine and arginine, and oxidizing the cysteine residue favors coordinate Cu^+ ions (Scheme 3C(ii)).

We also investigated the fragmentation chemistry of the $[M + 2Cu - H]^+$ ions of CDPGYIGSR (Figure 20). Results from these experiments suggest that the fragmentation of $[M + 2Cu - H]^+$ ions is sensitive to the nature of the cysteine side chain, and different fragment ion spectra are observed when the cysteine side chain is modified (C_{alkyl} and C_{ox}). For example, the fragment ion spectrum of $[M + 2Cu - H]^+$ ions of CDPGYIGSR contains three types of fragment ions, *viz*. $[y_i + 2Cu - 2H]^+$, $[y_i + Cu - H]^+$ and y_i, and the relative abundance ratios of these ions are 42%, 48% and 10%, respectively (Table 3). We propose that $[y_i + 2Cu - 2H]^+$ and $[y_i + Cu - H]^+$ are formed from the coordination conformations such as 4A(i) and 4A(ii) shown in Scheme 4, respectively, note that the differences in these two conformations depend on where the deprotonation site is, *i.e*. cysteine thiol, or C-terminal carboxyl. We would expect that the conformation shown in 4A(iii) (Scheme 4) to yield predominantly y_i ions with no Cu^+ attached. That is, the two Cu^+ ions are charge-solvated by the cysteine thiolate and the carboxylate of the aspartic acid, respectively, and the arginine side chain is protonated via an intramolecular proton transfer. This assumption is supported by the fragment ion spectrum of C_{alkyl}DPGYIGSR. The fragment ion spectrum of the modified peptide C_{alkyl}DPGYIGSR contains only two types of fragment ions, *viz*. $[y_i + 2Cu - 2H]^+$ and $[y_i + Cu - H]^+$, and y_i ions are not observed. The absence of y_i

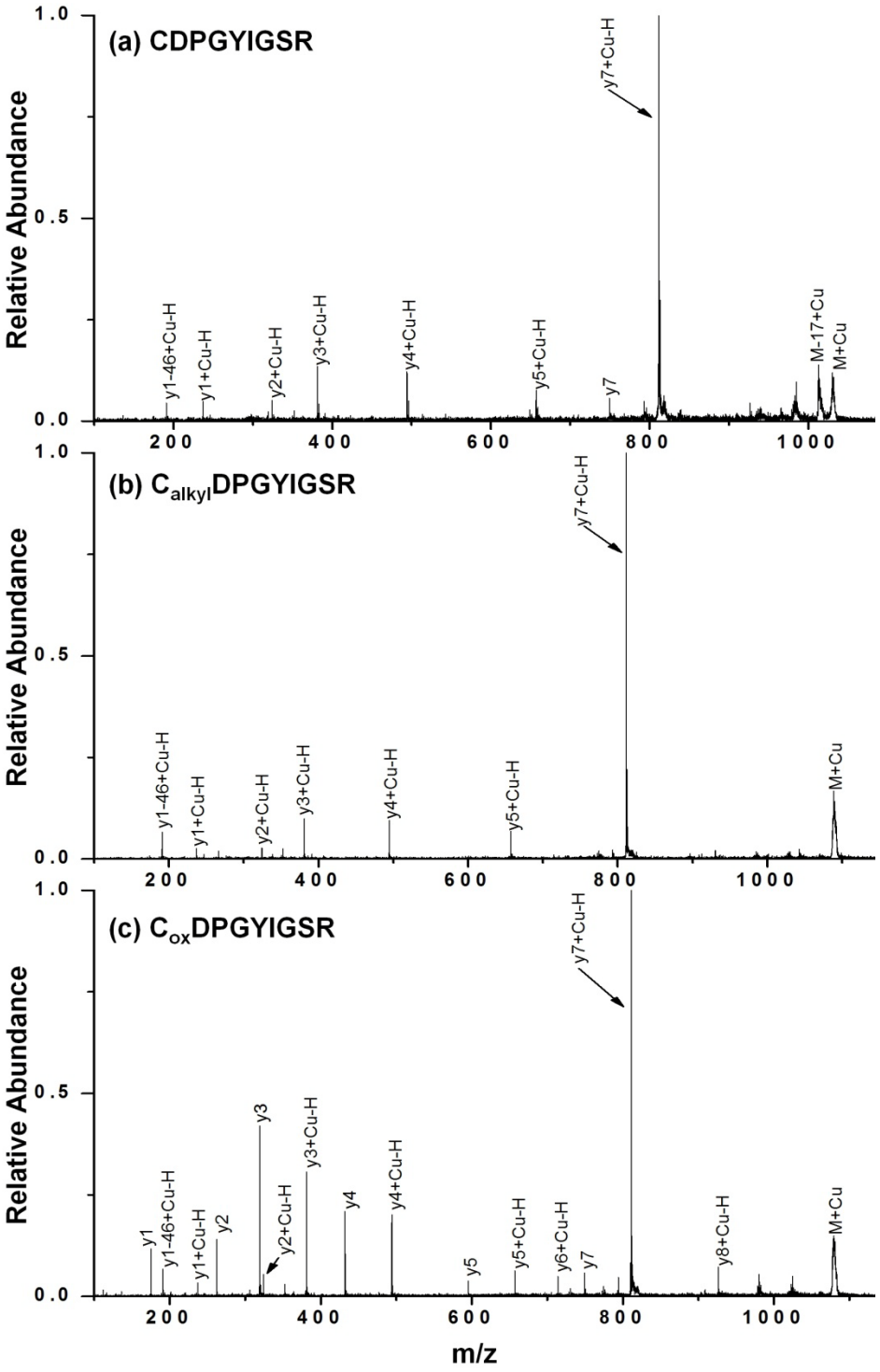

Figure 19. Fragment ion spectra of the $[M + Cu]^+$ ions of (a) CDPGYIGSR, (b) C_{alkyl}DPGYIGSR, (c) C_{ox}DPGYIGSR.

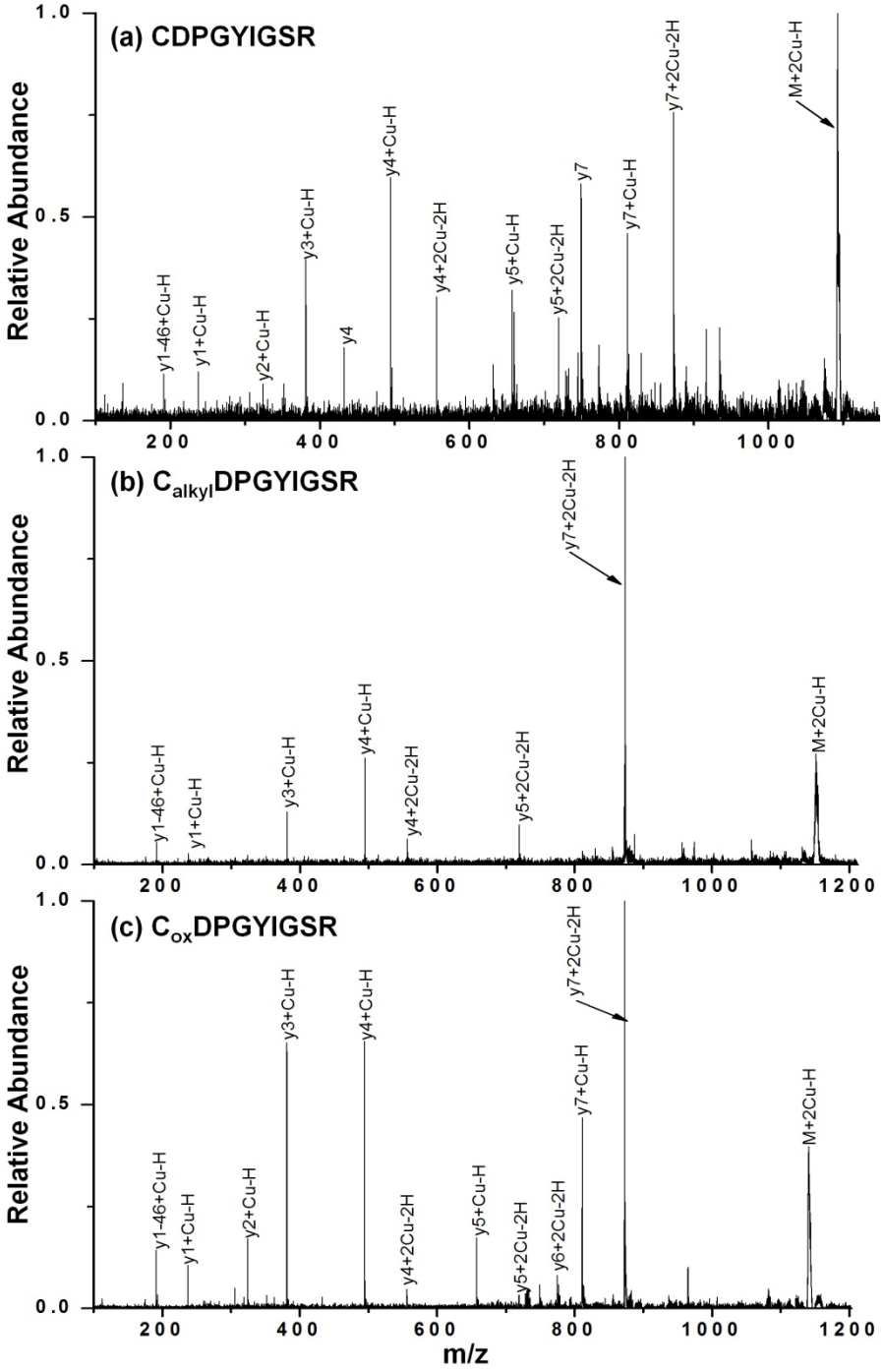

Figure 20. Fragment ion spectra of the $[M + 2Cu - H]^+$ ions of (a) CDPGYIGSR, (b) C_{alkyl}DPGYIGSR, (c) C_{ox}DPGYIGSR.

Table 3. Relative abundance ratio of the fragment ions for $[M + Cu]^+$ and $[M + 2Cu - H]^+$. For example, for $[M + Cu]^+$ ions, the relative abundance ratio of 'y_i + Cu - H' ions = $\sum(y_i + Cu - H) / (\sum(y_i + Cu - H) + \sum y_i)$.

	$[M + Cu]^+$		$[M + 2Cu - H]^+$		
	$\sum(y_i + Cu-H)$	$\sum y_i$	$\sum(y_i + 2Cu - 2H)$	$\sum(y_i + Cu - H)$	$\sum y_i$
CDPGYIGDR	>99%	<1%	42%	48%	10%
C_{alkyl}DPGYIGDR	100%	N/A	70%	30%	N/A
C_{ox}DPGYIGDR	65%	35%	44%	56%	N/A

ions for C_{alkyl}DPGYIGSR provides evidence that blocking the cysteine thiol group reduces the interaction with Cu^+ ion. In addition, these data suggests that at least one Cu^+ must be located at the C-terminus (charge-solvated by the C-terminal carboxyl and/or the arginine guanidine). For the $[M + 2Cu - H]^+$ ion of C_{ox}DPGYIGSR, we observed exclusively $[y_i + 2Cu - 2H]^+$ and $[y_i + Cu - H]^+$ fragment ions with relative abundance ratios of 44% and 56%, respectively (Table 3). The higher abundance of the $[y_i + Cu - H]^+$ ions suggests a larger population of the conformation (shown in Scheme 4C(ii)), where the sulfonic acid is the primary protonation site, and each Cu^+ ion is individually charge-solvated by the sulfonate and the arginine guanidine group, respectively. As a consequence, only one Cu^+ ion remains on the C-terminal fragment ions (Scheme 4C(ii)). A plausible explanation for the formation of higher abundance of $[y_i + Cu - H]^+$ ions is the fact that the deprotonation energy for sulfonic acid is less than that for carboxylic acid [88]. Thus, deprotonation of the sulfonic acid is more energetically favorable over that of the C-terminal carboxyl group, and the lower deprotonation energy of sulfonic acid results in a more stable coordination structure (Scheme 4C(ii)).

Conclusions

These studies clearly show that cysteine and cysteic acid side chains (-SH/SO_3H) are important Cu^+ ion ligands, and these metal ion-ligand interactions have a strong influence on the fragmentation chemistry of [M +

$Cu]^+$ and $[M + 2Cu - H]^+$ ions. In addition, we demonstrate that Cu^+ ions are competitively coordinated to the -SH/SO_3H groups versus guanidine group via an intramolecular proton transfer (Figures 21, 22, 23, 24). This is probably not surprising considering the Cu^+ binding energy for the two groups differs by ~5 kcal/mol [42,50]. It is particularly interesting to note that upon binding of Cu^+ ions to the cysteine or cysteic acid side chains the proton (on SH or SO_3H) is transferred to the arginine guanidine group, resulting in a thiolate-Cu^+ or sulfonate-Cu^+ group and a protonated arginine side chain. On the basis of the data reported herein we cannot determine whether this proton migration occurs as a result of Cu^+ attachment to SH or SO_3H ((*i.e.*, a process similar to that was proposed previously [36]) or whether the proton is mobilized as a result of the collisional activation process. We are currently investigating these issues further by comparing ion abundances observed by using 193 nm photodissociation with those observed by CID and by ion mobility-mass spectrometry (IM-MS) and molecular dynamics simulations. These studies underscore the role of peptide-metal ion interactions on the fragmentation chemistry of gas-phase peptide ions as well as the level of information that can be extracted regarding the specificity of metal ion binding.

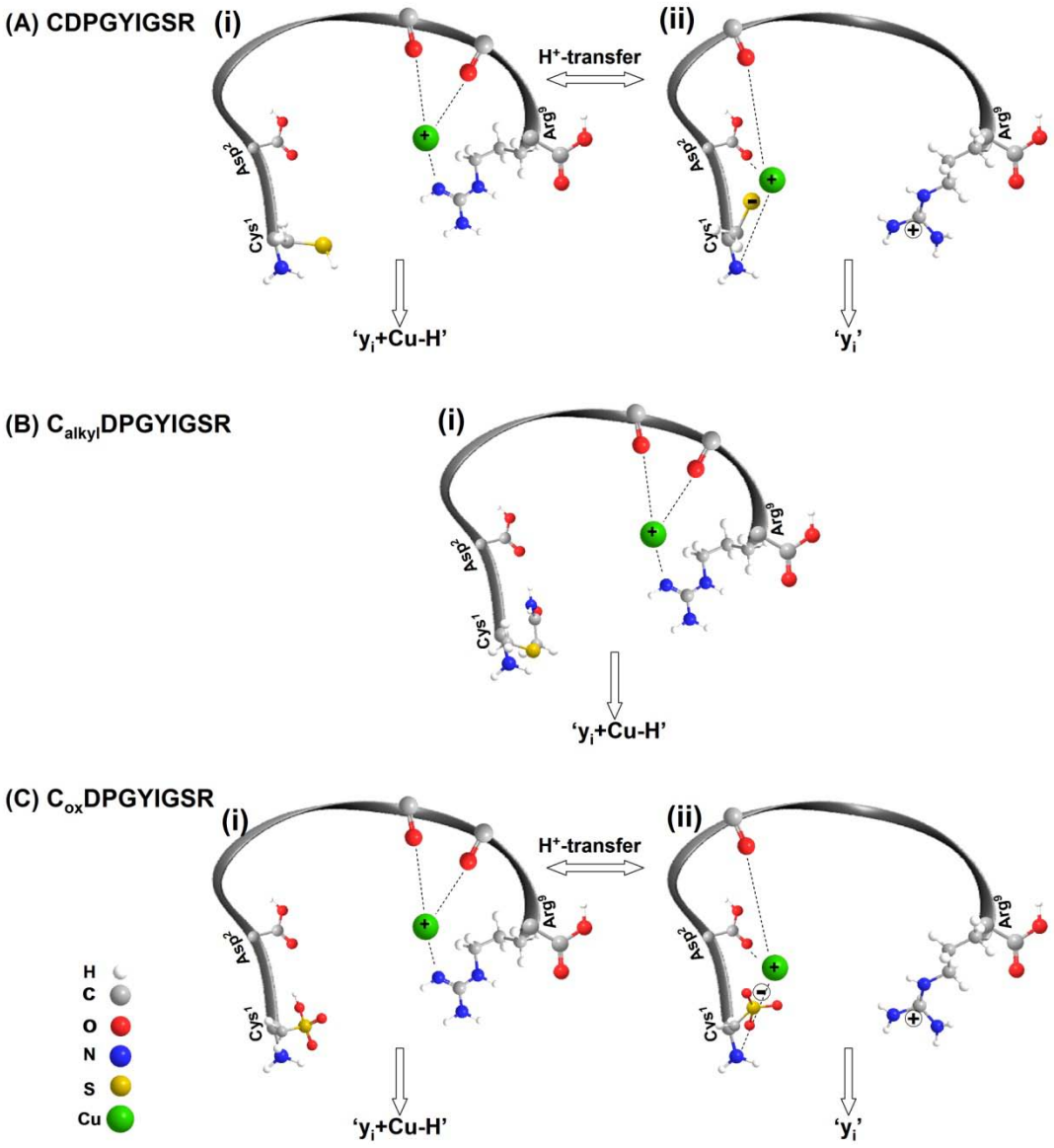
(A) CDPGYIGSR
(i)
H+-transfer
(ii)
Asp2
Arg8
Cys1
'yi+Cu-H'
'yi'
(B) CalkylDPGYIGSR
(i)
Asp2
Arg8
Cys1
'yi+Cu-H'
(C) CoxDPGYIGSR
(i)
H+-transfer
(ii)
Asp2
Arg8
Cys1
'yi+Cu-H'
'yi'
H
C
O
N
S
Cu

Scheme 3

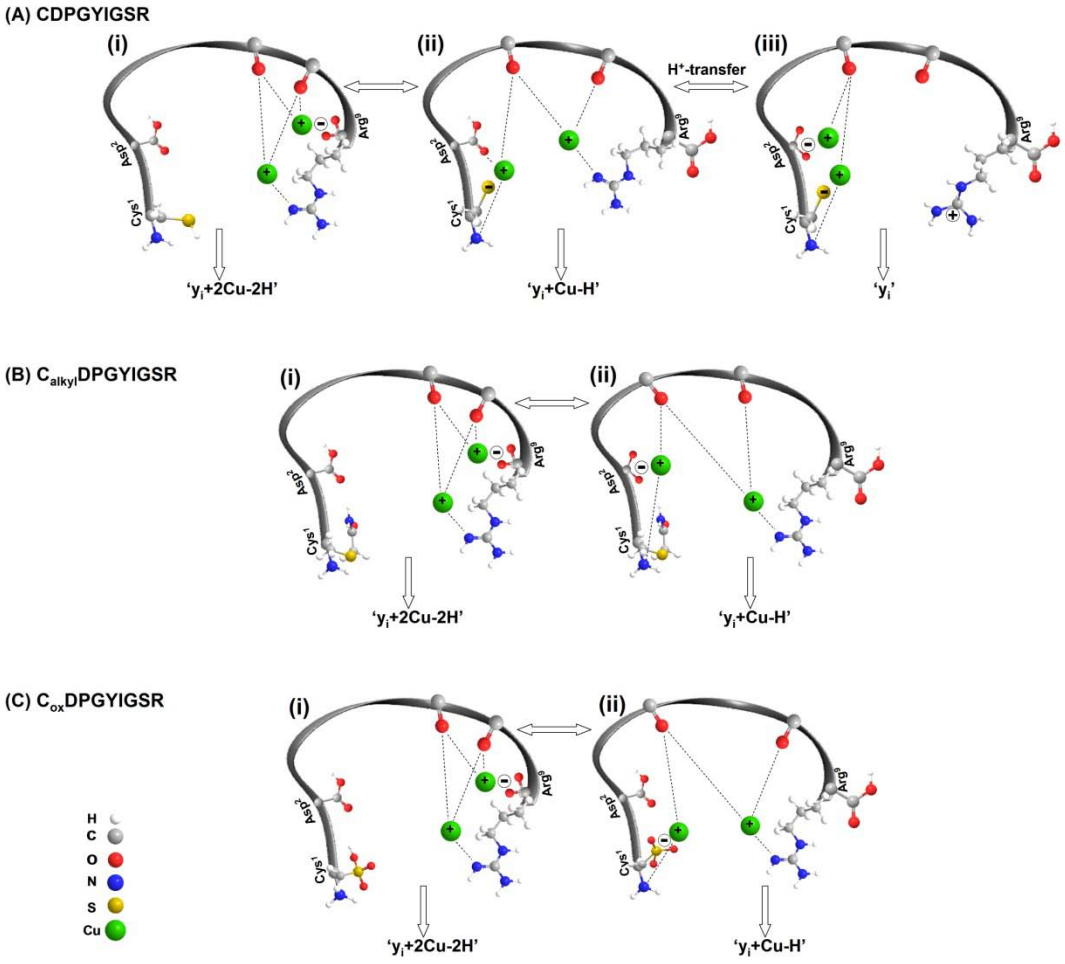
(A) CDPGYIGSR
(i)
(ii)
(iii)
H+-transfer
'yi+2Cu-2H'
'yi+Cu-H'
'yi'
(B) CalkylDPGYIGSR
(i)
(ii)
'yi+2Cu-2H'
'yi+Cu-H'
(C) CoxDPGYIGSR
(i)
(ii)
'yi+2Cu-2H'
'yi+Cu-H'
H
C
O
N
S
Cu

Scheme 4

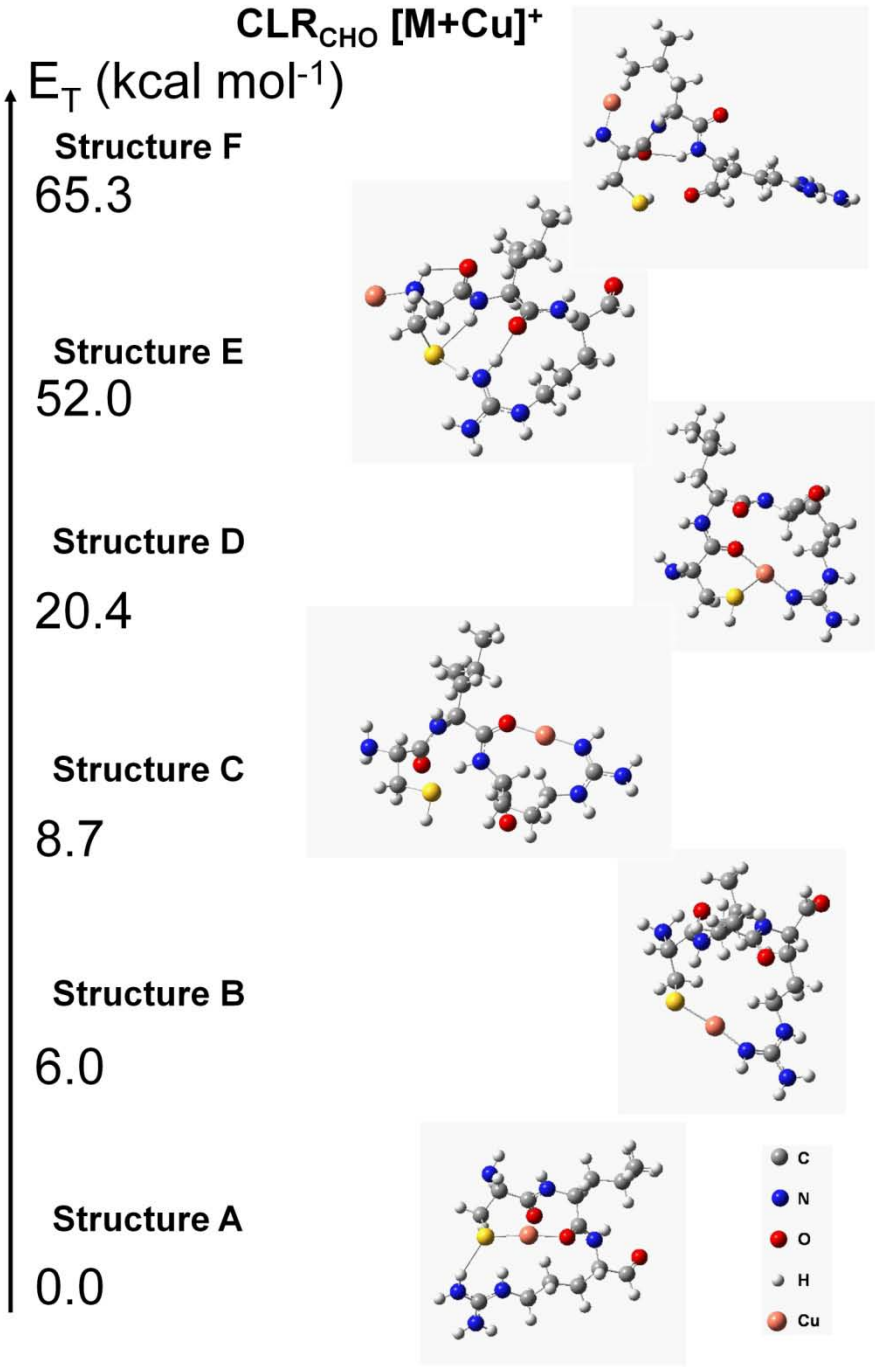

Figure 21. Candidate structures obtained at the DFT/B3LYP/LACV3P** level for the $[M + Cu]^+$ ions of the peptide motif CLR_{CHO}. The'$_{CHO}$' denotes an aldehyde C-terminus.

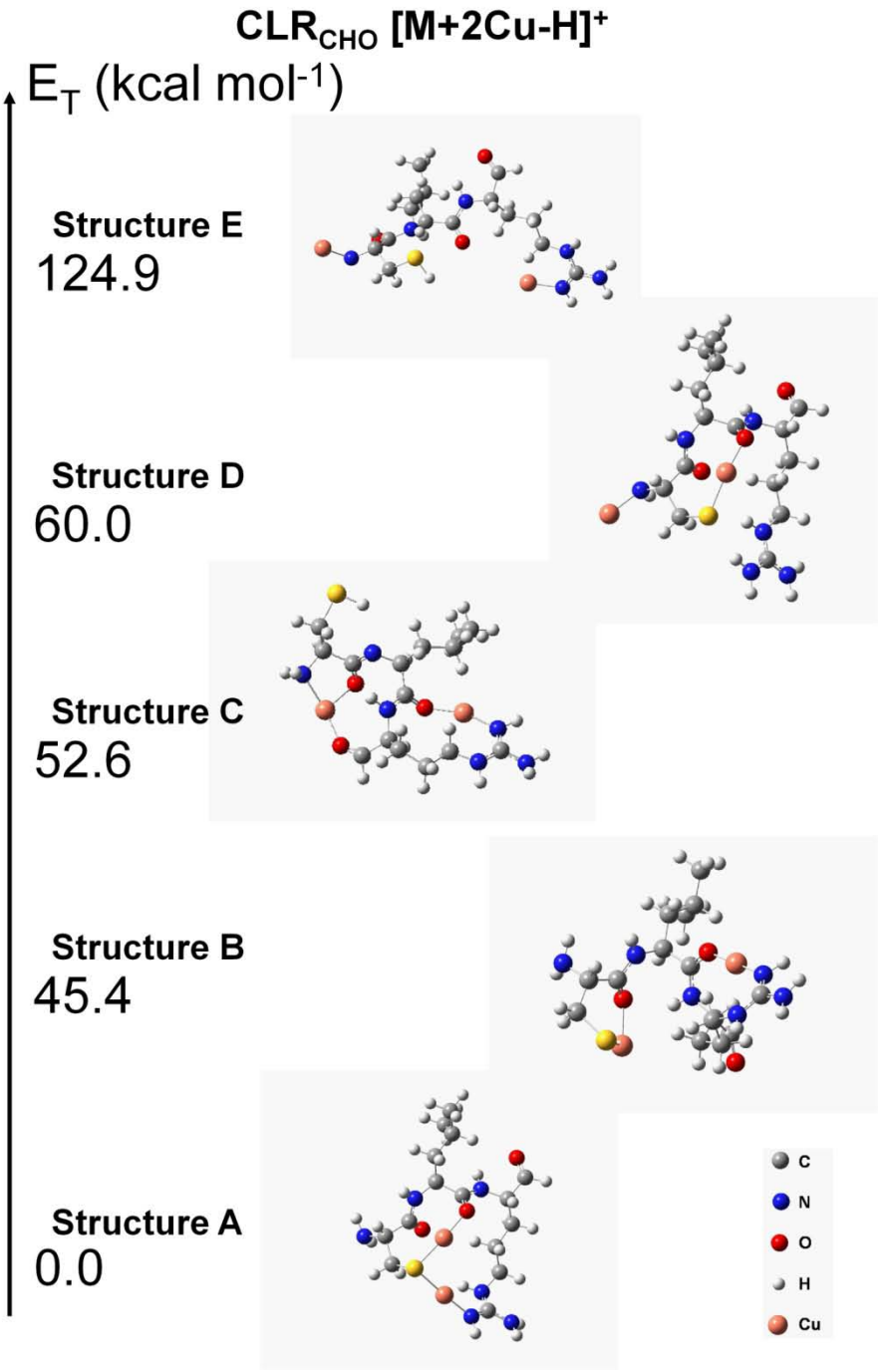

Figure 22. Candidate structures obtained at the DFT/B3LYP/LACV3P** level for the $[M + 2Cu - H]^+$ ions of the peptide motif CLR_{CHO}. The'$_{CHO}$' denotes an aldehyde C-terminus.

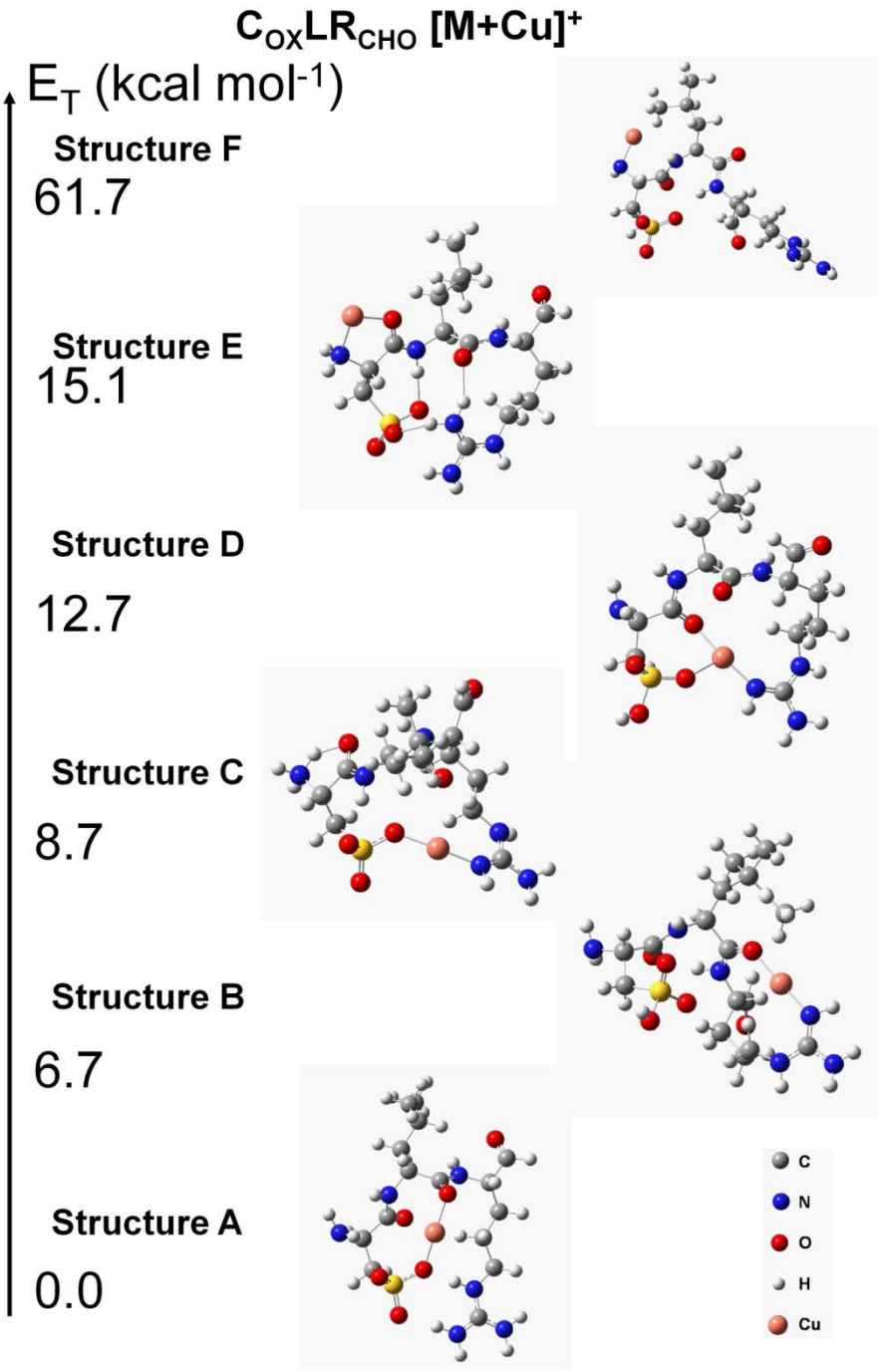

Figure 23. Candidate structures obtained at the DFT/B3LYP/LACV3P** level for the $[M + Cu]^+$ ions of the peptide motif $C_{ox}LR_{CHO}$. The'$_{CHO}$' denotes an aldehyde C-terminus.

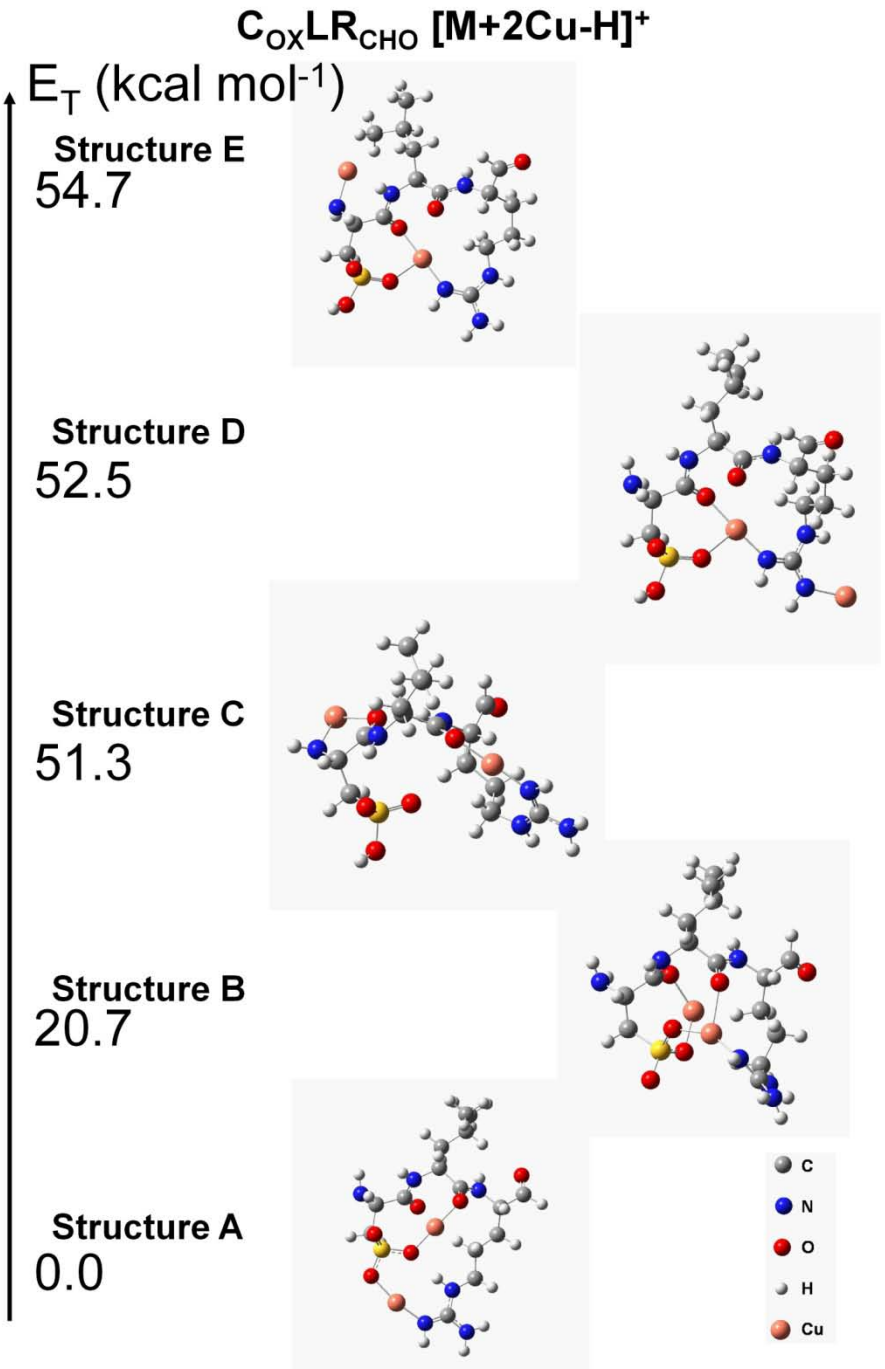

Figure 24. Candidate structures obtained at the DFT/B3LYP/LACV3P** level for the $[M + 2Cu - H]^+$ ions of the peptide motif $C_{ox}LR_{CHO}$. The'$_{CHO}$' denotes an aldehyde C-terminus.

CHAPTER IV

INFLUENCE OF SIDE-CHAIN INTERACTIONS ON PEPTIDE GAS-PHASE STRUCTURES*

Introduction

In previous chapters, tandem mass spectrometry has been used to investigate the Cu^+ binding chemistry for copper-peptide complexes. Combined with the results from theoretical calculations, the Cu^+ coordination structures for gas-phase peptide ions have been rationalized. For example, the role of the C-terminal carboxyl group in the Cu^+ binding was examined via tandem MS experiments and DFT calculations. In addition, chemical modifications (*i.e.*, oxidation and alkylation) were performed to evaluate the influence of functional groups on the competitive Cu^+ binding to peptides in gas phase. Results indicate that chemical modifications could help understand the fragmentation reactions for gas-phase peptide-Cu^+ ions.

Acetylation and methylation reactions have been performed in the context of protein identification and characterization for many reasons [62,89,90]. For example, methylation of a peptide converts carboxylic acids,

---

* Reproduced with permission from McLean, J.R.; McLean, J.A.; Wu, Z.; Becker, C.; Perez, L.M.; Pace, N.C.; Scholtz, M.J.; Russell, D.H. Factors that Influence Helical Preferences for Singly-Charged Gas-Phase Peptide Ions: The Effects of Multiple Charge-Carrying Sites. *J. Phys. Chem. B*. **2010**, 104, 809-816. Copyright [2010] by American Chemical Society.

such as those present on the side chains of aspartic (D) and glutamic acid (E) as well as the free carboxyl terminus, to their corresponding methyl esters. This method has been applied to peptide and protein quantitation, de novo sequencing, and reduction of nonspecific binding in immobilized metal affinity chromatography for enrichment of phosphorylated peptides [91]. Acetylation of proteins at specific lysine residues has also been considered as an important posttranslational modification of high biological impact. The reversible lysine acetylation plays a vital role in the regulation of many cellular processes including chromatin dynamics and transcription, cell cycle progression, apoptosis, DNA replication and DNA repair [92-95]. After acetylation the lysine residue of protein should be modified giving a mass shift of 42u, and this information will be useful in a peptide de novo sequencing experiment.

Previously, Baldwin and coworkers characterized the solution-phase structures of the peptides Ac-$(AAKAA)_n$Y-NH_2 (n = 3 – 7) and Ac-Y$(AEAAKA)_n$F-NH_2 (n = 2 – 5) using Circular Dichroism (CD) [96,97]. Their results suggest that the helical content of both series increases with increasing the peptide length, and the spacing of E and K side chains of the AEAAKA series is crucial to the stabilization of the helix structure, partially due to the potential side-chain interactions (*i.e.*, lysine-glutamic acid H-bonding and/or ion-pairing) [96,97]. Jarrold and coworkers have shown that insertion of an E/K pair into Ac-A_3G_{12}K decreased the helical content of the

anhydrous peptide ions compared to the unsubstituted peptide [98-100]. Janel and coworkers examined the relationship between helical content, primary sequence and peptide length in the AAKAA and AEAAKA series, and their results have shown that amino acid sequence and peptide length play important roles in the gas-phase structures for (AAKAA)n (n = 3 ~7) and (AEAAKA)n (n = 2 ~ 5) $[M + H]^+$ and $[M + Na]^+$ ions [101].

In this chapter, we investigate the fragmentation chemistry of the derivatives of AEAAKA and AAKAA series peptides (*i.e.*, $AE_{me}AAKA$ or $AEAAK_{actyl}A$) in an effort to determine the effects of amino acid positions on these modifications. In addition, we will compare the collision cross-sections of the AEAAKA and AAKAA series peptides with that of the modified forms using ion mobility-mass spectrometry (IM-MS). This study will provide a better understanding of the influence of side-chain interactions (*i.e.*, E/K H-bonding) on peptide gas-phase structures.

Experimental

All experiments were performed with 18-MΩ water (ddH_2O) purified using a water purification unit (Barnstead International, Dubuque, IA). The AEAAKA and AAKAA series peptides were purchased from Genscript Company and used without further purification. CHCA was recrystallized prior to use. All other chemicals were used as received. The lysine residue and/or the glutamic acid residue were modified by methylation and/or acetylation, respectively, following standard protocols [62,90]. Peptide

samples were mixed with matrix solution at a ratio of 1:3 (v:v), and an aliquot (1 µl) was applied to a stainless steel target. Samples were dried in air at room temperature.

Peptide Methylation

A solution of 2M hydrochloric acid in methanol was prepared by dropwise addition of acetyl chloride (800 µl) into anhydrous methanol (5 ml) and then stirring for 5 min at room temperature. The solution (1 ml) was added to the peptide (50 µg) and then the mixture was stirred for 3 h at room temperature. The resulting solution was dried by SC250DDA Speedvac Plus (Thermo Electron Corporation, Waltham, MA). The methylated peptide was mixed with metal complexes in each experiment without any further purification [62].

Peptide Acetylation

20 µL of acetic anhydride was added to 60 µL of anhydrous methanol and the mixture solution (acetylation reagent) was incubated at room temperature for 10 min. Peptide samples (1 nmol) were dissolved in 20µL of 50 mM ammonium bicarbonate (ABC) aqueous solution. 50µL of acetylation reagent was added to 20µL of peptide solution and incubated at room temperature for one hour, and the resulting solution was lyophilized to dryness [90]. The product of the acetylation reaction was analyzed by MALDI-TOF MS.

MALDI-TOF Mass Spectrometry

The MALDI experiments described herein were performed on a tandem time-of-flight mass spectrometer (4700 Proteomics Analyzer, Applied Biosystems, Framingham, MA). Tandem mass experiments were performed using a collision energy setting of 1 kV and air as the collision gas.

MALDI-IM TOF MS

Ion mobility spectrometry is a gas phase separation technique by which ions are separated based on mobility under an electric field. By assuming the ion and buffer gas molecule are hard spheres, the gas-phase mobility and the collision cross section (Ω) of ions can be determined by a number of factors, including the field strength (*E/L*), the temperature and pressure of the separation medium (*T*, *P*), the mass (m_b) of the separation medium, the mass (m_i) and charge (*z*) of the analyte. .The collision cross section (Ω) is calculated from the drift time (t_D) using the following equation [102]:

$$\Omega = \frac{(18\pi)^{\frac{1}{2}}}{16}\frac{Ze}{(K_b T)^{\frac{1}{2}}}\left(\frac{1}{m_i}+\frac{1}{m_b}\right)^{\frac{1}{2}}\frac{t_D E}{L}\frac{760}{P}\frac{T}{273.3}\frac{1}{N}$$

Coupling of ion mobility (IM) spectrometry with mass spectrometry (MS) provides a powerful analytical tool for the study of gas-phase peptide and protein structures [103-105]. Analysis using IM-MS results in a two-dimensional correlation between collision cross-section (Ω) which depends on ion structure and the mass-to-charge ratio (m/z) of the ion, allowing detection of multiple conformations of the same m/z.

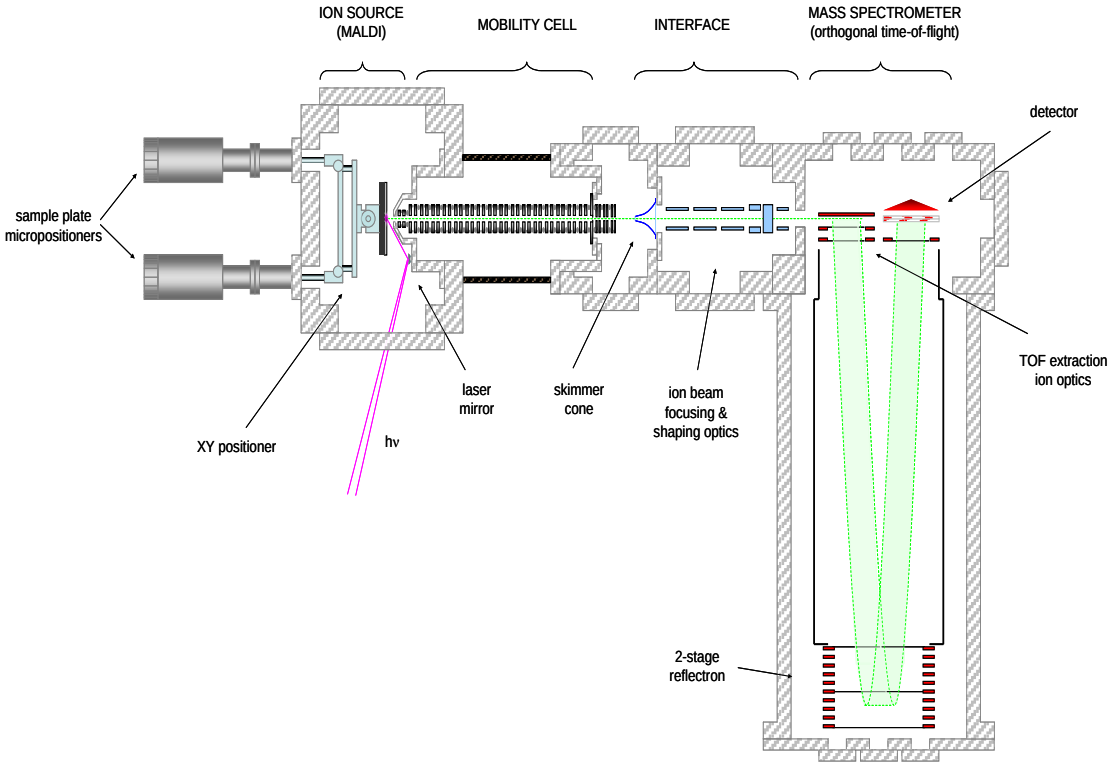

Figure 25. Schematic of the MALDI-IM-TOF-MS instrument used in experiments.

The MALDI-IM orthogonal time-of-flight mass spectrometer (MALDI-IM-TOF MS) (Figure 25) used in these studies was constructed in collaboration with Ionwerks, Inc. (Houston, TX). MALDI was performed using a frequency-tripled solid-state Nd:YAG laser (355 nm, Power Chip) operated at a frequency of 300 Hz. IMS separations occur in a 15 cm-long periodic-field drift cell, maintained at ~3 Torr with helium as a buffer gas (UHP grade). Typical IMS field strength/pressure (E/p) ratios were 10–20 V cm^{-1} $torr^{-1}$ and all measurements were performed at room temperature (ca. 297.15 K).

Results and Discussion

Acetylation reaction introduces an acetyl group into the lysine side chain. For the peptides Ac-Y(AEAAKA)$_2$F-NH$_2$ and Ac-(AAKAA)$_2$Y-NH$_2$ examined in the experiments, both mono- and di-acetylated forms were observed under our experimental conditions. For example, Figure 26a contains the MS spectrum of the acetylation products of the peptide Ac-(AAKAA)$_2$Y-NH$_2$. The ion at m/z 1089.6 is assigned as the protonated peptide of the mono-acetylated form ([M + H + 42]$^+$), and the ion at m/z 1031.6 is assigned as the protonated peptide of the di-acetylated form ([M + H + 84]$^+$). Note that, the lower abundance of the protonated ion of the di-acetylated form is due to the lower proton affinity of the backbone carbonyl [106-108], which is the only potential protonation site since the N-terminal amine and all the lysine residues are acetylated. For the mono-acetylated forms of the peptides Ac-(AAKAA)$_2$Y-NH$_2$ and Ac-Y(AEAAKA)$_2$F-NH$_2$ ([M + H + 42]$^+$ ions shown in Figure 26), which lysine residue is acetylated? Whether or not the acetylation reaction is sensitive to the lysine position?

Acetylation of Ac-(AAKAA)$_2$Y-NH$_2$ and Ac-Y(AEAAKA)$_2$F-NH$_2$

Theoretically, Lys^3 and Lys^8 are the two possible acetylation sites for the peptide Ac-(AAKAA)$_2$Y-NH$_2$; however, fragmentation results suggest that the acetylation reaction is sensitive to the lysine positions, and Lys^3 appears to have higher reactivity than Lys^8. That is, the fragment ion spectrum of the mono-acetylated Ac-(AAKAA)$_2$Y-NH$_2$ (Figure 27a) contains a series of N-

terminal *b*-type fragment ions with mass shift of 42u (*i.e.,* 'b_i + 42' (i = 3 – 7)), while we do not observe the 42u mass shift to C-terminal *y*-type fragment ions (*i.e.,* y_i (i = 4 – 7). The typical fragments such as 'b_i+42' (i = 3 – 7) ions indicate that the acetyl group was attached to Lys^3 rather than Lys^8. A plausible explanation for the higher reactivity of N-terminal lysine may have to do with the peptide secondary structure (*i.e.*, Lys^8 may not be accessible to the acetylation reagent due to steric effects of the tyrosine side chain).

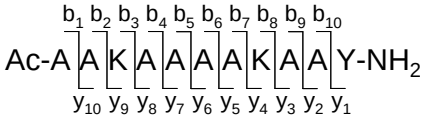

We also examined the fragmentation chemistry of the mono-acetylated Ac-Y$(AEAAKA)_2$F-NH_2, and similar results to that of Ac-$(AAKAA)_2$Y-NH_2 are observed. Based on the typical fragment ions observed (*i.e.*, 'b_6 + 42' (i = 6 – 11) and 'y_j" (j = 4 – 8)) in the spectrum (Figure 28a), we determine that the acetylation site for the mono-acetylated Ac-Y$(AEAAKA)_2$F-NH_2 is Lys^6 over Lys^{12}. Here again, we interpret this result as evidence that the reactivity of lysine residues is dependent on their position, and the N-terminal lysine appears to have higher reactivity than the ones at other positions.

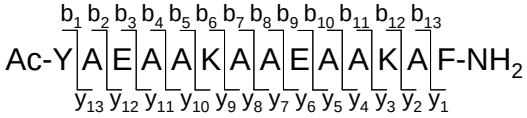

The fragment ion spectrum of the di-acetylated peptides (Ac-$(AAKAA)_2$Y-NH_2 and Y$(AEAAKA)_2$F-NH_2) is relatively simple compared to

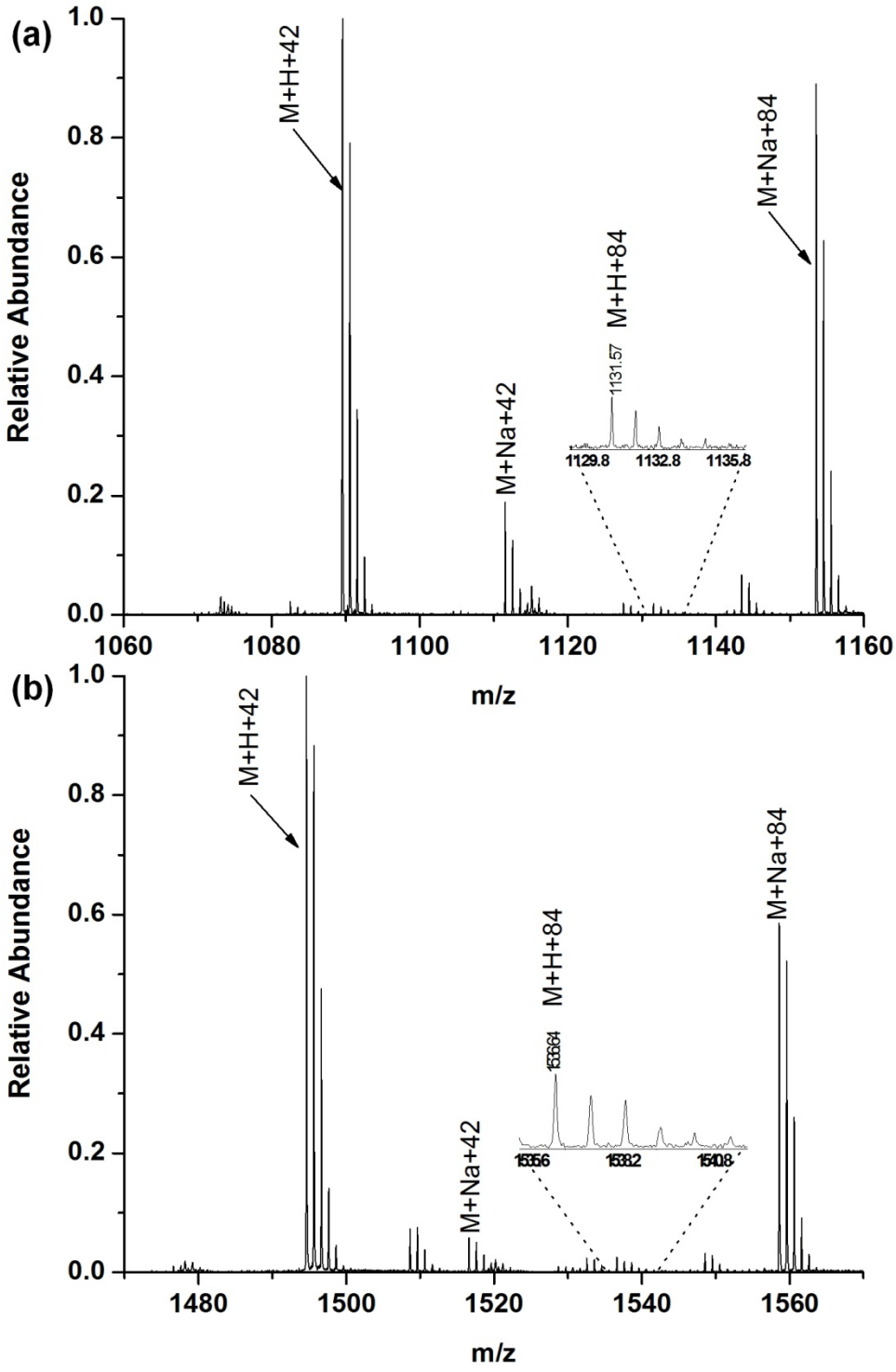

Figure 26. Partial MS spectra of the acetylation products of (a) Ac-$(AAKAA)_2$Y-NH_2 and (b) Ac-Y$(AEAAKA)_2$F-NH_2.

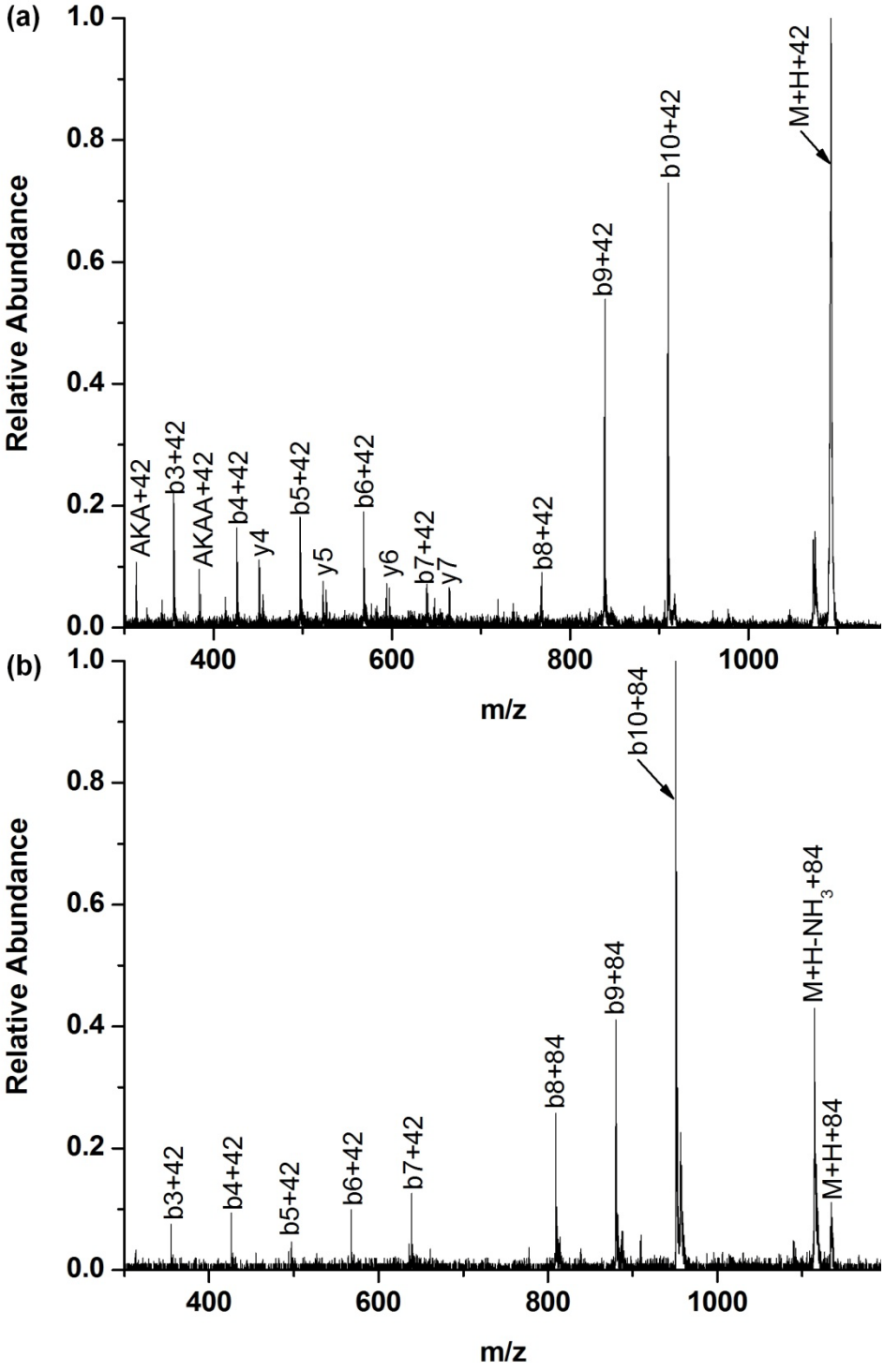

Figure 27. Fragment ion spectra of the $[M+H]^+$ ions (a) Ac-$(AAKAA)_2$Y-NH_2 (-CH_3CO) and (b) Ac-$(AAKAA)_2$Y-NH_2 (-$2CH_3CO$).

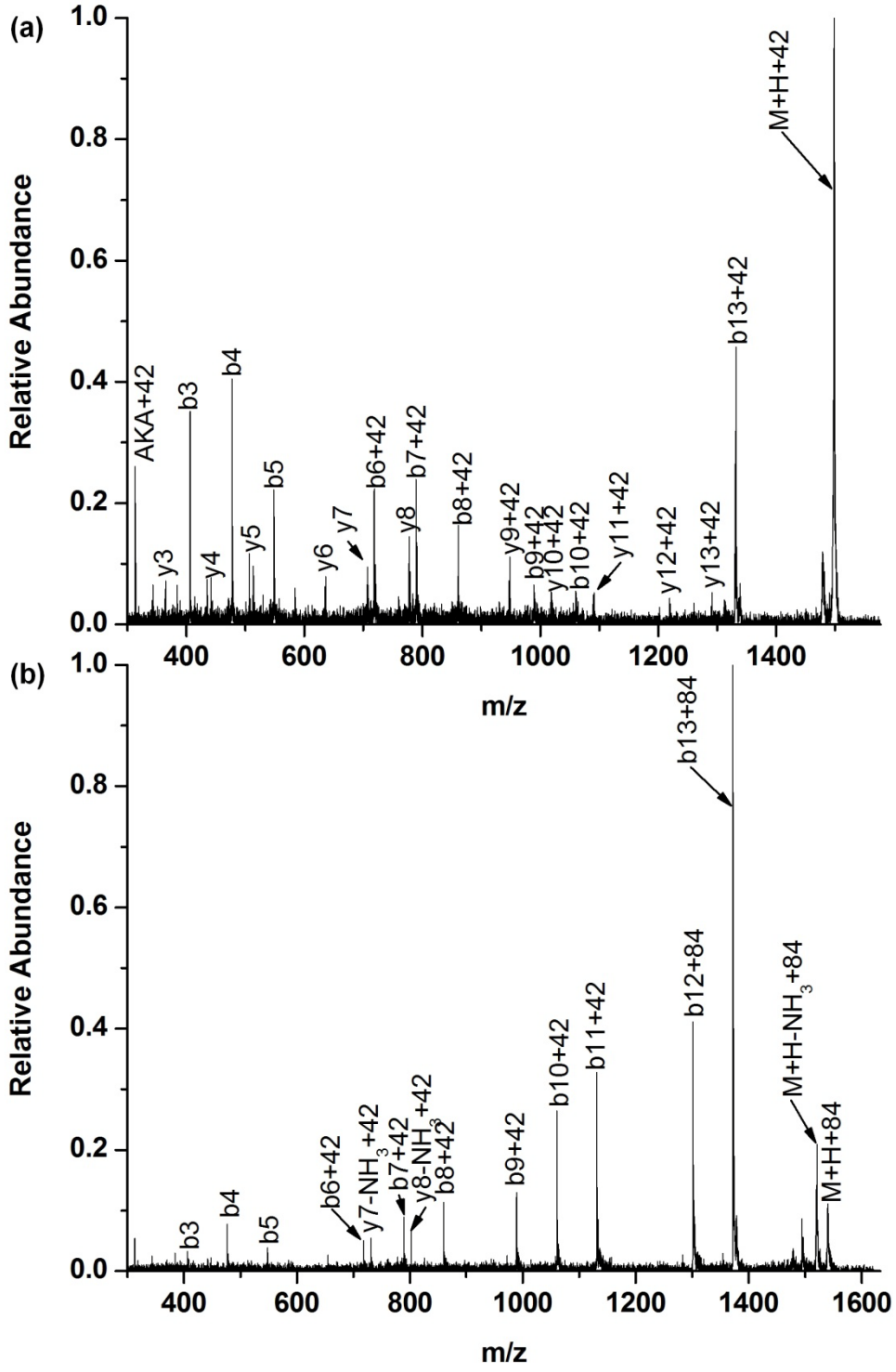

Figure 28. Fragment ion spectra of the $[M+H]^+$ ions (a) Ac-Y(AEAAKA)$_2$F-NH_2 (-CH_3CO) and (b) Ac-Y(AEAAKA)$_2$F-NH_2 (-2CH_3CO).

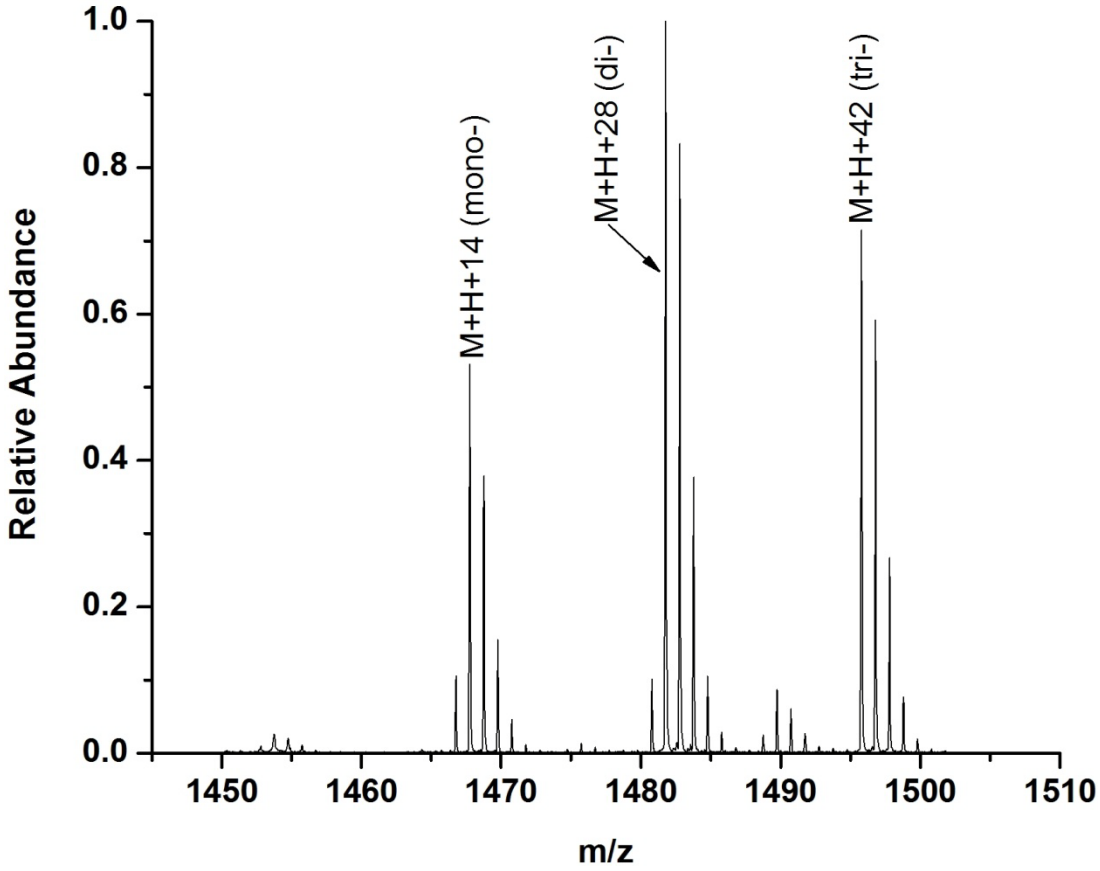

Figure 29. Partial MS spectra of the methylation products of Ac-Y(AEAAKA)$_2$F-NH$_2$.

that of the mono-acetylated forms. For example, for the di-acetylated peptide Ac-$(AAKAA)_2$Y-NH_2 (Figure 27b), we observe exclusively *b*-type fragment ions, including 'b_i + 42' (i = 3 – 7) and 'b_j + 84' (j = 8 – 10), and y-type fragment ions are absent. The 84u mass shift to the N-terminal fragment ions suggests that the two lysine residues were acetylated.

Methylation of Ac-Y(AEAAKA)$_2$F-NH$_2$

Methylation reaction was performed to modify the glutamic acid and/or the C-terminal amide group. For the peptide Ac-Y$(AEAAKA)_2$F-NH_2, Glu^3, Glu^9 and the C-terminal amide are the potential methylation sites; however, unlike the acetylation reaction we discussed above, we do not observe a significant site preference for the methylation reaction. That is, fragmentations results suggest that the mono- and di-methylated Ac-Y$(AEAAKA)_2$F-NH_2 may contain different conformational isomers (Figure 29). For example, the fragment ion spectra (Figure 30a) of the $[M + H]^+$ ions of the mono-methylated Ac-Y$(AEAAKA)_2$F-NH_2 are dominated by a series of 'b_i' and 'b_i+14' (i = 3,4,7,8,9,12,13) ions. The formation of 'b_i' (i =3,4,7,8) ions suggests the existence of a conformational isomer where Glu^9/C-terminal amide was methylated, while the formation of 'b_i+14' (i =3,4,7,8) ions conforms the existence of another isomer where Glu^3 was methylated instead. Therefore, on the basis of the fragmentation results, it is difficult to determine the exact methylation sites for the mono- and di-methylated

peptide; however, this is not a major concern for the following IM-MS experiments.

Influence of Methylation/Acetylation on Peptide Gas-phase Structures (IM-MS)

In previous work, Janel and coworkers used IM-MS and simulated annealing to generate the candidate structures for the $[M + H]^+$ ions of AEAAKA series peptides. Their results suggest that the presence of multiple E/K pairs promotes formation of closely related charge-solvated structures, resulting in a broad peak of the arrival time distributions (ATDs) for the $[M + H]^+$ ions [101]. Note that, the arrival time distributions (ATDs) were generated by integrating 2-dimensional IM-MS spectra across a range of *m/z* values that correspond to the isotopic cluster of the peptide ion. The peak width of ATDs is a function of the number of the collision cross-sections of the peptide ion. In other words, a single observed mobility peak may consist of a population of multiple structurally-related conformers, considering that the peak broadening arises exclusively from ion diffusion [109]. These conformers could be the result of distinct, unresolved structures or structures that are rapidly inter-converting on the timescale of the experiment (microseconds). Therefore, less charge-solvated structures are expected to form in gas phase if we decrease the interactions between E/K pairs (E_{methyl} and/or K_{actyl}). How would these modifications affect the ATDs profile of peptides?

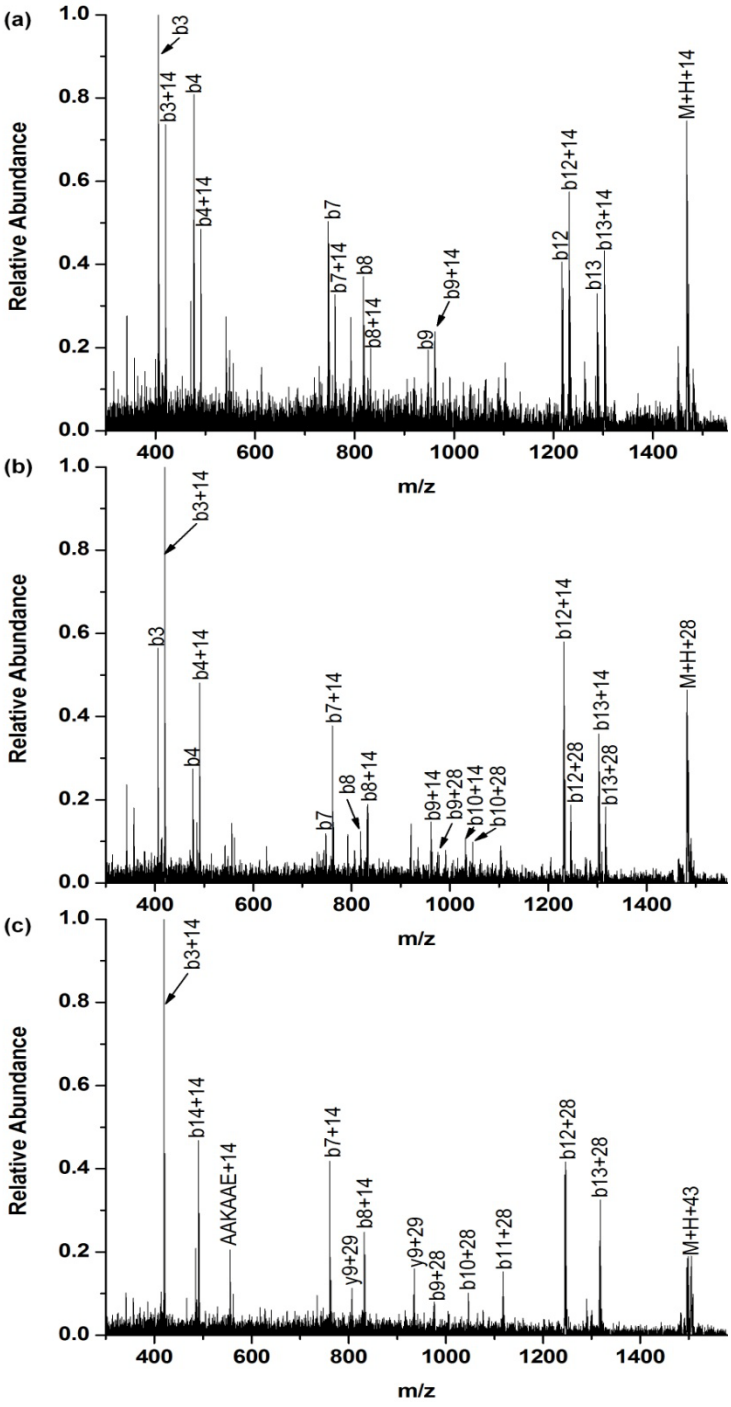

Figure 30. Fragment ion spectra of the $[M+H]^+$ ions (a) Ac-Y(AEAAKA)$_2$F-NH_2 (-OCH_3), (b) Ac-Y(AEAAKA)$_2$F-NH_2 (-2OCH_3) and (c) Ac-Y(AEAAKA)$_2$F-NH_2 (-3CH_3).

Figure 31 contains the experimental ATDs of the $[M + H]^+$ ions for the methylated Ac-Y(AEAAKA)$_2$F-NH$_2$ (tri-, di- and mono-) versus Ac-Y(AEAAKA)$_2$F-NH$_2$. Note that, the ATDs of the methylated peptide was significantly narrower compared to that of the unmodified peptide. In particular, the peak width of the tri-methylated peptide is only half of that for the unmodified peptide (FWHM for the ATDs of tri-methylated versus unmodified peptide is 14μs and 31μs, respectively). The peak narrowing suggests that the methyl ester groups decrease the side-chain interactions (*i.e.,* E/K H-bonding), and thus limit the formation of closely related charge-solvated structures. In addition, it is noteworthy that the ester groups do not change the peptide collision cross-sections significantly, considering that the average ATDs (centroid of the peak) of the methylated peptides only increase slightly than that of the unmodified peptide.

A similar result is observed for the acetylated Ac-Y(AEAAKA)$_2$F-NH$_2$. Figure 32 contains the experimental ATDs of the $[M + H]^+$ ions for the acetylated Ac-Y(AEAAKA)$_2$F-NH$_2$ (di- and mono-) versus Ac-Y(AEAAKA)$_2$F-NH$_2$. The FWHM for the ATDs of di-acetylated versus unmodified peptide is 19μs and 32μs, respectively. Here again, we interpret this result as evidence that E/K pairs contribute to the gas-phase structure of the peptide Ac-Y(AEAAKA)$_2$F-NH$_2$, and modifications of E/K will decrease the E/K side-chain interactions, limiting the formation of structurally-related charge-solvated conformers. For comparison, we also examined the ATDs for the

acetylated Ac-$(AAKAA)_2$Y-NH_2, and we do not observe any significant difference for the acetylated peptides versus non-acetylated peptide (Figures 33, 34). It is probably not surprising considering that the side-chains interactions are not significant for Ac-$(AAKAA)_2$Y-NH_2, owing to the absence of E/K pairs.

Conclusions

In this chapter, we discussed the fragmentation chemistry of the $[M + H]^+$ ions for methylated and acetylated peptides, and we utilized these modifications to study the influence of side-chain interactions on peptide gas-phase structures. Fragmentation results suggest that acetylation reaction is sensitive to the amino acid positions, and it favors the lysine near the N-terminus rather than other positions; however, no significant site preference is observed for the methylation reaction. These modifications strongly influence on the arrival time distributions for the Ac-Y$(AEAAKA)_2$F-NH_2 peptide ions. That is, narrower ATDs peaks are observed for the methylated/acetylated peptide Ac-Y$(AEAAKA)_2$F-NH_2, implying that the side-chain interactions of E/K pairs play important roles in peptide gas-phase structures, and blocking the E/K side chains will limit the formation of structurally-related charge-solvated conformers.

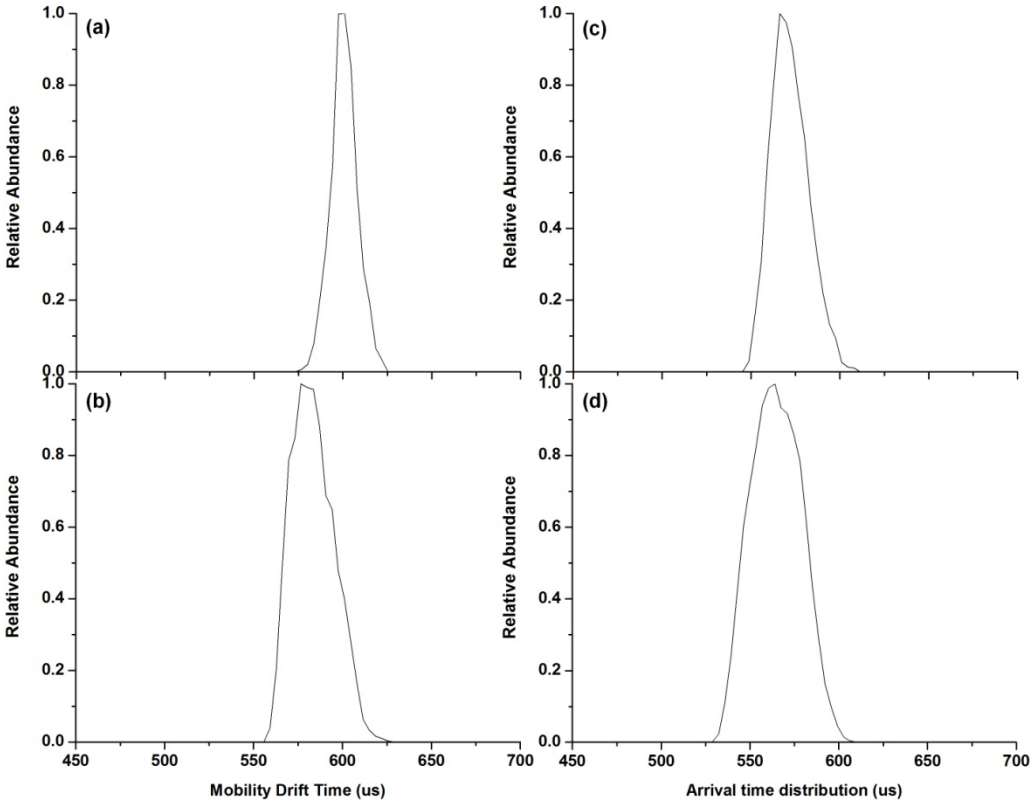

Figure 31. Arrival time distribution (ATD) of the $[M+H]^+$ ions of (a) Ac-Y(AEAAKA)$_2$F-NH$_2$ (3OCH$_3$) (FWHM:14), (b) Ac-Y(AEAAKA)$_2$F-NH$_2$ (2OCH$_3$) (FWHM:25), (c) Ac-Y(AEAAKA)$_2$F-NH$_2$ (OCH$_3$) (FWHM:21) and (d) Ac-Y(AEAAKA)$_2$F-NH$_2$ (FWHM:31).

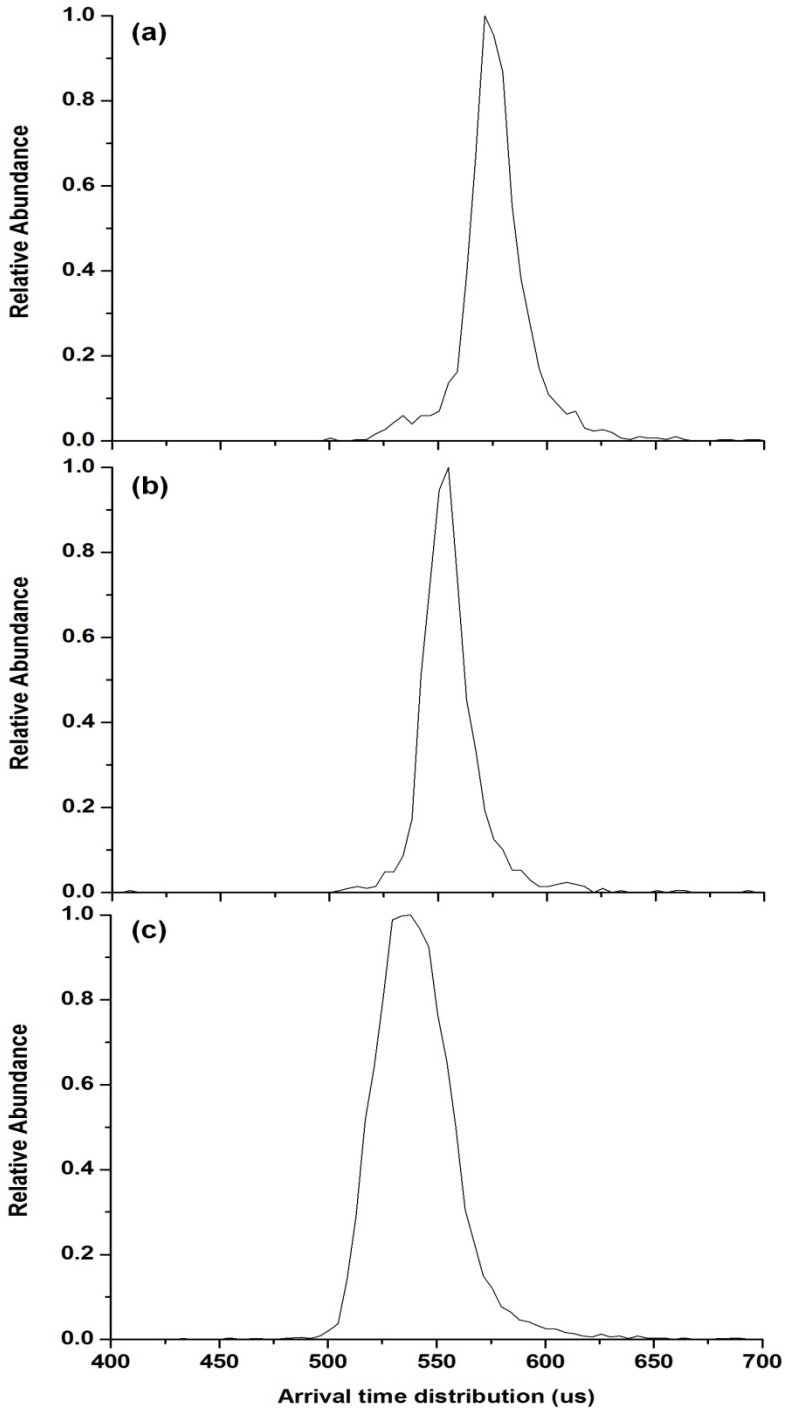

Figure 32. Arrival time distribution (ATD) of the $[M+H]^+$ ions of (a) Ac-Y(AEAAKA)$_2$F-NH$_2$ (2CH$_3$CO) (FWHM:19), (b) Ac-Y(AEAAKA)$_2$F-NH$_2$ ((CH$_3$CO) (FWHM:18) and (c) Ac-Y(AEAAKA)$_2$F-NH$_2$ (FWHM:33).

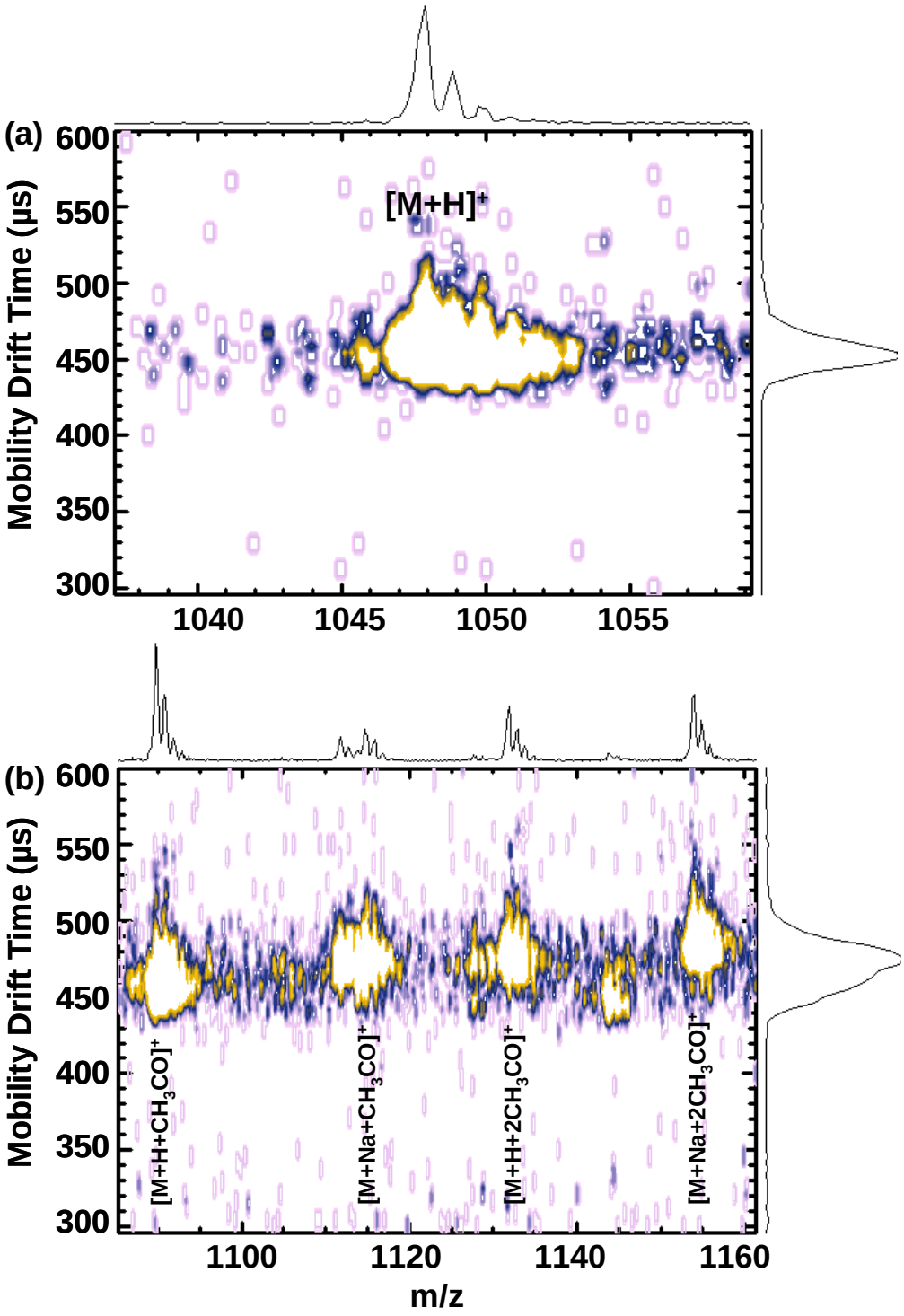

Figure 33. 2-D IM-MS spectra of (a) Ac-$(AAKAA)_2Y$-NH_2 versus (b) Ac-$(AAKAA)_2Y$-NH_2 (acetylated).

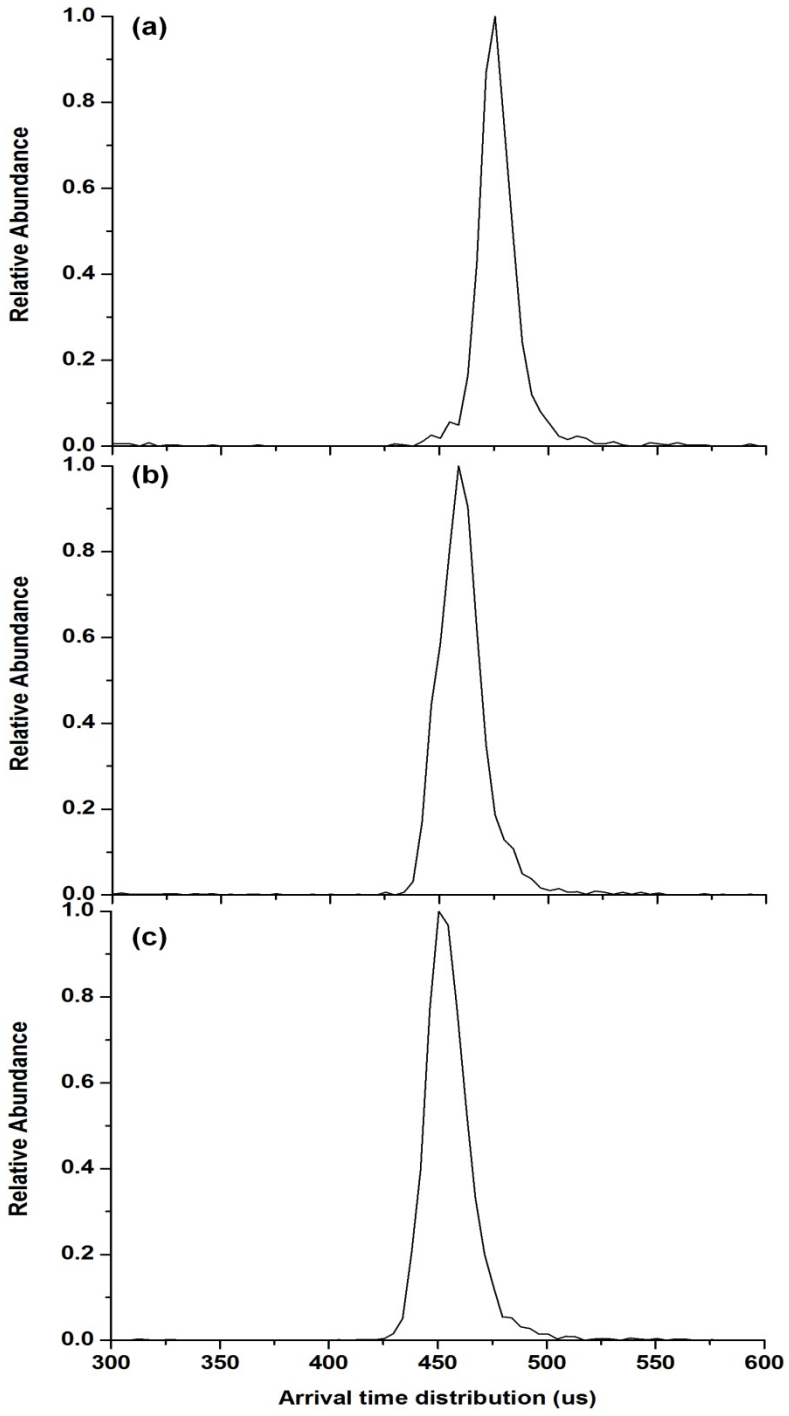

Figure 34. Arrival time distribution (ATD) of the $[M+H]^+$ ions of (a) Ac-$(AAKAA)_2Y$-NH_2 ($2CH_3CO$) (FWHM:14), (b) Ac-$(AAKAA)_2Y$-NH_2 ((CH_3CO) (FWHM: 18) and (c) Ac-$(AAKAA)_2Y$-NH_2 (FWHM:18).

CHAPTER V

CONCLUSIONS AND FUTURE DIRECTIONS

In this work, MALDI TOF mass spectrometry was used to investigate the coordination chemistry of peptide-Cu complexes as well as the gas-phase conformations. MALDI was used as the ionization source of choice in these studies because MALDI results almost exclusively in singly-charged ions, which greatly simplifies MS and MS/MS spectral interpretation. In addition, peptide-Cu ion complexes formed in MALDI process yields primarily peptide-Cu^+ complex ions, which can mimic the coordination environments of Cu^+ ions in biological systems.

Here, we developed a novel copper containing MALDI matrix (Cu-CHCA) to enhance the detection of copper binding peptide ions. This new method generates higher abundances of $[M + xCu - (x-1)H]^+$ ions in gas phase compared to other commonly used methods (*i.e.,* (i) co-mixing a metal salt such as $CuCl_2$, CuO or $CuSO_4$ with the peptide and organic matrix [22,23,26,28,30-32,58] and (ii) desorbing the sample from a CHCA matrix deposited onto an oxidized copper plate [59]). The increased abundances $[M + xCu - (x-1)H]^+$ ions produced by Cu-CHCA reveal rich MS/MS spectra containing Cu^+, which improves our ability to investigate Cu-peptide and Cu-protein complexes. In addition, Cu-CHCA affords opportunities to study the competitive binding of Cu^+ in $[M + xCu - (x-1)H]^+$ ions. For example, for [M +

$Cu]^+$ ions of Ac-$(AAKAA)_n$-NH_2 (n = 2, 3, 4) peptides, we found that the Cu^+ anchoring site is sensitive to the lysine positions, and the lysine residue close to the N-terminus appears to have larger Cu^+ affinity than the other ones (Chapter II). The influence of the C-terminal functional groups on Cu^+ binding was also discussed in Chapter II. Our results suggest that the C-terminal carboxyl strongly affects the fragmentation reactions of $[M + 2Cu – H]^+$ ions of Ac-$(AAKAA)_2$Y, whereas the C-terminal amide or methyl ester group has less influence on the fragmentation chemistry. For example, the fragment ion spectrum of the Ac-$(AAKAA)_2$Y-COOH is dominated by exclusively C-terminal y-type ions (*i.e.,* $[y_i + 2Cu – 2H]^+$). We interpret this result as evidence that the C-terminal carboxyl is a primary deprotonation site for $[M + 2Cu – H]^+$ ions of peptides compared to amide (C-terminal/backbone) or methyl ester (C-terminal), resulting in an energetically favorable structure, where the Cu^+ ions are charged-solvated by the €-amino group of Lys^8, the C-terminal carboxylate and the backbone carbonyl(s).

In Chapter III, we discussed the amino acid influence on Cu^+ coordinating chemistry, in particular, the competitive Cu^+ binding to cysteine versus arginine (note that the binding energy (BE) for the two groups differs by ~5 kcal/mol (BE_{arg} - BE_{cys} = ~ 5 kcal/mol)) [36,42,50]. Our studies have clearly shown that cysteine and cysteic acid side chains (-SH/SO_3H) are important Cu^+ ion ligands, and these metal ion-ligand interactions have a strong influence on the fragmentation chemistry of $[M + Cu]^+$ and [M + 2Cu -

$H]^+$ ions. In addition, we demonstrate that Cu^+ ions are competitively coordinated to the -SH/SO_3H groups versus arininine guanidino group via an intramolecular proton transfer. That is, upon binding of Cu^+ ions to the cysteine or cysteic acid side chains the proton (on SH or SO_3H) is transferred to the arginine guanidine group, resulting in a thiolate-Cu^+ or sulfonate-Cu^+ group and a protonated arginine side chain. However, on the basis of the data reported herein it is difficult to determine whether this proton migration occurs as a result of Cu^+ attachment to SH or SO_3H or whether the proton is mobilized as a result of the collisional activation process. We have measured collision cross-sections for the $[M + Cu]^+$ and $[M + 2Cu - H]^+$ ions using IM-MS, but it is unclear as to whether the observed changes in the cross-sections are the result of structural changes. We are currently investigating these issues using IM-MS and molecular dynamics simulations. Addressing these issues will shed light on the role of peptide-metal ion interactions on the fragmentation chemistry of gas-phase peptide ions as well as the level of information that can be extracted regarding the specificity of metal ion binding.

Using a similar strategy to that for studies of peptide-metal ion interactions, we investigated the fragmentation chemistry of the derivatized AEAAKA and AAKAA series peptides (*i.e.,* acetylation of lysine (K) and methylation of glutamic acid (E)) in an effort to understand the influence of the amino acid positions on the E/K reactivity. In addition, we examined how

the side-chain interactions of E/K pairs affect the peptide gas-phase structures via IM-MS. On the basis of the fragmentation data, it appears that acetylation reaction is sensitive to the lysine positions, and it favors the lysine near the N-terminus rather than other positions; however, no significant site preference is observed for methylation reaction. The derivatization of E/K strongly affects the arrival time distributions (ATDs) in terms of the peak width for the Ac-Y$(AEAAKA)_2$F-NH_2 peptide ions, which indicates that the side-chain interactions of E/K pairs play important roles in the peptide gas-phase structures. In other words, the salt bridges between the E/K pairs likely contribute to the gas-phase structures, and blocking the side chains of E/K will limit the formation of structurally-related charge-solvated structures.

All in all, this dissertation focuses on developing the methodology of using mass spectrometry to understand the intrinsic peptide-metal interactions, and in particular, the relationship between the peptide gas-phase conformations and the metal coordination geometry. We proved that peptide fragmentation coupling with IM-MS and molecular simulations is a powerful approach to investigate the metal binding systems. Future directions would be focusing on using this methodology to investigate the metal binding for biologically important proteins and peptides. For example, one of the on-going projects in our group is studying the Cu^+ ions aggregation in β-amyloid, which is a crucial peptide involved in Alzheimer's disease. Some preliminary data suggests that the Cu^+ aggregation is

responsible for the gas-phase conformation change of β-amyloid. This study may shed light on the biological functions and pathways of copper aggregation in the development of Alzheimer's disease. In addition, as we mentioned in Chapter III, we have examined the arrival time distributions of the peptide-Cu^+ complexes for several histidine rich peptides via IM-MS; however, we only observe slightly difference of the collision cross-sections between the protonated peptide ions and Cu^+ adducted peptide ions (up to five Cu^+ ions attached). Considering that the ion mobility resolution of the instrument used for this study is not very high at present (<50), we will revisit this issue when the new IM-MS instrument building in our lab is ready for work (with a longer drift tube, it is expected to increase the ion mobility resolution up to 200).

The fragmentation chemistry of hybrid-metal binding systems, such as the peptide-metal complexes containing both alkali metal and copper ions is also an interesting issue. The binding chemistry of alkali metal to peptides is significantly different from that of the copper ions (Cu^+ and Cu^{2+}). That is, alkali metal ions do not bind to specific amino acid residues and the binding of alkali metal ions to peptides usually involves charge-charge or charge-dipole interactions (*i.e.*, alkali metal ions versus C-terminal carboxylate group). Our preliminary data suggests that the fragmentation reactions of the hybrid-metal complexes (*i.e.*, $[M + Na + Cu - H]^+$) are different from either that of the sodiated ions (*i.e.,* $[M + Na]^+$ and $[M + 2Na - H]^+$) or the

cupperated ions (*i.e.,* $[M + Cu]^+$ and $[M + 2Cu - H]^+$). For example, the fragment ion spectra of the $[M + Na + Cu - H]^+$ contains a series of c-type fragment ions which are not typical CID fragment ions for peptides, indicating that the fragmentation pathway for the hybrid metal complexes appears to be different from that for single metal containing complexes; however, the fragmentation mechanism for the hybrid-metal complexes is unclear at this moment. It is assumed that the correlation of the Na^+ and the Cu^+ ions might be involved in the fragmentation chemistry of peptide ions. Additional experiments and molecular modeling are needed to address this issue in the future.

We are also developing a modified trypsin digestion method on the basis of metal binding to facilitate peptide mapping via mass spectrometry. That is, protein samples are incubated with metal ions and thermally denatured, and then digested with trypsin. We observed significantly different mass spectra for the protein digest with Cu-incubation from that of the standard trypsin digestion, in terms of peptide mapping and amino acid sequence coverage. In particular, the Cu-incubation method seems to be more sensitive to the protein sequence. For example, the Cu-incubated Cytochrome C digest favors the detection of peptide fragments containing a specific sequence (TGPNLHGLFGRK); however, a similar pattern is not observed for the standard or the Ni-incubated digestion. It is possible that incubating with copper ions changes the protein structure in solution, which

affects the following enzymatic digestion experiments. This method could potentially increase the amino acid sequence coverage for peptide mapping, and thus enhance the confidence level for protein identification and characterization. Here again, the preliminary data discussed above reveals the potential advantages of studying metal ion binding chemistry in understanding the intrinsic functions of metal ions in biological systems and the applications in mass spectrometry based proteomics studies.

REFERENCES

1. Lippard, S. J.; Berg, J. M. *Principles of Bioinorganic Chemistry*; University Science Books: Mill Valley, CA, 1994.

2. Villafranca, J. J.; Desai, P. R. Copper Proteins: A Review of the Different Classes of Copper Proteins and an in-Depth Investigation of the Active Copper Sites in Dopamine Beta-Hydroxylase., *Biol. Oxid. Syst.* **1990**, *1*, 297-327.

3. Linder, M. C.; Hazegh-Azam, M. Copper Biochemistry and Molecular Biology, *Am J Clin Nutr*. **1996**, *63*, 797-811.

4. Kitajima, N.; Fujisawa, K.; Fujimoto, C.; Morooka, Y.; Hashimoto, S.; Kitagawa, T.; Toriumi, K.; Tatsumi, K.; Nakamura, A. A New Model for Dioxygen Binding in Hemocyanin - Synthesis, Characterization, and Molecular-Structure of the Mu-Eta-2-Eta-2 Peroxo Dinuclear Copper (II) Complexes, [Cu(Hb(3,5-R2pz)3)]2(O2) (R = Iso-Pr and Ph), *J. Am. Chem. Soc.* **1992**, *114*, 1277-1291.

5. Karlin, K. D.; Cruse, R. W.; Gultneh, Y.; Farooq, A.; Hayes, J. C.; Zubieta, J. Dioxygen Copper Reactivity - Reversible Binding of O_2 and Co to a Phenoxo-Bridged Dicopper(I) Complex, *J. Am. Chem. Soc.* **1987**, *109*, 2668-2679.

6. Decker, H.; Tuczek, F. Tyrosinase/Catecholoxidase Activity of Hemocyanins: Structural Basis and Molecular Mechanism, *Trends in Biochemical Sciences*. **2000**, *25*, 392-397.

7. Linder, M. C. *Biochemistry of Copper*; Plenum Press: New York, 1991.

8. Tsukihara, T.; Aoyama, H.; Yamashita, E.; Tomizaki, T.; Yamaguchi, H.; Shinzawaitoh, K.; Nakashima, R.; Yaono, R.; Yoshikawa, S. Structures of

Metal Sites of Oxidized Bovine Heart Cytochrome-C-Oxidase at 2.8 Angstrom, *Science*. **1995**, *269*, 1069-1074.

9. Alonso, J. R.; Cardellach, F.; Lopez, S.; Casademont, J.; Miro, O. Carbon Monoxide Specifically Inhibits Cytochrome C Oxidase of Human Mitochondrial Respiratory Chain, *Pharmacology & Toxicology*. **2003**, *93*, 142-146.

10. Voet, D.; Voet, J. G. *Biochemistry*; John Wiley & Sons: New York, 2004.

11. Sancenon, V.; Puig, S.; Mira, H.; Thiele, D. J.; Penarrubia, L. Identification of a Copper Transporter Family in *Arabidopsis Thaliana*, *Plant Molecular Biology*. **2003**, *51*, 577-587.

12. Pilon, M.; Abdel-Ghany, S. E.; Cohu, C. M.; Gogolin, K. A.; Ye, H. Copper Cofactor Delivery in Plant Cells, *Curr. Opin. Plant Biol.* **2006**, *9*, 256-263.

13. Marschner, H. *Mineral Nutrition of Higher Plants*; Academic Press: New York, 1995.

14. Masters, C. L.; Simms, G.; Weinman, N. A.; Multhaup, G.; McDonald, B. L.; Beyreuther, K. Amyloid Plaque Core Protein in Alzheimer's Disease and Down Syndrome, *Proc. Nat. Acad. Sci. USA*. **1985**, *82*, 4245-4249.

15. Roher, A. E.; Chaney, M. O.; Kuo, Y. M.; Webster, S. D.; Stine, W. B.; Haverkamp, L. J.; Woods, A. S.; Cotter, R. J.; Tuohy, J. M.; Krafft, G. A.; Bonnell, B. S.; Emmerling, M. R. Morphology and Toxicity of a Beta-(1-42) Dimer Derived from Neuritic and Vascular Amyloid Deposits of Alzheimer's Disease, *J. Biol. Chem*. **1996**, *271*, 20631-20635.

16. Raffa, D. F.; Gomez-Balderas, R.; Brunelle, P.; Rickard, G. A.; Rauk, A. Ab Initio Model Studies of Copper Binding to Peptides Containing a His-His

Sequence: Relevance to the Beta-Amyloid Peptide of Alzheimer's Disease, *J. Biol. Inorg. Chem*. **2005**, *10*, 887-902.

17. Valentine, J. S.; Gralla, E. B. *Advances in Protein Chemistry: Copper-Containing Proteins*; Academic Press: San Diego, CA, 2002.

18. Martell, A. E. *Metal Complexes in Aqueous Solutions*; Plenum Press: New York, 1996.

19. Lontie, R. *Copper Proteins and Copper Enzymes*; CRC Press, Boca Raton, FL, 1984.

20. Russell, D. H. *Gas Phase Inorganic Chemistry*; Plenum Press: New York, 1989.

21. Turecek, F. Copper-Biomolecule Complexes in the Gas Phase. The Ternary Way, *Mass Spectrometry Reviews*. **2007**, *26*, 563-582.

22. Gatlin, C. L.; Turecek, F.; Vaisar, T. Copper(II) Amino-Acid Complexes in the Gas-Phase, *J. Am. Chem. Soc.* **1995**, *117*, 3637-3638.

23. Russell, D. H.; McGlohon, E. S.; Mallis, L. M. Fast-Atom Bombardment Tandem Mass-Spectrometry Studies of Organo-Alkali-Metal Ions of Small Peptides - Competitive Interaction of Sodium with Basic Amino-Acid Substituents, *Anal. Chem.* **1988**, *60*, 1818-1824.

24. Grese, R. P.; Cerny, R. L.; Gross, M. L. Metal-Ion Peptide Interactions in the Gas-Phase - A Tandem Mass-Spectrometry Study of Alkali-Metal Cationized Peptides, *J. Am. Chem. Soc.* **1989**, *111*, 2835-2842.

25. Lausarot, P. M.; Operti, L.; Vaglio, G. A. Reactions of Cu(II) with Alpha-Amino-Acids Investigated by Fast-Atom-Bombardment (Fab) Mass-Spectrometry, *Org. Mass Spectrom*. **1991**, *26*, 51-52.

26. Hu, P. F.; Gross, M. L. Strong-Interactions of Anionic Peptides and Alkaline-Earth Metal-Ions - Metal-Ion-Bound Peptides in the Gas-Phase, *J. Am. Chem. Soc.* **1992**, *114*, 9153-9160.

27. Nelson, R. W.; Hutchens, T. W. Mass-Spectrometric Analysis of a Transition-Metal-Binding Peptide Using Matrix-Assisted Laser-Desorption Time-of-Flight Mass-Spectrometry - A Demonstration of Probe Tip Chemistry, *Rapid Commun. Mass Spectrom*. **1992**, *6*, 4-8.

28. Reiter, A.; Adams, J.; Zhao, H. Intrinsic (Gas-Phase) Binding of Co^{2+} and Ni^{2+} by Peptides - a Direct Reflection of Aqueous-Phase Chemistry, *J. Am. Chem. Soc.* **1994**, *116*, 7827-7838.

29. Bouchonnet, S.; Hoppilliard, Y.; Ohanessian, G. Formation and Fragmentations of Organometallic Complexes Involving Aliphatic Alpha-Amino-Acids and Transition-Metal Cations - A Plasma Desorption Mass-Spectrometry Study, *J. Mass Spectrom*. **1995**, *30*, 172-179.

30. Gatlin, C. L.; Turecek, F.; Vaisar, T. Gas-Phase Complexes of Amino-Acids with Cu(II) and Diimine Ligands.1. Aliphatic and Aromatic-Amino-Acids, *J. Mass Spectrom*. **1995**, *30*, 1605-1616.

31. Gatlin, C. L.; Turecek, F.; Vaisar, T. Gas-Phase Complexes of Amino-Acids with Cu(II) and Diimine Ligands.2. Amino-Acids with O, N and S Functional-Groups in the Side-Chain, *J. Mass Spectrom*. **1995**, *30*, 1617-1627.

32. Jiao, C. Q.; Freiser, B. S.; Carr, S. R.; Cassady, C. J. An Electrospray-Ionization Mass-Spectrometry Study of Copper Adducts of Protonated Ubiquitin, *J. Am. Soc. Mass. Spectrom*. **1995**, *6*, 521-524.

33. Wen, D.; Yalcin, T.; Harrison, A. G. Fragmentation Reactions of Cu^+-Cationated Alpha-Amino-Acids, *Rapid Commun. Mass Spectrom*. **1995**, *9*, 1155-1157.

34. Woods, A. S.; Buchsbaum, J. C.; Worrall, T. A.; Berg, J. M.; Cotter, R. J. Matrix-Assisted Laser Desorption/Ionization of Noncovalently Bound Compounds, *Anal. Chem*. **1995**, *67*, 4462-4465.

35. Hornshaw, M. P.; McDermott, J. R.; Candy, J. M. Copper-Binding to the N-Terminal Tandem Repeat Regions of Mammalian and Avian Prion Protein, *Biochemical and Biophysical Research Communications*. **1995**, *207*, 621-629.

36. Shields, S. J.; Bluhm, B. K.; Russell, D. H. Fragmentation Chemistry of $[M+Cu]^+$ Peptide Ions Containing an N-Terminal Arginine, *J. Am. Soc. Mass. Spectrom*. **2000**, *11*, 626-638.

37. McLuckey, S. A.; Cameron, D.; Cooks, R. G. Proton Affinities from Dissociations of Proton-Bound Dimers, *J. Am. Chem. Soc.* **1981**, *103*, 1313-1317.

38. Cooks, R. G.; Patrick, J. S.; Kotiaho, T.; McLuckey, S. A. Thermochemical Determinations by the Kinetic Method, *Mass Spectrometry Reviews*. **1994**, *13*, 287-339.

39. McLuckey, S. A.; Schoen, A. E.; Cooks, R. G. Silver Ion Affinities of Alcohols as Ordered by Mass-Spectrometry Mass-Spectrometry, *J. Am. Chem. Soc.* **1982**, *104*, 848-850.

40. Eberlin, M. N.; Majumdar, T. K.; Cooks, R. G. Structures and Mechanisms of Reactions of Isomeric $C_2H_3O^+$ and $C_2H_3S^+$ Ions Revealed

through Ion Molecule Reactions in Conjunction with 2d and 3d Mass-Spectrometry, *J. Am. Chem. Soc.* **1992**, *114*, 2884-2896.

41. Burinsky, D. J.; Fukuda, E. K.; Campana, J. E. Electron-Affinities from Dissociations of Mixed Negative-Ion Dimers, *J. Am. Chem. Soc.* **1984**, *106*, 2770-2771.

42. Cerda, B. A.; Wesdemiotis, C. The Relative Copper(I) Ion Affinities of Amino-Acids in the Gas-Phase, *J. Am. Chem. Soc.* **1995**, *117*, 9734-9739.

43. Robinson, P. J.; Holbrook, K. A. *Unimolecular Reactions*; Wiley Interscience: London, 1972.

44. Hillenkamp, F.; Karas, M.; Holtkamp, D.; Klusener, P. Energy Deposition in Ultraviolet-Laser Desorption Mass-Spectrometry of Biomolecules, *Int. J. Mass Spectrom.* **1986**, *69*, 265-276.

45. Karas, M.; Bachmann, D.; Hillenkamp, F. Influence of the Wavelength in High-Irradiance Ultraviolet-Laser Desorption Mass-Spectrometry of Organic-Molecules, *Anal. Chem.* **1985**, *57*, 2935-2939.

46. Karas, M.; Bahr, U. Laser Desorption Mass-Spectrometry, *Trac-Trends in Analytical Chemistry*. **1986**, *5*, 90-93.

47. Karas, M.; Bachmann, D.; Bahr, U.; Hillenkamp, F. Matrix-Assisted Ultraviolet-Laser Desorption of Nonvolatile Compounds, *Int. J. Mass Spectrom.* **1987**, *78*, 53-68.

48. Karas, M.; Hillenkamp, F. Laser Desorption Ionization of Proteins with Molecular Masses Exceeding 10000 Daltons, *Anal. Chem*. **1988**, *60*, 2299-2301.

49. Koichi, T.; Hiroaki, W.; Yutaka, I.; Satoshi, A.; Yoshikazu, Y.; Tamio, Y.; Matsuo, T. Protein and Polymer Analyses up to M/Z 100 000 by Laser Ionization Time-of-Flight Mass Spectrometry, *Rapid Commun. Mass Spectrom*. **1988**, *2*, 151-153.

50. Bluhm, B. K.; Shields, S. J.; Bayse, C. A.; Hall, M. B.; Russell, D. H. Determination of Copper Binding Sites in Peptides Containing Basic Residues: A Combined Experimental and Theoretical Study, *Int. J. Mass Spectrom.* **2001**, *204*, 31-46.

51. Prudent, M.; Girault, H. H. On-Line Electrogeneration of Copper-Peptide Complexes in Microspray Mass Spectrometry, *J. Am. Soc. Mass. Spectrom*. **2008**, *19*, 560-568.

52. Zenobi, R.; Knochenmuss, R. Ion Formation in MALDI Mass Spectrometry, *Mass Spectrometry Reviews*. **1998**, *17*, 337-366.

53. Zhang, J.; Frankevich, V.; Knochenmuss, R.; Friess, S. D.; Zenobi, R. Reduction of Cu(II) in Matrix-Assisted Laser Desorption/Ionization Mass Spectrometry, *J. Am. Soc. Mass. Spectrom*. **2003**, *14*, 42-50.

54. Lim, J.; Vachet, R. W. Development of a Methodology Based on Metal-Catalyzed Oxidation Reactions and Mass Spectrometry to Determine the Metal Binding Sites in Copper Metalloproteins, *Anal. Chem*. **2003**, *75*, 1164-1172.

55. Bridgewater, J. D.; Vachet, R. W. Using Microwave-Assisted Metal-Catalyzed Oxidation Reactions and Mass Spectrometry to Increase the Rate at Which the Copper-Binding Sites of a Protein Are Determined, *Anal. Chem*. **2005**, *77*, 4649-4653.

56. Bridgewater, J. D.; Lim, J.; Vachet, R. W. Using Metal-Catalyzed Oxidation Reactions and Mass Spectrometry to Identify Amino Acid Residues within 10 Angstrom of the Metal in Cu-Binding Proteins, *J. Am. Soc. Mass. Spectrom*. **2006**, 1552-1559.

57. Biemann, K. Nomenclature for Peptide Fragment Ions (Positive-Ions), *Methods Enzymol*. **1990**, *193*, 886-887.

58. Yalcin, T.; Wang, J. Y.; Wen, D.; Harrison, A. G. C-C and C-H Bond Activation in the Fragmentation of the [M+Ni](+) Adducts of Aliphatic Amino Acids, *J. Am. Soc. Mass. Spectrom*. **1997**, *8*, 749-755.

59. Shields, S. J.; Bluhm, B. K.; Russell, D. H. Novel Method for $[M+Cu]^+$ Ion Formation by Matrix-Assisted Laser Desorption Ionization, *Int. J. Mass Spectrom.* **1999**, *183*, 185-195.

60. Wu, Z.; Fernandez-Lima, F. A.; Perez, L. M.; Russell, D. H. A New Copper Containing Maldi Matrix That Yields High Abundances of [Peptide + $Cu]^+$ Ions, *J. Am. Soc. Mass. Spectrom.* **2009**, *20*, 1263-1271.

61. Greenlee, W. J.; Thorsett, E. D. Mild Conversion of Carboxamides and Carboxylic-Acid Hydrazides to Acids and Esters, *J. Org. Chem.* . **1981**, *46*, 5351-5353.

62. Corey, N. W. L.; Eric, D. L. R.; Ma, C. Y.; Ivan, K. C. Non-Zwitterionic Structures of Aliphatic-Only Peptides Mediated the Formation and Dissociation of Gas Phase Radical Cations, *J. Mass Spectrom*. **2006**, *41*, 931-938.

63. Agterberg, F. P. W.; Kluit, H.; Driessen, W. L.; Oevering, H.; Buijs, W.; Lakin, M. T.; Spek, A. L.; Reedijk, J. Dinuclear Paddle-Wheel Copper(Ii) Carboxylates in the Catalytic Oxidation of Carboxylic Acids. Unusual

Polymeric Chains Found in the Single-Crystal X-Ray Structures of [Tetrakis(Mu-1-Phenylcyclopropane-1-Carboxylato-O,O')Bis(Ethanol-O)Dicop Per(Ii)] and Catena-Poly[[Bis(Mu-Diphenylacetato-O:O')Dicopper](Mu(3)-Diphenylacetato -1-O:2-O':1'-O')-(Mu(3)-Diphenylacetato-1-O:2-O':2'-O')], *Inorg. Chem*. **1997**, *36*, 4321-4328.

64. Lee, C. T.; Yang, W. T.; Parr, R. G. Development of the Colle-Salvetti Correlation-Energy Formula into a Functional of the Electron-Density, *Phys. Rev. B*. **1988**, *37*, 785-789.

65. Becke, A. D. Density-Functional Thermochemistry. 3. The Role of Exact Exchange, *J. Chem. Phys.* **1993**, *98*, 5648-5652.

66. Stephens, P. J.; Devlin, F. J.; Chabalowski, C. F.; Frisch, M. J. *Ab Initio* Calculation of Vibrational Absorption and Circular-Dichroism Spectra Using Density-Functional Force-Fields, *J. Phys. Chem.* **1994**, *98*, 11623-11627.

67. Dolg, M.; Wedig, U.; Stoll, H.; Preuss, H. Energy-Adjusted *Ab Initio* Pseudopotentials for the 1st-Row Transition-Elements, *J. Chem. Phys.* **1987**, *86*, 866-872.

68. Krishnan, R.; Binkley, J. S.; Seeger, R.; Pople, J. A. Self-Consistent Molecular-Orbital Methods. 20. Basis Set for Correlated Wave-Functions, *J. Chem. Phys.* **1980**, *72*, 650-654.

69. Frisch, M. J.; Pople, J. A.; Binkley, J. S. Self-Consistent Molecular-Orbital Methods. 25. Supplementary Functions for Gaussian-Basis Sets, *J. Chem. Phys.* **1984**, *80*, 3265-3269.

70. Frisch, M. J.; Schlegel, H. B.; Scuseria, G. E.; Robb, M. A.; Cheeseman, J. R.; et al. Gaussian 03, Revision C.02 ed.; Gaussian: Wallingford, CT, 2004.

71. Liu, F.; Press, M. R.; Khanna, S. N.; Jena, P. Stability of Doubly Charged Transition-Metal Dimers, *Phys. Rev. Lett*. **1987**, *59*, 2562-2565.

72. Salih, B.; Masselon, C.; Zenobi, R. Matrix-Assisted Laser Desorption/Ionization Mass Spectrometry of Noncovalent Protein Transition Metal Ion Complexes, *J. Mass Spectrom*. **1998**, *33*, 994-1002.

73. Abajian, C.; Yatsunyk, L. A.; Ramirez, B. E.; Rosenzweig, A. C. Yeast Cox17 Solution Structure and Copper(I) Binding, *J. Biol. Chem*. **2004**, *279*, 53584-53592.

74. Arnesano, F.; Balatri, E.; Banci, L.; Bertini, I.; Winge, D. R. Folding Studies of Cox17 Reveal an Important Interplay of Cysteine Oxidation and Copper Binding, *Structure*. **2005**, *13*, 713-722.

75. Fujiwara, N.; Nakano, M.; Kato, S.; Yoshihara, D.; Ookawara, T.; Eguchi, H.; Taniguchi, N.; Suzuki, K. Oxidative Modification to Cysteine Sulfonic Acid of Cys(111) in Human Copper-Zinc Superoxide Dismutase, *J. Biol. Chem*. **2007**, *282*, 35933-35944.

76. De Beus, M. D.; Chung, J. Y.; Colon, W. Modification of Cysteine 111 in Cu/Zn Superoxide Dismutase Results in Altered Spectroscopic and Biophysical Properties, *Protein Science*. **2004**, *13*, 1347-1355.

77. Hay, R. W. *Bio-Inorganic Chemistry*; Ellis Honvood Limited: Chichester, UK, 1984.

78. Kaim, W.; Schwederski, B. *Bioinorganic Chemistry: Inorganic Elements in the Chemistry of Life*; John Wiley & Sons: Chichester, UK, 1994.

79. Zheng, H.; Chruszcz, M.; Lasota, P.; Lebioda, L.; Minor, W. Data Mining of Metal Ion Environments Present in Protein Structures, *Journal of Inorganic Biochemistry*. **2008**, *102*, 1765-1776.

80. Hodgson, E. K.; Fridovich, I. Interaction of Bovine Erythrocyte Superoxide-Dismutase with Hydrogen-Peroxide-Chemiluminescence and Peroxidation, *Biochemistry*. **1975**, *14*, 5299-5303.

81. Chaparro, A. L.; Vachet, R. W. Tandem Mass Spectrometry of Cu(II) Complexes: The Effects of Ligand Donor Group on Dissociation, *J. Mass Spectrom*. **2003**, *38*, 333-342.

82. Combariza, M. Y.; Fahey, A. M.; Milshteyn, A.; Vachet, R. W. Gas-Phase Ion-Molecule Reactions of Divalent Metal Complex Ions: Toward Coordination Structure Analysis by Mass Spectrometry and Some Intrinsic Coordination Chemistry Along the Way, *Int. J. Mass Spectrom.* **2005**, *244*, 109-124.

83. Tian, Z. X.; Pawlow, A.; Poutsma, J. C.; Kass, S. R. Are Carboxyl Groups the Most Acidic Sites in Amino Acids? Gas-Phase Acidity, H/D Exchange Experiments, and Computations on Cysteine and Its Conjugate Base, *J. Am. Chem. Soc.* **2007**, *129*, 5403-5407.

84. Sechi, S.; Chait, B. T. Modification of Cysteine Residues by Alkylation. A Tool in Peptide Mapping and Protein Identification, *Anal. Chem*. **1998**, *70*, 5150-5158.

85. Crankshaw, M. W.; Grant, G. A. Modification of Cysteine, *Current Protocols in Protein Science*. **1996**, *15*, 1-18.

86. Hay, P. J.; Wadt, W. R. *Ab Initio* Effective Core Potentials for Molecular Calculations-Potentials for K to Au Including the Outermost Core Orbitals, *J. Chem. Phys.* **1985**, *82*, 299-310.

87. Jaguar 6.0 manual; Schroedinger Inc: Portland, OR, 2004.

88. Men, L. J.; Wang, Y. S. Fragmentation of the Deprotonated Ions of Peptides Containing Cysteine, Cysteine Sulfinic Acid, Cysteine Sulfonic Acid, Aspartic Acid, and Glutamic Acid, *Rapid Commun. Mass Spectrom*. **2006**, *20*, 777-784.

89. Bestor, T. H. Gene Silencing - Methylation Meets Acetylation, *Nature*. **1998**, *393*, 311-312.

90. Hisada, M.; Konno, K.; Itagaki, Y.; Naoki, H.; Nakajima, T. Advantages of Using Nested Collision Induced Dissociation/Post-Source Decay with Matrix-Assisted Laser Desorption/Ionization Time-of-Flight Mass Spectrometry: Sequencing of Novel Peptides from Wasp Venom, *Rapid Commun. Mass Spectrom*. **2000**, *14*, 1828-1834.

91. Ma, M. M.; Kutz-Naber, K. K.; Li, L. J. Methyl Esterification Assisted MALDI FT MS Characterization of the Orcokinin Neuropeptide Family, *Anal. Chem*. **2007**, *79*, 673-681.

92. Kuo, M. H.; Allis, C. D. Roles of Histone Acetyltransferases and Deacetylases in Gene Regulation, *Bioessays*. **1998**, *20*, 615-626.

93. Marzio, G.; Wagener, C.; Gutierrez, M. I.; Cartwright, P.; Helin, K.; Giacca, M. E2f Family Members Are Differentially Regulated by Reversible Acetylation, *J. Biol. Chem*. **2000**, *275*, 10887-10892.

94. Fu, M. F.; Wang, C. G.; Zhang, X. P.; Pestell, R. G. Acetylation of Nuclear Receptors in Cellular Growth and Apoptosis, *Biochemical Pharmacology*. **2004**, *64*, 1199-1208.

95. Abraham, J.; Kelly, J.; Thibault, P.; Benchimol, S. Post-Translational Modification of P53 Protein in Response to Ionizing Radiation Analyzed by Mass Spectrometry, *Journal of Molecular Biology*. **2000**, *295*, 853-864.

96. Scholtz, J. M.; Hong, Q.; York, E. J.; Stewart, J. M.; Baldwin, R. L. Parameters of Helix-Coil Transition Theory for Alanine-Based Peptides of Varying Chain Lengths in Water, *Biopolymers*. **1991**, *31*, 1463-1470.

97. Rohl, C. A.; Scholtz, J. M.; York, E. J.; Stewart, J. M.; Baldwin, R. L. Kinetics of Amide Proton-Exchange in Helical Peptides of Varying Chain Lengths - Interpretation by the Lifson-Roig Equation, *Biochemistry*. **1992**, *31*, 1263-1269.

98. Hudgins, R. R.; Ratner, M. A.; Jarrold, M. F. Design of Helices That Are Stable in Vacuo, *J. Am. Chem. Soc.* **1998**, *120*, 12974-12975.

99. Hudgins, R. R.; Mao, Y.; Ratner, M. A.; Jarrold, M. F. Conformations of Gly(N)H(+) and Ala(N)H(+) Peptides in the Gas Phase, *Biophysical Journal*. **1999**, *76*, 1591-1597.

100. Sudha, R.; Kohtani, M.; Breaux, G. A.; Jarrold, M. F. Pi-Helix Preference in Unsolvated Peptides, *J. Am. Chem. Soc.* **2004**, *126*, 2777-2784.

101. McLean, J. R.; McLean, J. A.; Wu, Z.; Becker, C.; Perez, L. M.; Pace, C. N.; Scholtz, J. M.; Russell, D. H. Factors That Influence Helical Preferences for Singly Charged Gas-Phase Peptide Ions: The Effects of Multiple Potential Charge-Carrying Sites, *J. Phys. Chem. B*. **2009**, *109*, 809-816.

102. Mason, E. A.; McDaniel, E. W. *Transport Properties of Ions in Gases*; Wiley Interscience: New York, 1988.

103. Jarrold, M. F. Peptides and Proteins in the Vapor Phase, *Annual Review of Physical Chemistry*. **2000**, *51*, 179-207.

104. Wyttenbach, T.; Bowers, M. T. *Gas-Phase Conformations: The Ion Mobility/Ion Chromatography Method*; Springer-Verlag: Berlin, 2003.

105. McLean, J. A.; Ruotolo, B. T.; Gillig, K. J.; Russell, D. H. Ion Mobility-Mass Spectrometry: A New Paradigm for Proteomics, *Int. J. Mass Spectrom.* **2005**, *240*, 301-315.

106. Meot-Ner, M. The Proton Affinity Scale, and Effects of Ion Structure and Solvation, *Int. J. Mass Spectrom.* **2003**, *227*, 525-554.

107. McMahon, T. B. Thermochemical Ladders: Scaling the Ramparts of Gaseous Ion Energetics, *Int. J. Mass Spectrom.* **2000**, *200*, 187-199.

108. Harrison, A. G. The Gas-Phase Basicities and Proton Affinities of Amino Acids and Peptides, *Mass Spectrometry Reviews*. **1997**, *16*, 201-217.

109. Raznikov, V. V.; Soulimenkov, I. V.; Kozlovski, V. I.; Pikhtelev, A. R.; Raznikova, M. O.; Horwath, T.; Kholomeev, A. A.; Zhou, Z.; Wollnik, H.; Dodonov, A. F. Ion Rotating Motion in a Gas-Filled Radio-Frequency Quadrupole Ion Guide as a New Technique for Structural and Kinetic Investigations of Ions, *Rapid Commun. Mass Spectrom*. **2001**, *15*, 1912-1921.

APPENDIX A

FIGURE Page

FIGURE Page

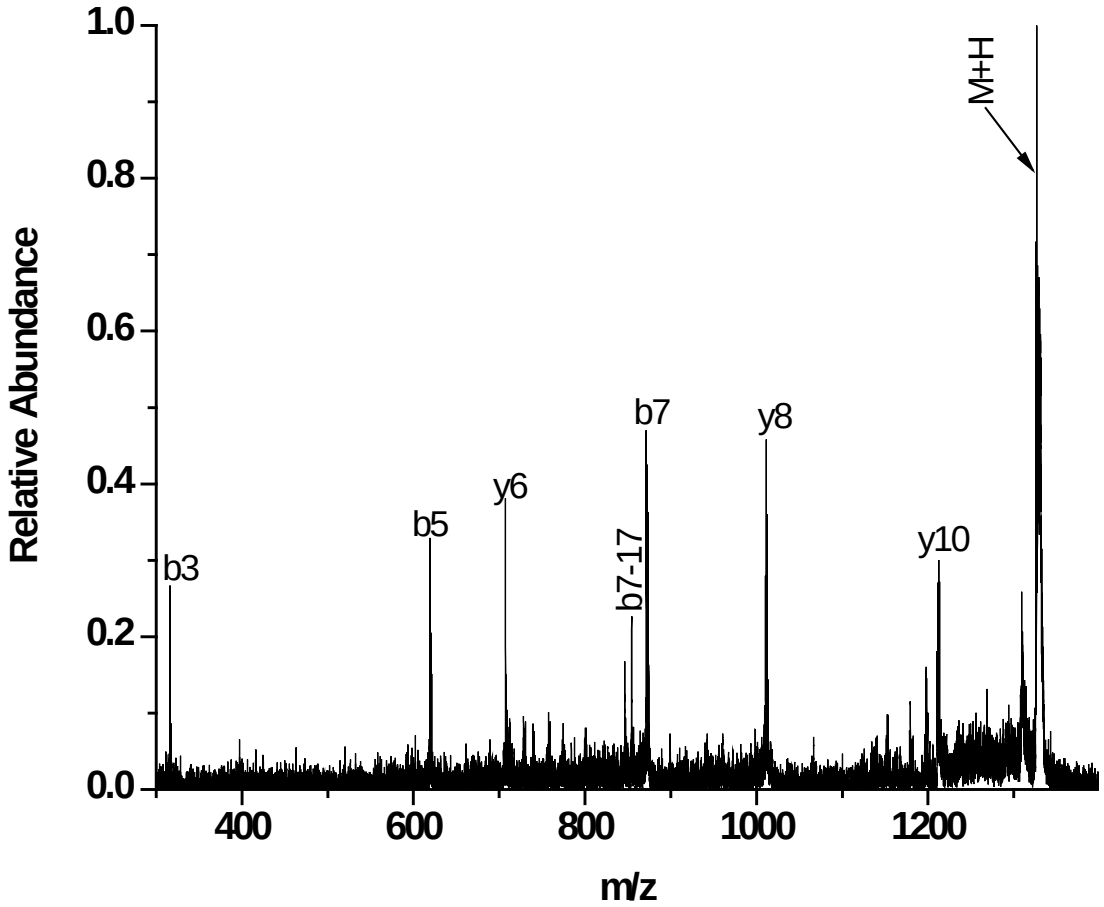

Figure A1. Fragment ion spectrum of the $[M + H]^+$ ion of β-amyloid (1-11) (DAEFRHDSGYE).

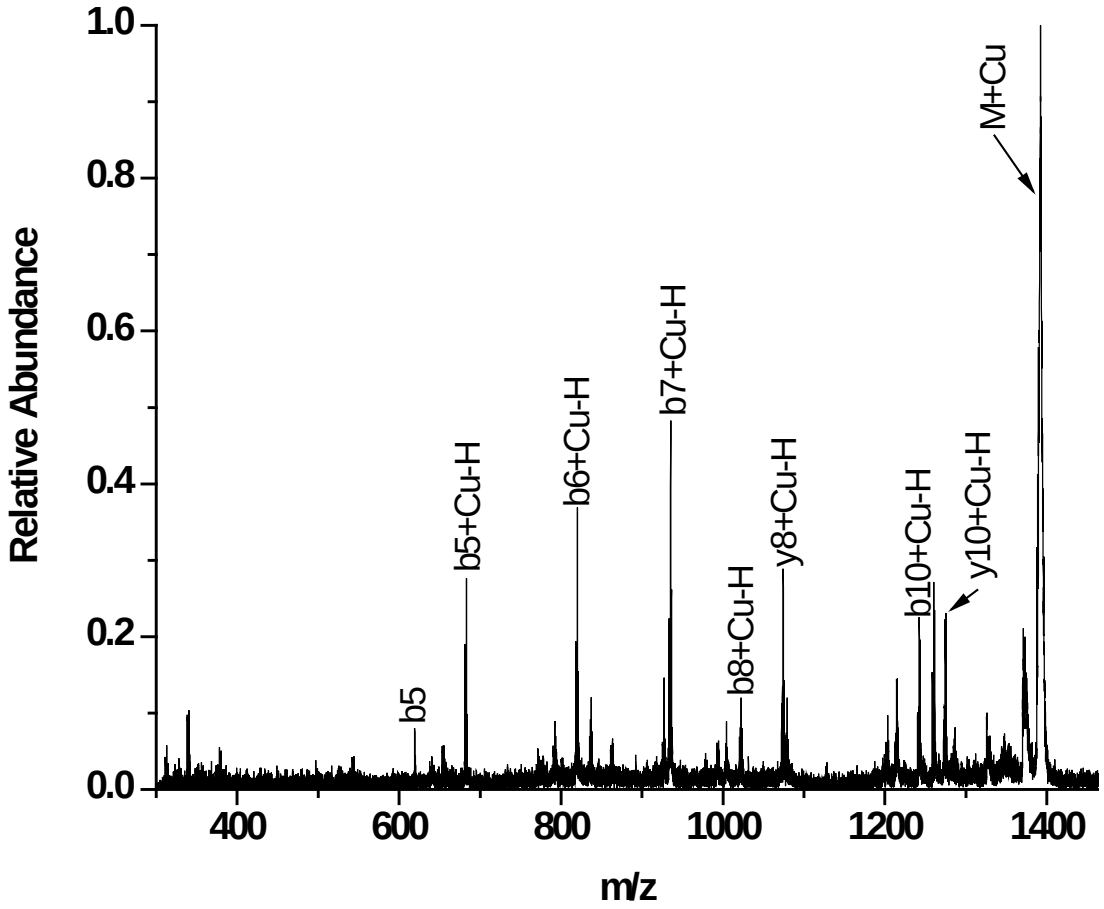

Figure A2. Fragment ion spectrum of the $[M + Cu]^+$ ion of β-amyloid (1-11) (DAEFRHDSGYE).

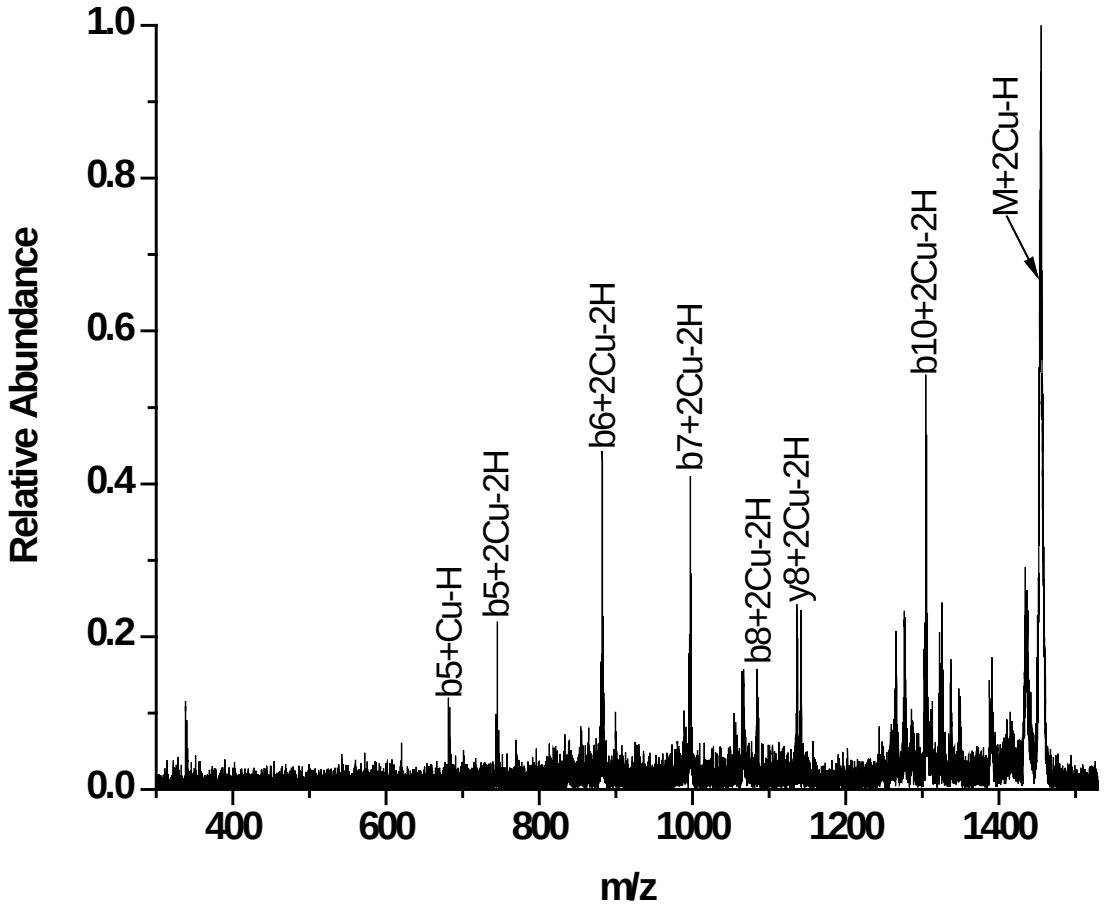

Figure A3. Fragment ion spectrum of the $[M + 2Cu - H]^+$ ion of β-amyloid (1-11) (DAEFRHDSGYE).

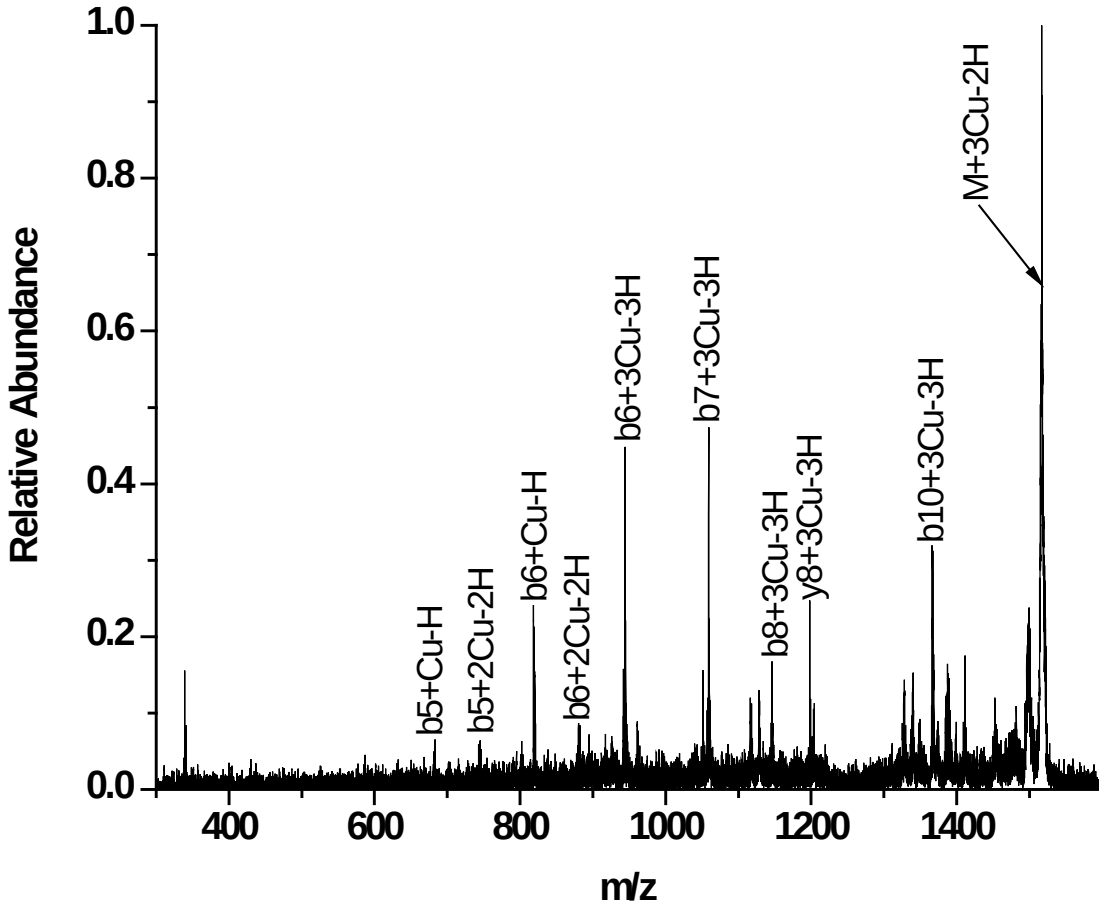

Figure A4. Fragment ion spectrum of the $[M + 3Cu - 2H]^+$ ion of β-amyloid (1-11) (DAEFRHDSGYE).

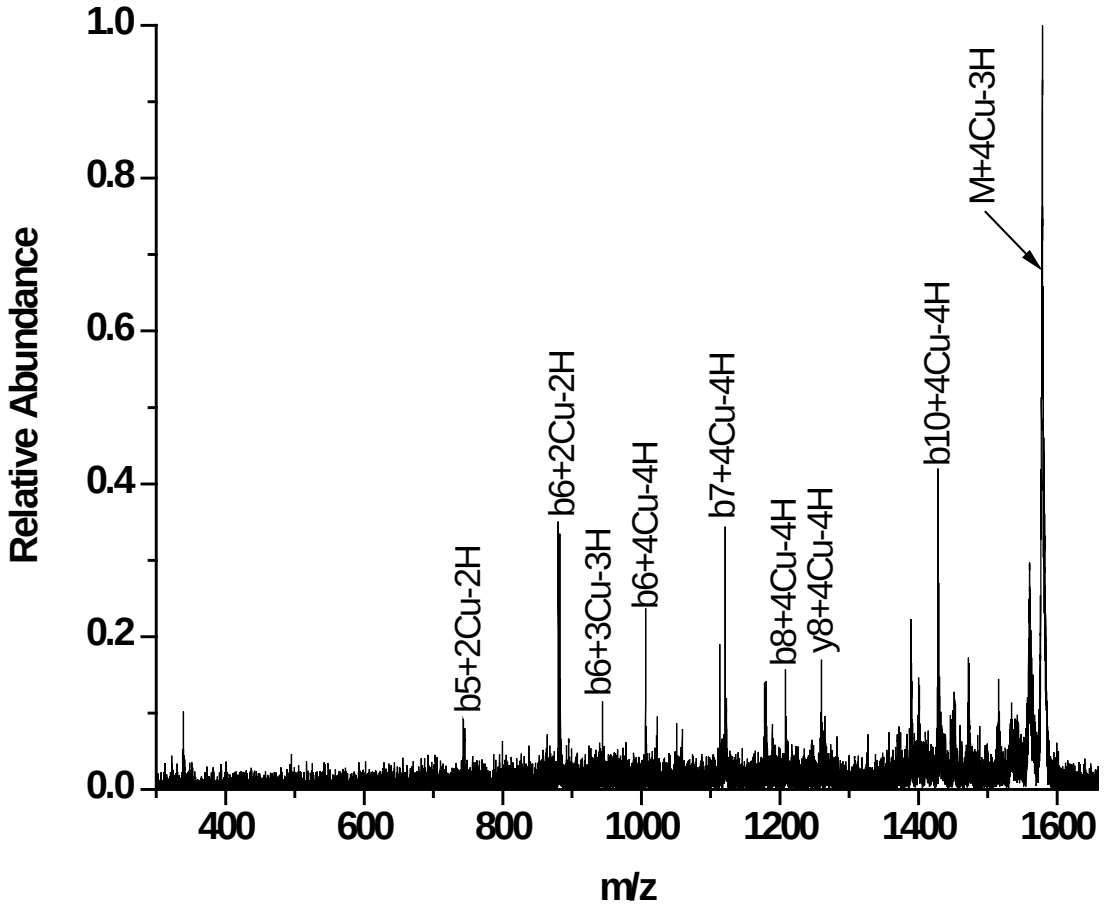

Figure A5. Fragment ion spectrum of the $[M + 4Cu - 3H]^+$ ion of β-amyloid (1-11) (DAEFRHDSGYE).

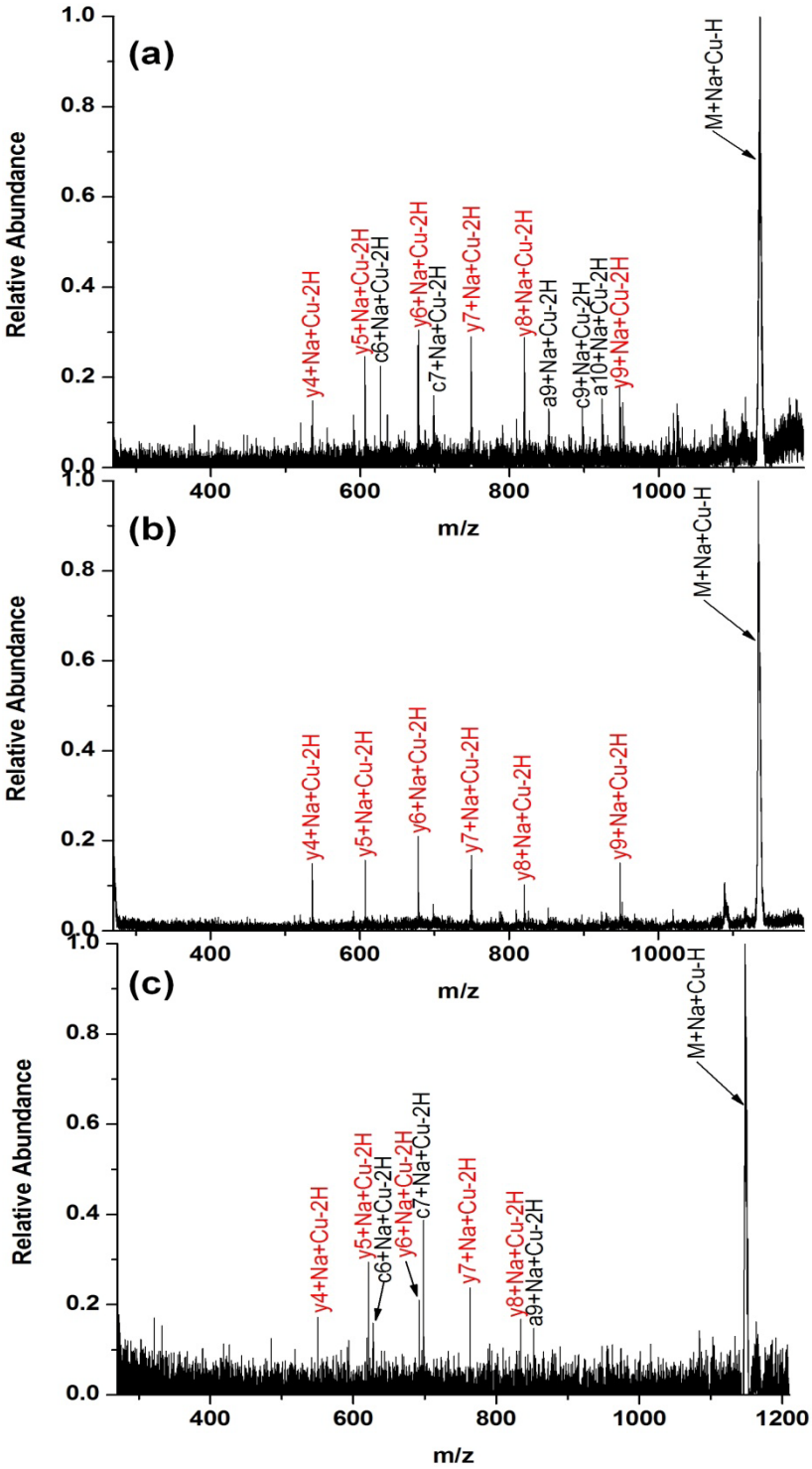

Figure A6. Fragment ion spectra of the $[M+Na+Cu-H]^+$ ions of (a) Ac-$(AAKAA)_2$Y-amide, (b) Ac-$(AAKAA)_2$Y-acid and (c) Ac-$(AAKAA)_2$Y-ester.

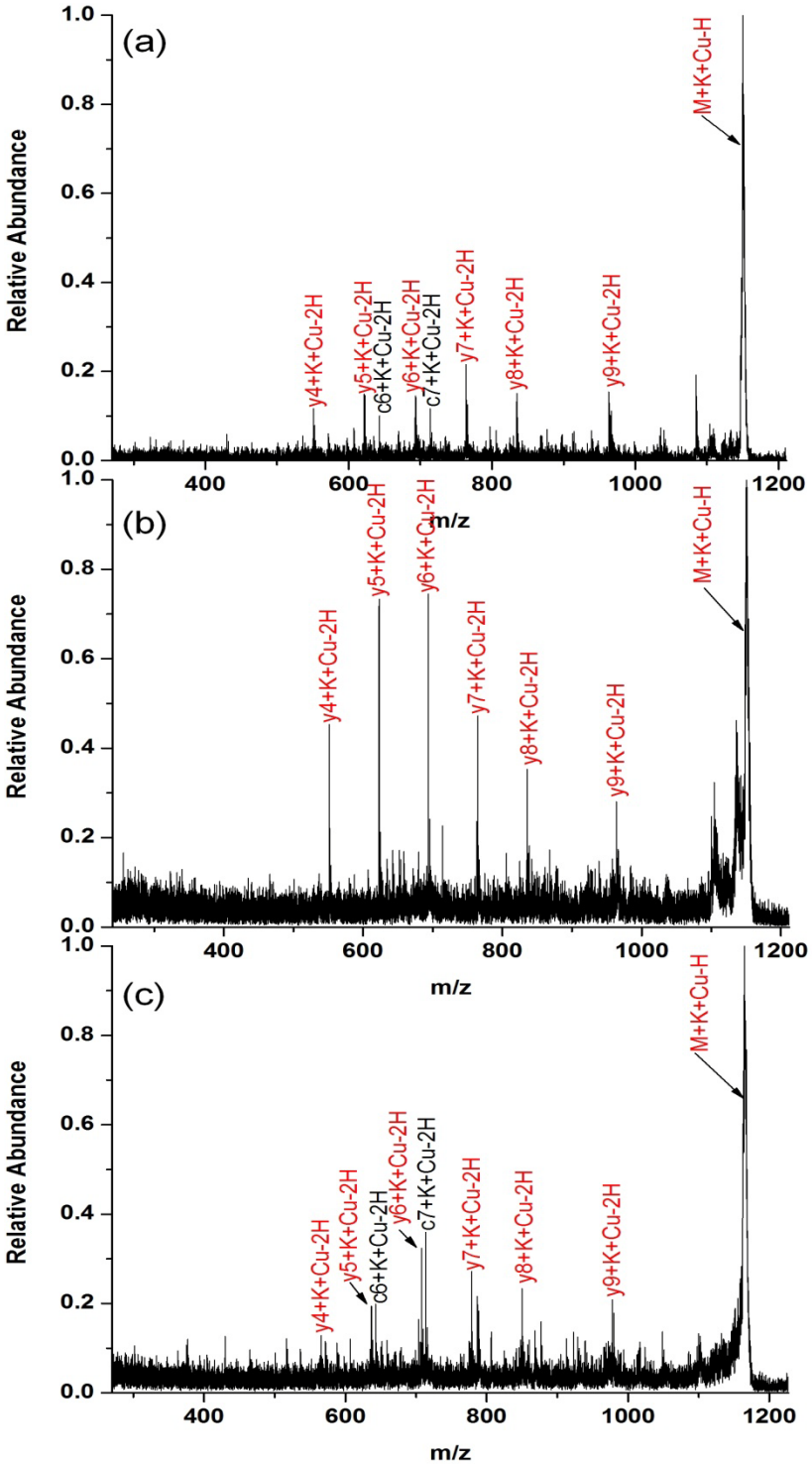

Figure A7. Fragment ion spectra of the $[M+K+Cu-H]^+$ ions of (a) Ac-$(AAKAA)_2$Y-amide, (b) Ac-$(AAKAA)_2$Y-acid and (c) Ac-$(AAKAA)_2$Y-ester.

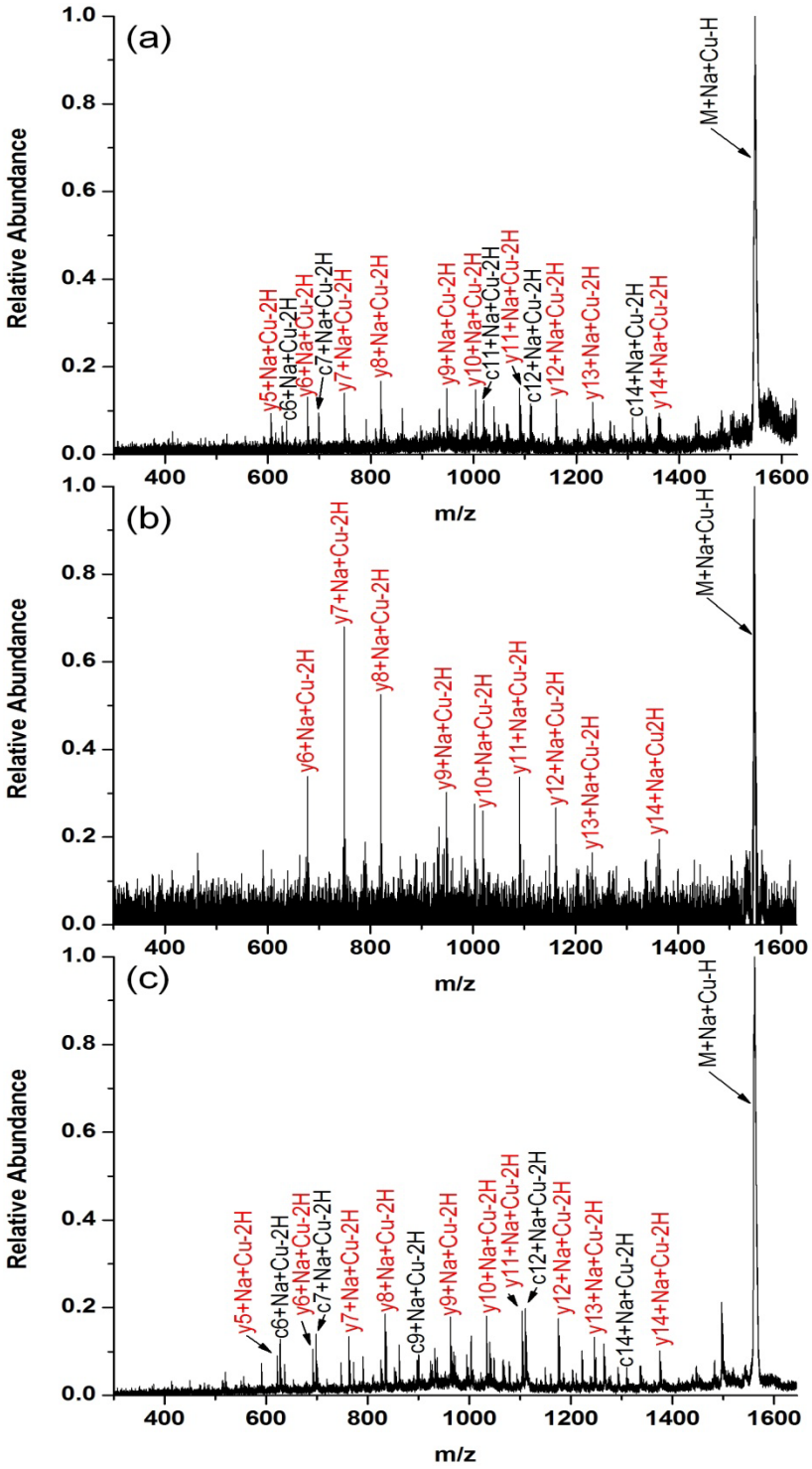

Figure A8. Fragment ion spectra of the $[M+Na+Cu-H]^+$ ions of (a) Ac-$(AAKAA)_3$Y-amide, (b) Ac-$(AAKAA)_3$Y-acid and (c) Ac-$(AAKAA)_3$Y-ester.

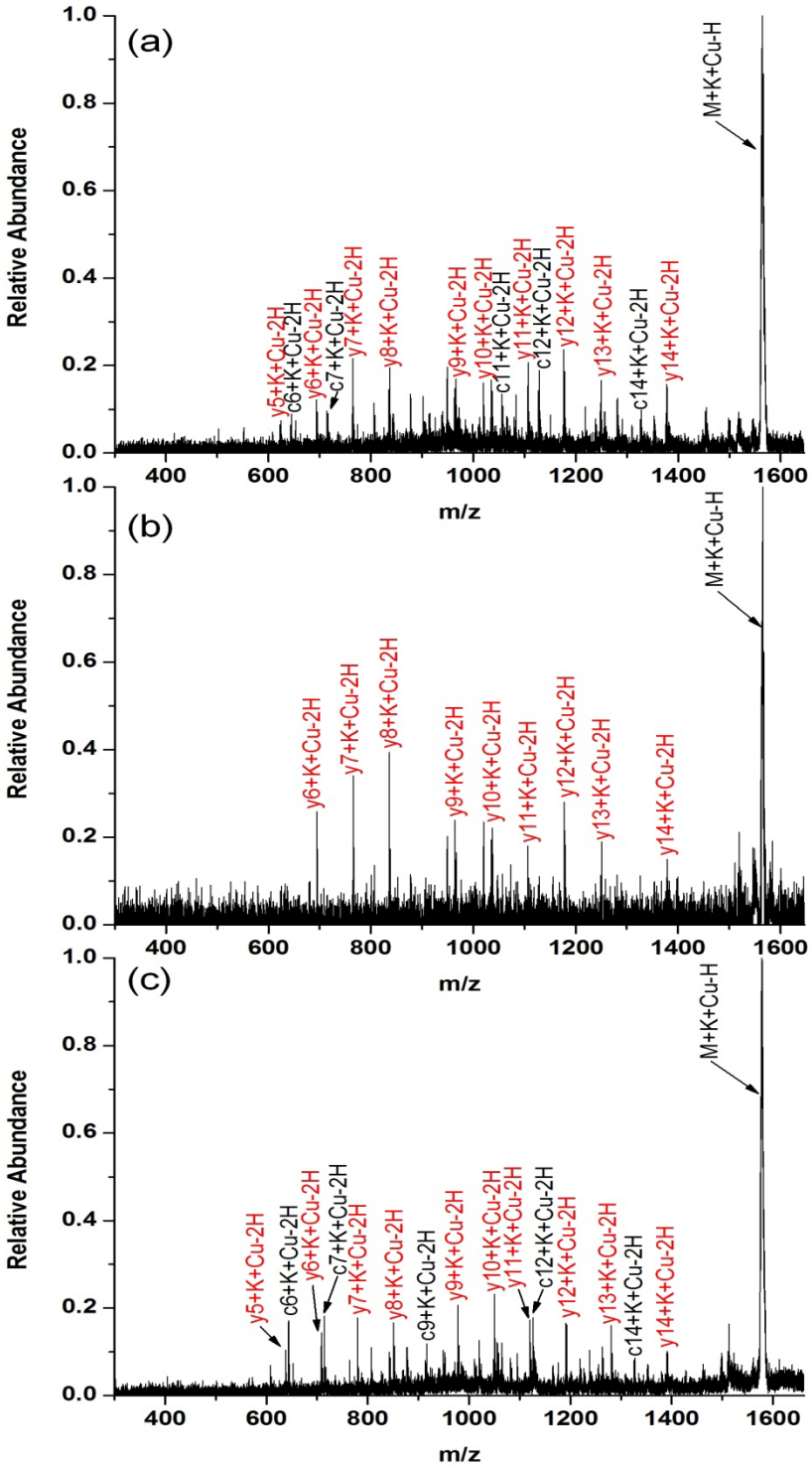

Figure A9. Fragment ion spectra of the $[M+K+Cu-H]^+$ ions of (a) Ac-$(AAKAA)_3$Y-amide, (b) Ac-$(AAKAA)_3$Y-acid and (c) Ac-$(AAKAA)_3$Y-ester.

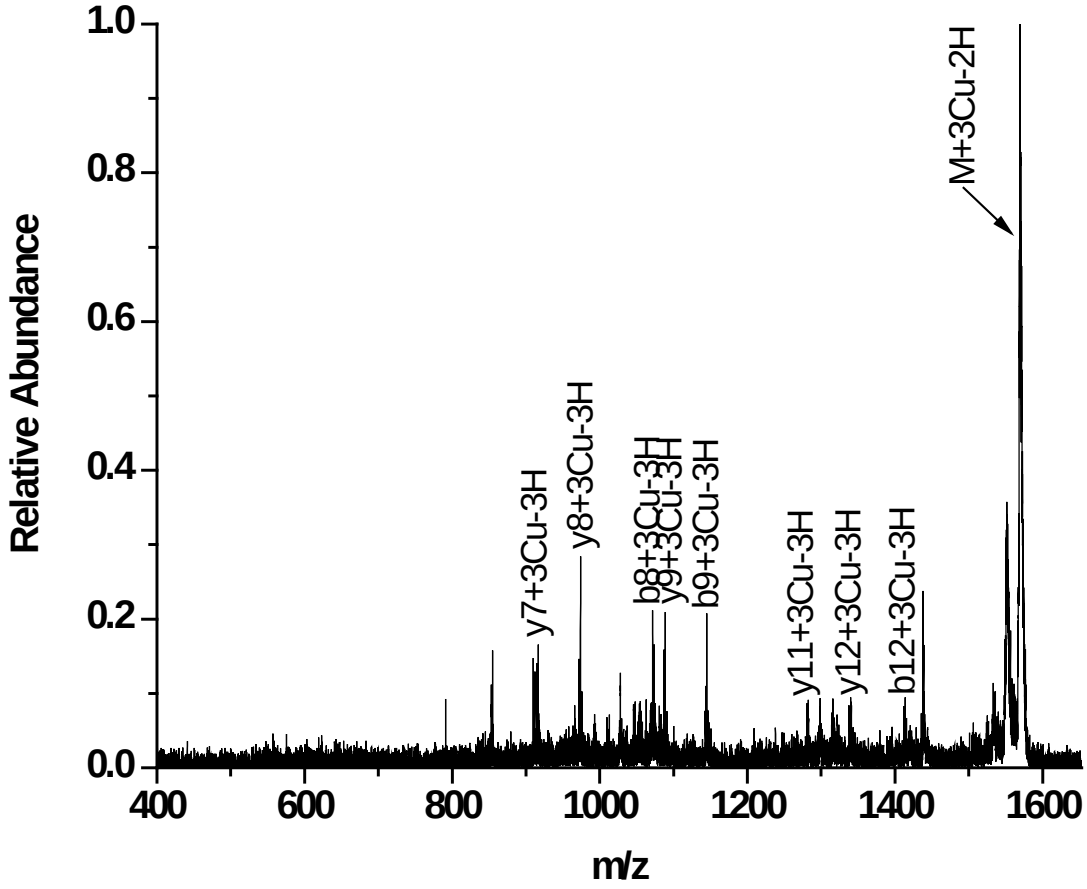

Figure A10. Fragment ion spectra of the $[M + 3Cu - 2H]^+$ ions of Ac-WGGHDGPHAPGDH-NH_2.

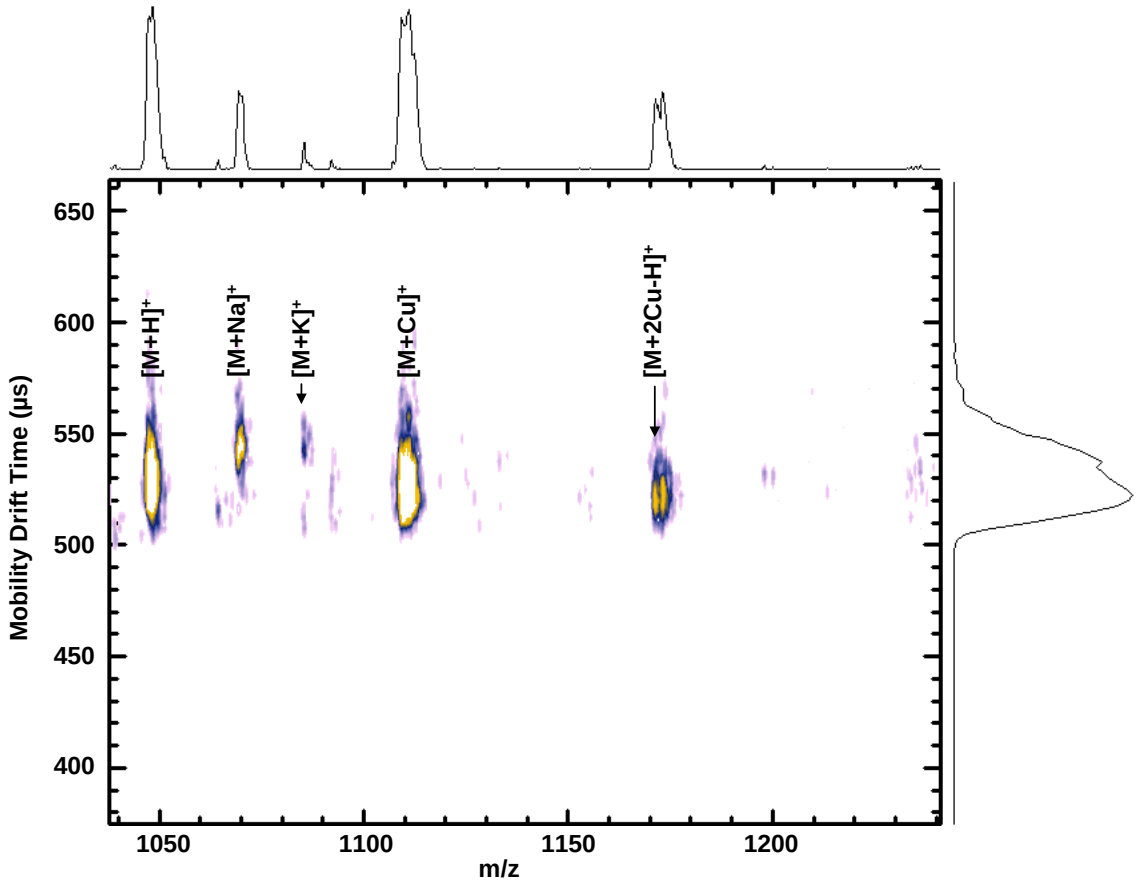

Figure A11. 2-D ion mobility mass spectrum of the $[M + xCu – (x-1)H]^+$ (x = 1 – 2) ions for the peptide Ac-AAKAAAAKAAY-NH_2.

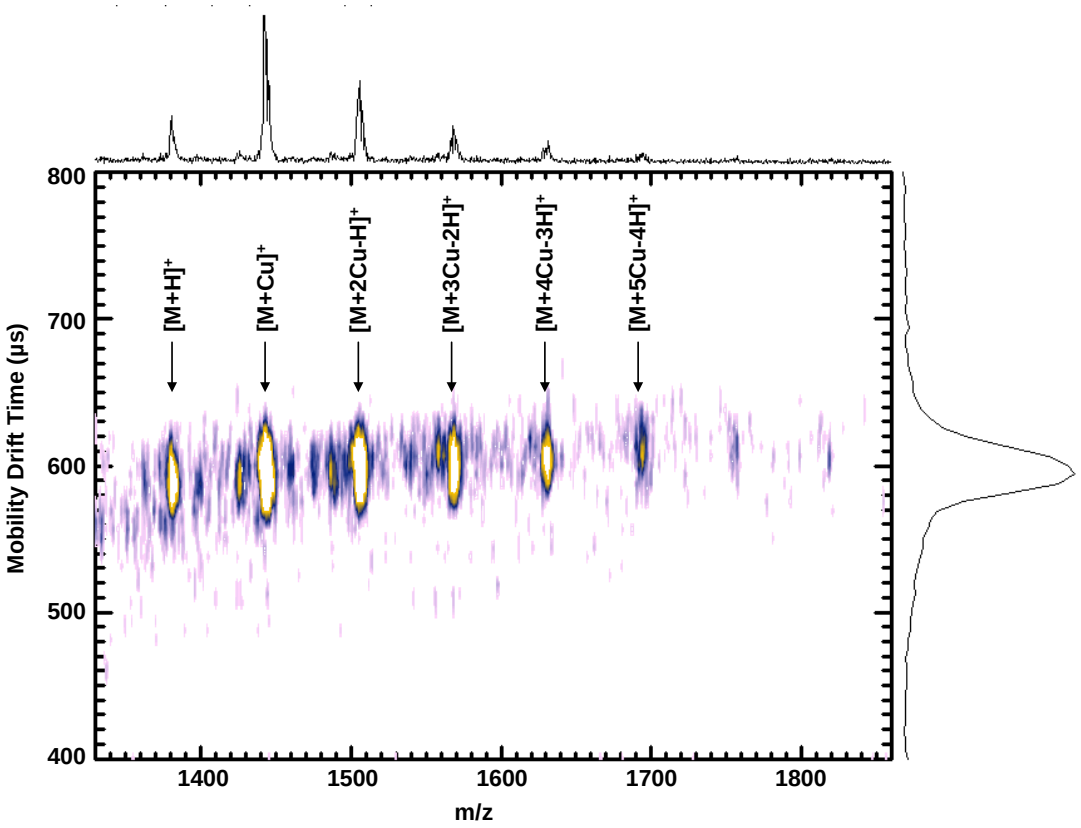

Figure A12. 2-D ion mobility mass spectrum of the $[M + xCu – (x-1)H]^+$ (x = 1 - 5) ions for the peptide Ac-WGGHDGPHAPGDH-NH_2.

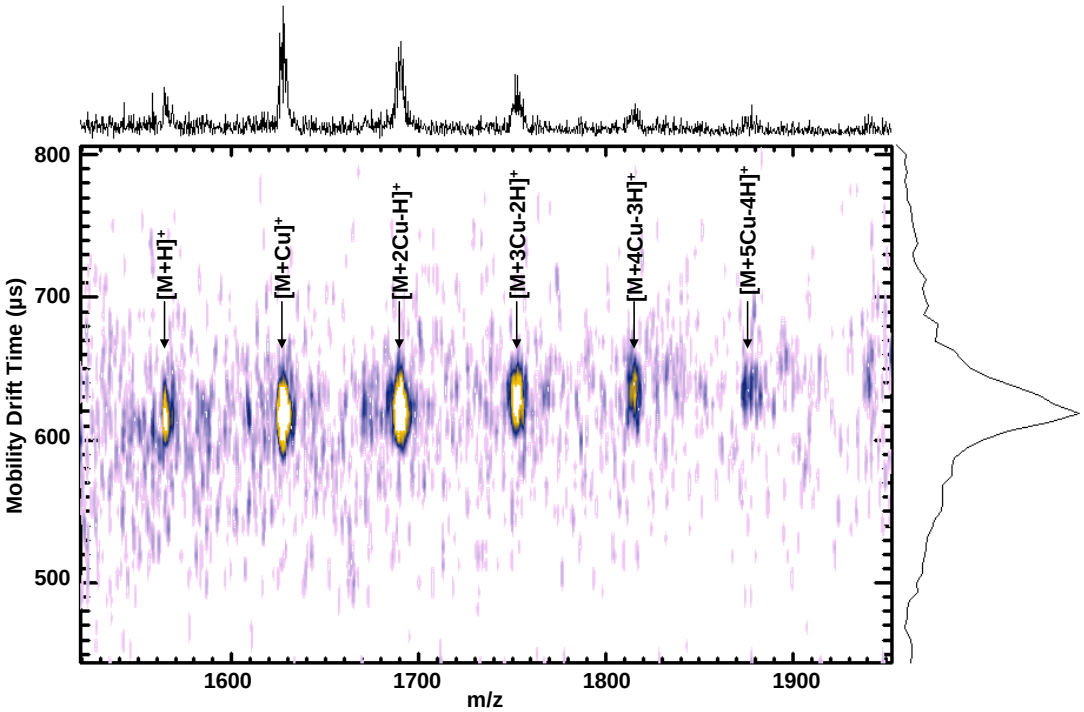

Figure A13. 2-D ion mobility mass spectrum of the $[M + xCu – (x-1)H]^+$ (x = 1 - 5) ions for the peptide Ac-WGHGHGHGPGHGHGH-NH_2.

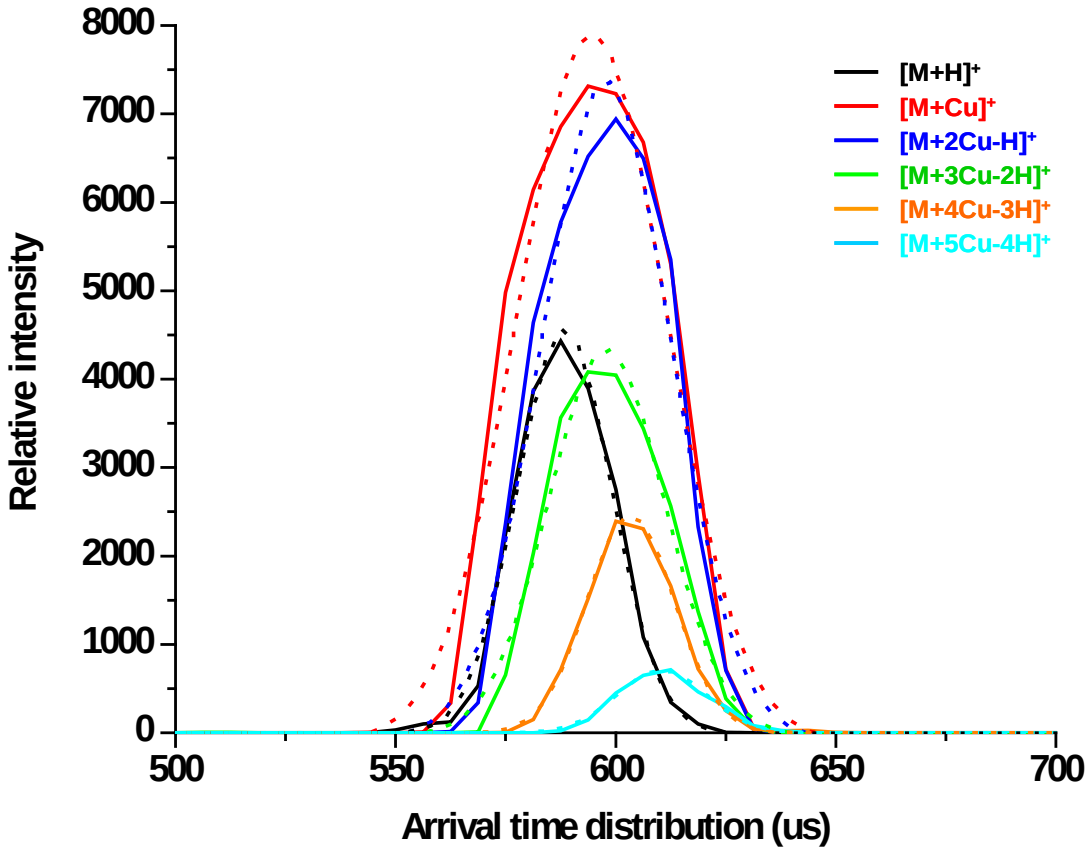

Figure A14. Arrival time distributions (ATDs) of the $[M + xCu - (x-1)H]^+$ (x = 1 - 5) ions for the peptide Ac-WGGHDGPHAPGDH-NH_2 (The solid line represents the data and the dotted line represents the Gaussian fit).

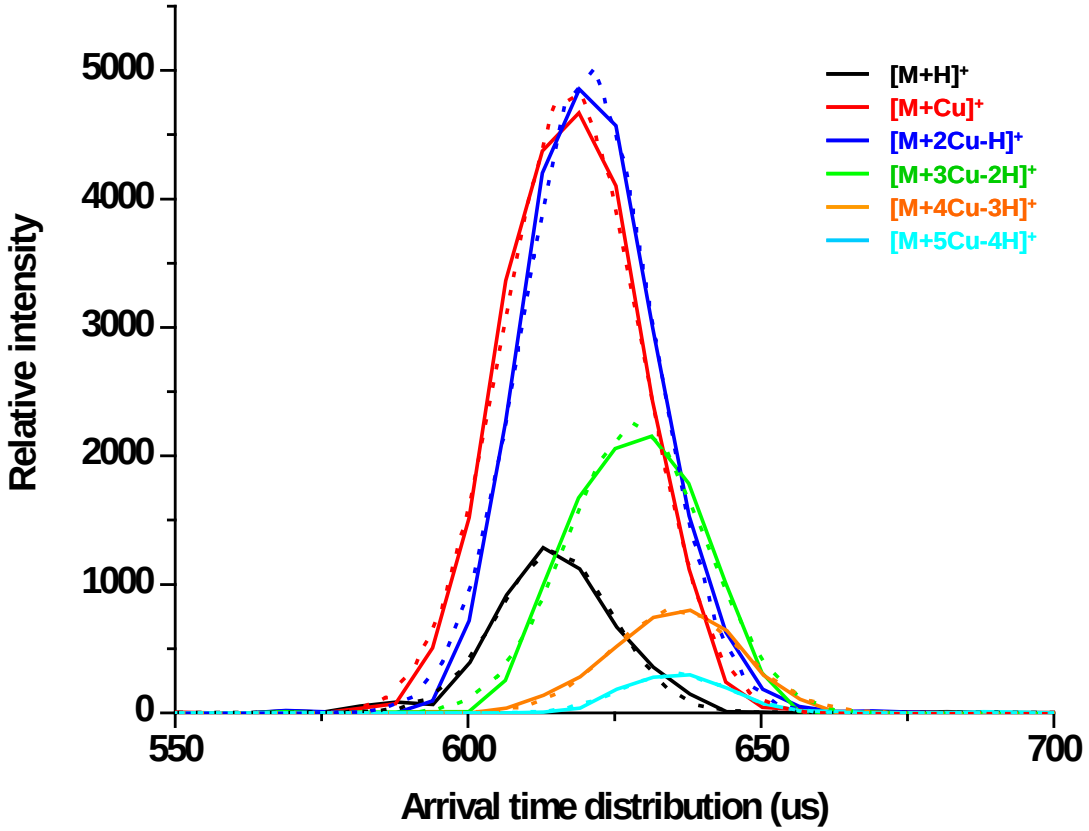

Figure A15. Arrival time distributions (ATDs) of the $[M + xCu - (x-1)H]^+$ (x = 1 - 5) ions for the peptide Ac-WGHGHGHGPGHGHGH-NH_2 (The solid line represents the data and the dotted line represents the Gaussian fit).

APPENDIX B

FIGURE Page

TABLE Page

Table B1. Partial peptide fragment list of the cytochrome C tryptic digest.

	Theoretical mass	Position	#MC	Peptide Sequence
1	1092.6299	93-101	1	EDLIAYLKK
2	1168.6221	29-39	0	TGPNLHGLFGR
3	1296.7171	29-40	1	TGPNLHGLFGRK
4	1350.7263	90-100	1	TEREDLIAYLK
5	1433.7760	27-39	1	HKTGPNLHGLFGR
6	1438.8126	75-87	1	YIPGTKMIFAGIK
7	1470.6859	41-54	0	TGQAPGFTYTDANK
8	1478.8213	90-101	2	TEREDLIAYLKK
9	1495.6985	62-73	0	EETLMEYLENPK
10	1561.8710	27-40	2	HKTGPNLHGLFGRK
11	1598.7809	40-54	1	KTGQAPGFTYTDANK
12	1606.9162	89-101	3	KTEREDLIAYLKK
13	1623.7934	62-74	1	EETLMEYLENPKK
14	1633.6150	15-23	0	heme|CAQCHTVEK|
15	1675.9139	24-39	2	GGKHKTGPNLHGLFGR
16	1712.8238	41-56	1	TGQAPGFTYTDANKNK
17	1735.0112	88-101	4	KKTEREDLIAYLKK
18	1761.9138	9-23	2	KIFVQKCAQCHTVEK
19	1804.0088	24-40	3	GGKHKTGPNLHGLFGRK
20	1840.9188	40-56	2	KTGQAPGFTYTDANKNK
21	2081.0259	57-73	1	GITWKEETLMEYLENPK
22	2140.9067	15-28	2	heme|CAQCHTVEKGGKHK|
23	2209.1209	57-74	2	GITWKEETLMEYLENPKK

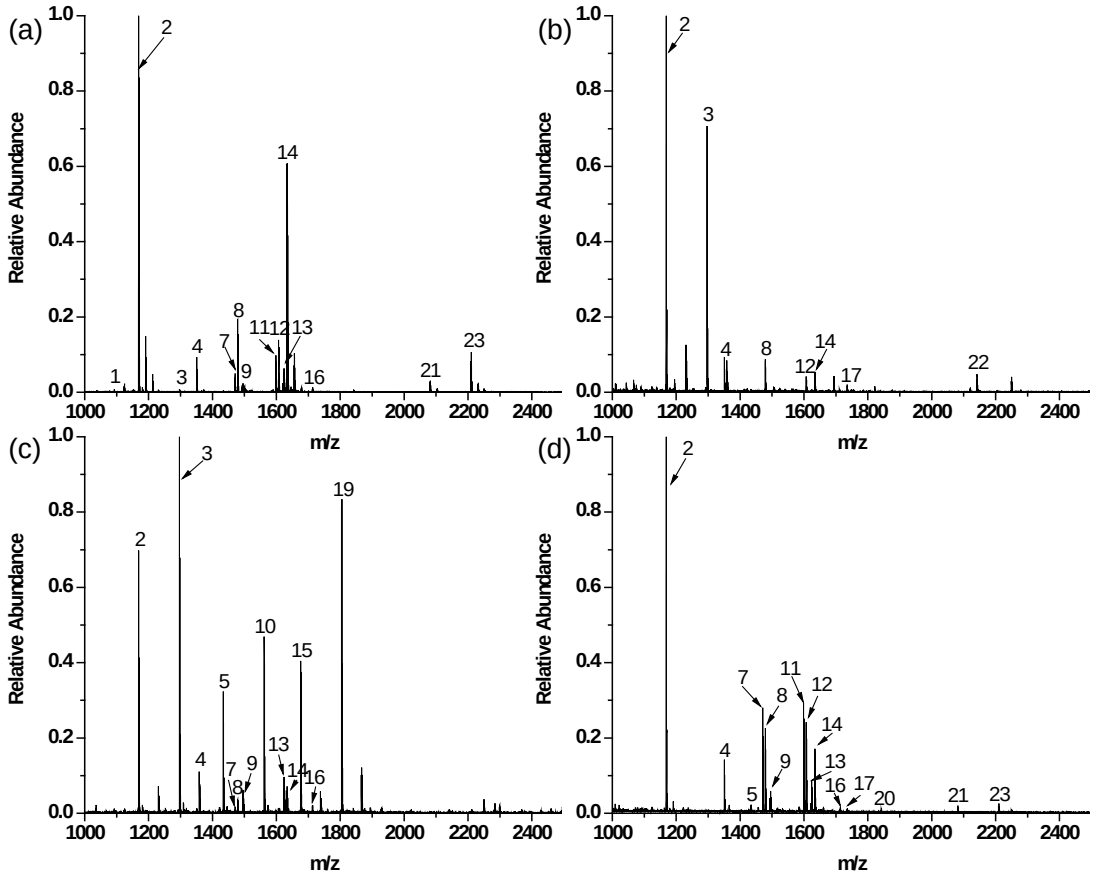

Figure B1. Partial mass spectra of Cytochrome C digest. (a) w/o metal; (b) w/$CuSO_4$; (c) w/Cu-CHCA and (d) w/$NiSO_4$.

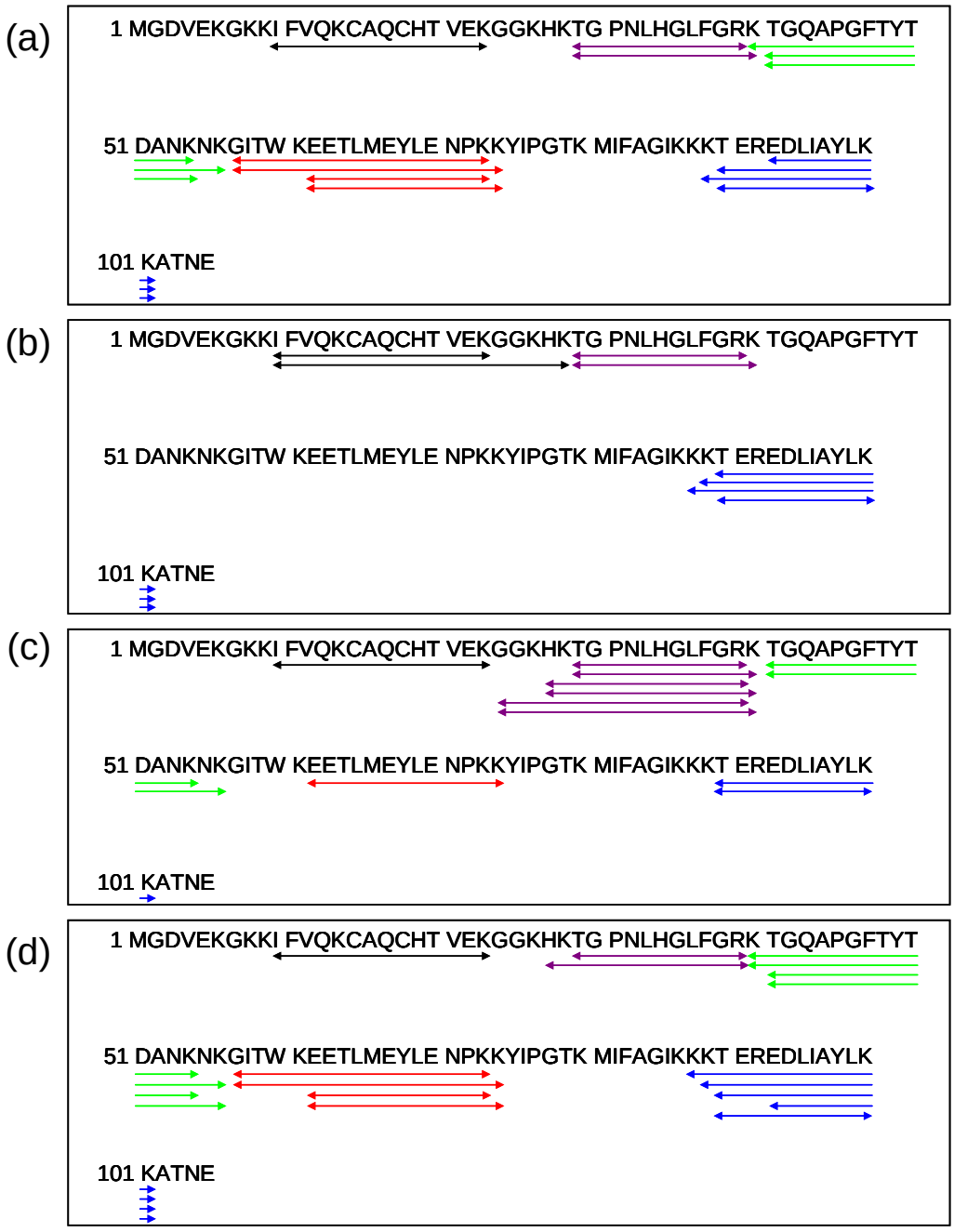

Figure B2. Peptide mapping for the tryptic digestion of Cytochrome C incubated with (a) No metal, (b) $CuSO_4$, (c) Cu-CHCA, and (d) $NiSO_4$.

VITA

Name: Zhaoxiang Wu

Address: Department of Chemistry, 3255 TAMU
College Station, TX 77843

Email: zxwu8056@gmail.com

Education: Ph.D/ Chemistry 2010
Texas A&M University, College Station, TX

B.S./ Chemistry
University of Science and Technology of China 2004
Hefei, Anhui, China

AFFILIATIONS: Member of American Society for Mass Spectrometry
Member of American Chemical Society
Associate Vice President for Chinese Students and Scholars Association (2006-2007)